



Delft University of Technology

# Ship collision on temporary structures

Combi-walls under collision loading

J. Jansen



# Ship collision on temporary structures

Combi-walls under collision loading

by

J. Jansen

in partial fulfilment of the requirements for the degree of

**Master of Science**  
in Civil Engineering

at the Delft University of Technology,  
to be defended publicly on Thursday December 19, 2019 at 16:00.

Student number: 4171225  
Project duration: October, 2018 – December, 2019  
Thesis committee: Prof. dr. ir. S.N. Jonkman, TU Delft, chairman  
Ir. W. F. Molenaar, TU Delft  
Dr. Ir. R. Abspoel, TU Delft  
Ir. E. Van Putten, BAAK/DIMCO



An electronic version of this thesis is available at <http://repository.tudelft.nl/>

*Cover photo: Construction of the Maasdelatunnel  
Photo by Rijkswaterstaat*



# Preface

This master thesis is the final chapter of my studies at the Delft University of Technology. Since the beginning of my studies I learned a lot about several different subjects, including Civil Engineering. I really enjoyed my years in Delft and I would like to thank everyone that was involved during these years of studying.

In the first place I would like to thank the members of my graduation committee for their contribution in making this thesis possible and guiding me through the process. I especially would like to thank Eelco van Putten for giving me the opportunity to have a look inside the kitchen of a mega project. I enjoyed my time at the office, getting some inside information about the project and experiencing a little bit of how it is to work on such a big project.

Furthermore I would like to thank my family and friends for providing support and motivating me to the end of this study. Special thanks to my parents who have always supported me, although it took me some years. Liesje, thank you for your in-depth feedback during the final stages of my thesis, it was really helpful. And finally I would like to thank my girlfriend Rachèl for always supporting me and helping me through the process, we did it!

*Johan Jansen*  
*Delft, December 2019*



# Abstract

When designing a construction pit adjacent to a navigation channel, the event of a ship colliding with the structure is something to take into account in the design of the pit. However, several aspects regarding ship collisions, i.e. the probability of occurrence of a collision, the magnitude of the collision force and the influence on the safety of the pit, are uncertain. The goal of this research is to develop a method to determine the safety of a temporary construction pit.

The Blankenburg Connection, which is being built by BAAK, is used as a case study in this thesis. The construction pit in this project is located in the Scheur and has to deal with a busy navigation channel. The end-wall of the pit is a temporary wall, as it has to be removed in order to be able to float a tunnel element to the middle of the channel.

The safety of a construction pit is expressed by the difference between the loading and resistance of the pit. Out of the several design methods that are proposed, a level IV/III probabilistic method will be used in order to assess the safety of the pit. The required safety level for the construction pit can be calculated using the individual risk criteria and is found to be  $P_f < 10^{-5}$ .

The first aspect that is unknown when designing the construction pit, is the probability of a vessel collision at the Scheur. From scenarios it becomes clear that there are several causes that can lead to a collision on the structure. Out of historical data an estimate of the probability can be made, giving a general number for the probability of a collision. However, the influence of different parameters (i.e. pilot presence) is still unknown, making it difficult for the company to decide which measures to implement in order to reduce the probability of a collision.

A Bayesian Network is used as a method to take into account all the different parameters influencing the probability of collision. When comparing the outcome of the model with values based on historical data for the Scheur, it can be concluded that the probability of the model has the same order of magnitude as the data. A small difference can be noticed, which is probably explained by the fact that not all incidents are being reported to the Port authorities. This is a known phenomenon in shipping and it is estimated that approximately 20% of all marine incidents is not reported.

From the model it becomes clear that the probability of a collision is already below the safety limit found through the individual risk criteria. However, the influence of the different parameters is still measured and this makes it visible to the project owner what kind of measures can be taken in order to decrease the collision probability even more. As not all parameters can be adapted that easily in practice, a selection of parameters is made based on the adaptability from the perspective of the project owner.

To determine the magnitude of the force, a Monte Carlo simulation is used. In this way a probability density function of the magnitude of the force is generated, giving insight in the occurrence of forces on the structure. From the results it can be concluded that there is a small difference in magnitude of forcing between the North and South side of the channel. The reason for this is a combination of the velocity of the vessel and the impact angle. A vessel sailing downstream is accelerated, as where a vessel sailing upstream is slowed down. This is important, as vessels sailing downstream can hit the structure on the South side with a higher angle of impact, resulting in a higher collision load. Turning the construction pit on the south side to face more to the downstream vessels, could be feasible when looking at the magnitude of the force. As in general seagoing vessels are bigger than inland going vessels, the length of the seagoing vessels limits the possibility to hit the structure head-on. The kinetic energy stored inside the vessel is bigger, however, the forcing on the structure is lower for these type of vessels.

The design by BAAK with double end-wall has higher resistance due to the decreased arm of the impact force with respect to the turning point. Furthermore, the effects of the framework can not be neglected. The frame-

work couples all the piles in the wall and also couples the primary wall with the secondary wall, making it a more robust system. In the case of the variant with a single end-wall, the governing failure mechanism is the buckling of the primary elements. As no framework is present in this design, the piles should be considered separately.

In the last part of the thesis several different options are proposed in order to increase the safety of the pit. Out of this sensitivity analysis follows that increasing the amount of activated piles is the most beneficial option. This can increase the safety with a factor of 8, taking the single end-wall as a basic situation. Decreasing the friction between the hull of the vessel and the structure can also be beneficial, as this leads to a safety increase of 1.37.

From the analysis it can be concluded that constructing the pit under an angle can be beneficial. This is related to the ability of the vessel to hit the structure head-on. When vessels sailing by on the other side of the channel are going in the downstream direction, the safety of the pit can be increased with a factor of 1.16 by turning the pit 10 degrees downstream. In the case of the Blankenburg construction pit on the North bank, the vessels on the other side of the channel are sailing in upstream direction. The pit is turned almost 30 degrees downstream, decreasing the safety of the pit.



# Table of Contents

<b>Preface</b>	<b>iii</b>
<b>Abstract</b>	<b>v</b>
<b>1 Introduction</b>	<b>1</b>
1.1 Context . . . . .	1
1.2 Problem statement . . . . .	2
1.3 Research objective . . . . .	2
1.4 Research questions . . . . .	2
1.5 Research scope . . . . .	2
1.6 Methodology . . . . .	3
1.7 Document outline . . . . .	4
<b>2 Ship collisions and construction pits</b>	<b>5</b>
2.1 Safety of a construction pit . . . . .	5
2.1.1 Design methods . . . . .	6
2.1.2 Target reliability for construction pits . . . . .	7
2.2 Loading due to a vessel collision . . . . .	9
2.2.1 Type and number of accidents . . . . .	9
2.2.2 Contributing factors . . . . .	10
2.2.3 Influence parameters in ship collisions . . . . .	10
2.2.4 Determining the collision energy . . . . .	12
2.2.5 Vessels under an angle . . . . .	15
2.2.6 Evaluation . . . . .	17
2.3 Resistance of the structure . . . . .	18
2.3.1 Temporary construction pits . . . . .	18
2.3.2 Failure of a retaining wall . . . . .	21
2.3.3 Failure modes of a combi-wall under collision loading . . . . .	22
2.3.4 Lateral soil pressure . . . . .	23
2.3.5 Local buckling . . . . .	24
2.3.6 Bending moment resistance tubular pile . . . . .	27
2.3.7 Out-of-roundness . . . . .	28
2.4 Conclusion . . . . .	31
<b>3 Case description - Blankenburg Connection</b>	<b>33</b>
3.1 Project description . . . . .	33
3.1.1 Construction method . . . . .	34
3.1.2 Project phases . . . . .	36
3.2 Construction site . . . . .	39
3.2.1 Components of the construction pit . . . . .	40
3.2.2 Design of the end-wall . . . . .	42
3.3 Collision scenarios . . . . .	43
3.4 Consequences of a ship collision . . . . .	45
3.5 Conclusion . . . . .	46
<b>4 The probability of a collision</b>	<b>47</b>
4.1 Bayesian networks . . . . .	47
4.1.1 Collision model for the Scheur . . . . .	47
4.1.2 Existing collision models . . . . .	47
4.1.3 Overview of the existing model . . . . .	48
4.1.4 Adaptations to implement the model at the Scheur . . . . .	49

4.2	Setting up the new model . . . . .	52
4.2.1	Waterway complexity . . . . .	52
4.2.2	Type of vessels . . . . .	53
4.2.3	Meteorological conditions . . . . .	53
4.2.4	Pilot presence . . . . .	54
4.2.5	Scheur Model . . . . .	55
4.3	Probability of a collision according to the model . . . . .	56
4.3.1	Comparison with historical collision data . . . . .	56
4.3.2	Influence of the different parameters . . . . .	57
4.4	Conclusion . . . . .	60
<b>5</b>	<b>The magnitude of the collision force</b>	<b>61</b>
5.1	Model set-up . . . . .	61
5.1.1	Magnitude of the force . . . . .	62
5.2	Input parameters . . . . .	63
5.2.1	Classification and number of vessels . . . . .	63
5.2.2	Dead weight tonnage of the vessels . . . . .	64
5.2.3	Vessel dimensions . . . . .	64
5.2.4	Vessel velocity . . . . .	66
5.2.5	Water level . . . . .	67
5.2.6	Turning circle . . . . .	69
5.2.7	Position of the vessel . . . . .	70
5.2.8	Overview of the input parameters . . . . .	71
5.3	Model limitations . . . . .	73
5.4	Model overview . . . . .	74
5.4.1	Calculation example . . . . .	75
5.5	Results . . . . .	76
5.6	Conclusion . . . . .	78
<b>6</b>	<b>Resistance of the structure</b>	<b>79</b>
6.1	Variants of the structure . . . . .	79
6.1.1	Failure mechanisms . . . . .	80
6.1.2	Assumptions . . . . .	80
6.2	Original design . . . . .	81
6.2.1	Characteristics of the combi-walls . . . . .	81
6.2.2	Failure modes . . . . .	82
6.2.3	Failure of the secondary members . . . . .	85
6.2.4	Influence of interlocking after local buckling . . . . .	88
6.2.5	Failure of the welded joints . . . . .	91
6.2.6	Summary . . . . .	93
6.3	Single combi-wall . . . . .	94
6.3.1	Local buckling . . . . .	94
6.3.2	Rotational stability . . . . .	96
6.3.3	Summary . . . . .	97
6.4	Conclusion . . . . .	98
<b>7</b>	<b>Sensitivity analysis for the end-wall</b>	<b>99</b>
7.1	Safety of the construction pit . . . . .	99
7.1.1	Individual risk . . . . .	99
7.1.2	Probability of failure of the end-wall . . . . .	100
7.2	Parameters to study . . . . .	101
7.3	Conclusion . . . . .	108
<b>8</b>	<b>Conclusions and recommendations</b>	<b>109</b>
8.1	Conclusions . . . . .	109
8.2	Recommendations . . . . .	111

<b>List of Figures</b>	<b>117</b>
<b>List of Tables</b>	<b>121</b>
<b>A General requirements and boundary conditions</b>	<b>123</b>
A.1 Design lifetime of the structure . . . . .	123
A.2 Shipping lane . . . . .	123
A.3 Geotechnical conditions . . . . .	124
A.3.1 Classification of soil . . . . .	124
A.4 Navigational conditions. . . . .	127
<b>B Bayesian Networks - Basics</b>	<b>129</b>
B.1 Basic concepts in probability theory . . . . .	129
B.1.1 Graph theory. . . . .	130
B.1.2 Setting up a Bayesian Network . . . . .	130
<b>C Bayesian Network - Description of nodes</b>	<b>133</b>
<b>D Inland vessels</b>	<b>141</b>
<b>E Friction</b>	<b>145</b>
E.1 Definition . . . . .	145
E.2 Dry Friction. . . . .	145
E.3 Lubricated friction . . . . .	146
E.4 Friction at the interface of ship-structure . . . . .	146
E.5 Influence of the friction coefficient . . . . .	146
E.6 Reducing the friction coefficient . . . . .	147
<b>F Soil stiffness</b>	<b>149</b>
F1 Calculation procedure . . . . .	149
F2 Results . . . . .	152
<b>G Navigational properties</b>	<b>153</b>
G.1 Distribution of wind . . . . .	153
G.2 Tide variation . . . . .	154
<b>H Buckling calculation sheet</b>	<b>155</b>

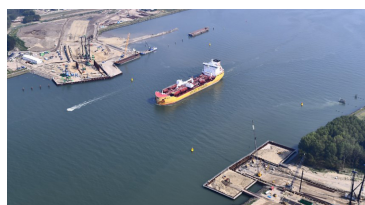


# Introduction

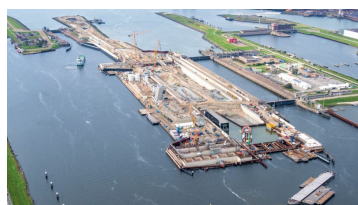
*In this chapter the reader is provided with a general introduction to the problem. In Section 1.1 the context and motivation of this research is given. Following this introduction, the problem is described in Section 1.2 and from this the research objective is formulated in Section 1.3. In Sections 1.6 and 1.7 the approach for this research and the document outline is given.*

## 1.1. Context

Construction works adjacent to or partly located in navigation channels are considered a complicated matter. Besides the self-evident considerations of stability and safety with respect to normal loading, in this case also the possibility of a ship collision with the structure should be considered. This type of loading is considered to be accidental and unlikely to happen.



(a) Maasdelatunnel near Rozenburg



(b) Sealock IJmuiden



(c) Maeslandtbarrier

Figure 1.1: Three recent examples of temporary construction pits vulnerable to ship collisions.

Recently the safety during construction and on construction sites has been an important topic of debate in the Netherlands ([Onderzoeksraad voor de veiligheid, 2018](#)). The Dutch Safety Board concludes, after studying the failure of the unfinished parking garage near Eindhoven Airport, that;

*"the construction sector is insufficiently successful in organizing the process of design and implementation in such a way that constructive safety risks are properly managed."*

In order to prevent accidents and failures on construction sites, the safety board believes that better risk management in the construction sector is needed.

In light of these recent projects and the investigation by the Dutch Safety Board, the safety of temporary construction sites with regard to ship collisions is questioned. At the basis of this thesis is the case of the Blankenburg Connection, which is being realized by BAAK near Rotterdam. The construction pit in this project is partly located in the waterway.

## 1.2. Problem statement

When designing a construction pit adjacent to a navigation channel, the event of a ship colliding with the structure is something to take into account in the design. However, several aspects regarding ship collisions, i.e. the probability of occurrence of a collision, the magnitude of the collision force and the influence on the safety of the pit, are uncertain. As the Dutch Safety Board concluded that the construction sector is insufficiently successful in organizing the process of design and implementation in such a way that constructive safety risks are properly managed, a clear process should be available to assess the safety of a construction pit. As of this moment, no clear process or method exists to take into account all the different aspects to come to a safe design.

## 1.3. Research objective

Based on the problem description the objective of this thesis is formulated as follows:

*Develop a method to determine the safety of a construction pit regarding ship collisions and taking into account the temporary aspect of the construction pit.*

## 1.4. Research questions

This research objective is approached by answering the following questions on basis of the case of the Blankenburg Connection:

- What is the likelihood of a collision event?
- What is the magnitude of the collision force?
- How does a combined wall react under collision loading and how can this be described?
- Is there any residual energy absorbing capacity after failure of a combined wall?
- Based on the findings, what are valuable solutions in order to increase the safety of a construction pit?

## 1.5. Research scope

The scope of this research is limited due to limited time and resources. This section provides an overview of the scope and provides justification for the choices that were made:

### **Scheur ⇔ Other rivers**

In this thesis only the case of the Scheur is considered. The main reason for this is that the project is quite unique and many details are known in this case. Also the Scheur has a mixed fleet, which is interesting as not that many rivers have such kind of composition.

### **Combi-walls ⇔ Other types of wall**

A multitude of methods exist for the construction of a pit in the water. As the time is limited and the project has decided to use combined walls, these will be considered in this thesis.

## 1.6. Methodology

To answer the research questions listed in Section 1.4 several steps are to be made.

### Ship collisions and construction pits

The first step is to set up a framework. This framework describes the current situation and codes as a basis for the rest of the study. The goal of this framework is to provide all the required information in a coherent way as input for the rest of the study.

### Describing the case

The second step is describing the case of the Blankenburg Connection as this is the basis for this research. In this several details of the case are explained, after which the problem becomes at hand becomes more clear.

### Determining the probability of a collision

The third step is to determine the probability of collision in the Scheur. This is done by adapting Bayesian Belief Network from the Finnish Gulf in order to describe all the different aspects that are involved when considering a ship collision at the Scheur.

### Determining the impact forces from colliding vessels

An important next step is to determine the actual occurrence of impact forces. The probability of a collision is now known, but the magnitude of the force is also of importance. Using statistical data, literature and engineering judgment impact forces are determined using a Monte Carlo simulation.

### Determining the resistance of the end-wall

The next step is to determine the resistance of the end-wall, as this is the structure of interest. Both the original design and a variant are checked. With the help of the information from literature, failure modes and failure forces are determined.

### Analyzing the sensitivity of the end-wall

The last step is to combine the previous steps into a combined probability of failure and to see what the sensitivity of the system is to certain parameters.

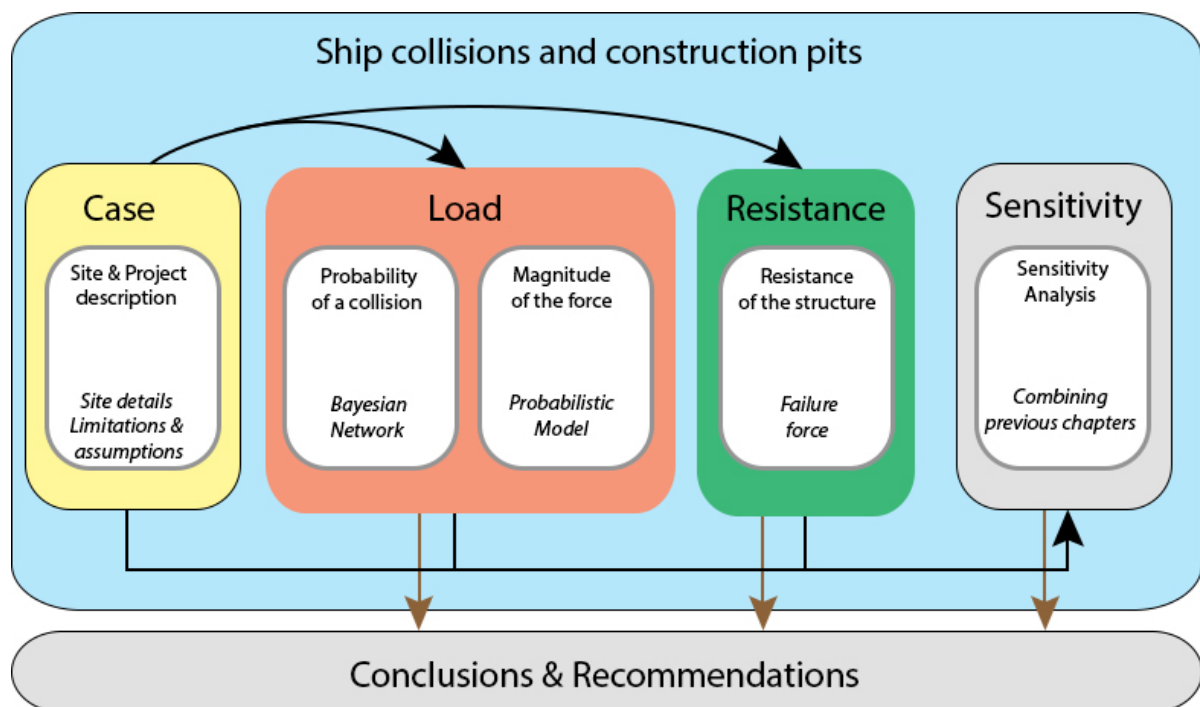


Figure 1.2: The different steps in this thesis visualized in a diagram.

## 1.7. Document outline

**Chapter 1** introduces the problem, research goal and scope.

**Chapter 2** reviews the relevant available literature on the subject and provides a framework for the rest of the thesis.

**Chapter 3** describes the actual case of the Blankenburg Connection which is being realized by BAAK.

**Chapter 4** presents the Bayesian Belief Network which is used to calculate the probability of a vessel collision.

**Chapter 5** presents the probabilistic collision model in which the magnitude of the collision forces is determined.

**Chapter 6** presents the structural analysis of the combined wall. It treats the different failure modes and failure forces on the structure.

**Chapter 7** combines the previous three chapters into a failure probability of the end-wall. After that the sensitivity of the end-wall to different parameters is reviewed.

**Chapter 8** concludes with a discussion about the validity of the proposed solutions and assumptions, provides a conclusion on the study, and gives recommendations on future research and implementation.

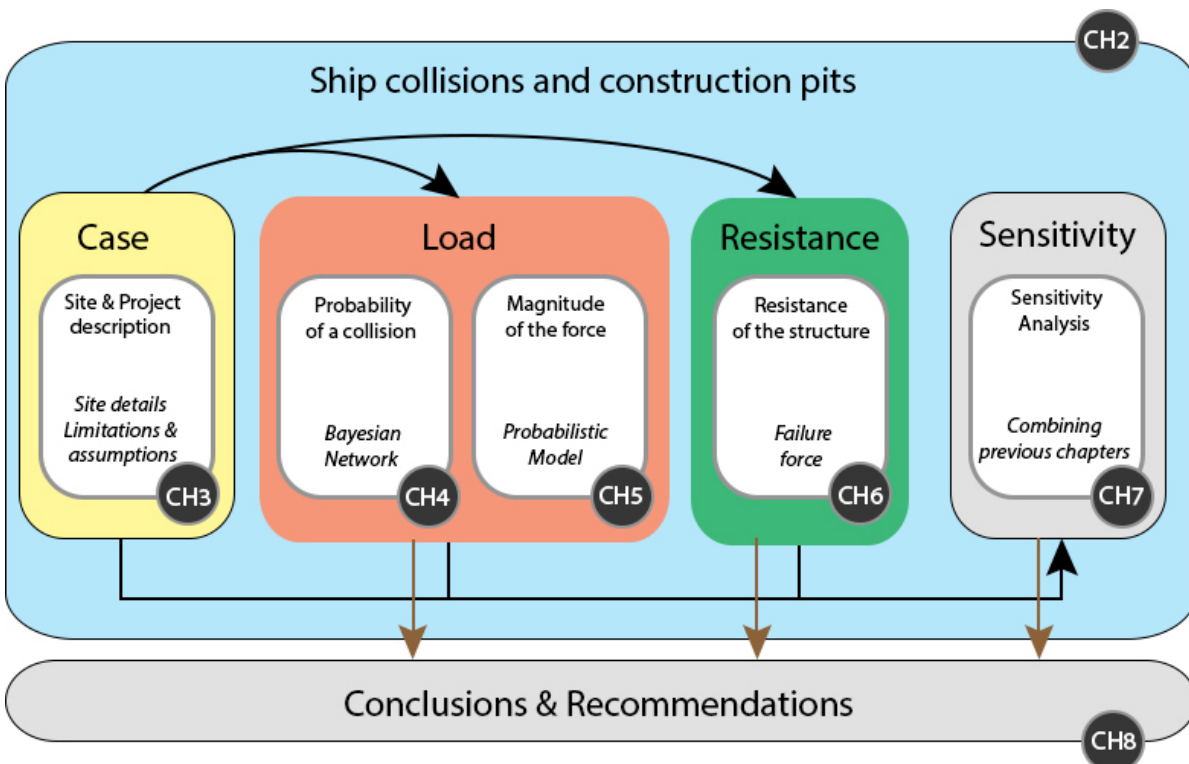


Figure 1.3: The different steps and the corresponding chapters in this thesis.



# 2

## Ship collisions and construction pits

In this chapter the reader is provided with the background knowledge of the subject. In Section 2.1 the safety principle and design methods are discussed. In the following section the loading due to vessels collisions is described. In Section 2.3 the resistance of the structure is treated, after which a short conclusion follows in Section 2.4.

### 2.1. Safety of a construction pit

The main function of a construction pit is providing a safe space for construction works to happen. The walls of the pit can be viewed as a flood defence system, preventing the pit from flooding. The definition of failure for flood defences is the loss of water-retaining function. This usually implies the initiation or development of a breach or excessive amount of water passing the defence line (i.e. a penetrating ship bow).

In order to determine whether failure of the wall occurs, various failure mechanisms need to be considered. For every failure mechanism the load and its resistance needs to be considered. A so-called limit state function  $Z$  can be defined for each failure mechanism:

$$Z = R - S \quad (2.1)$$

Failure occurs if the load ( $S$ ) is greater than the resistance ( $R$ ), so more generally when the limit state function has a negative value ( $Z < 0$ ). For a wall of a construction pit placed in a waterway, the most relevant loads include hydraulic loads, such as the water level and waves, but also loads due to colliding vessels. Relevant resistance properties include the method of construction, type of steel and soil properties.

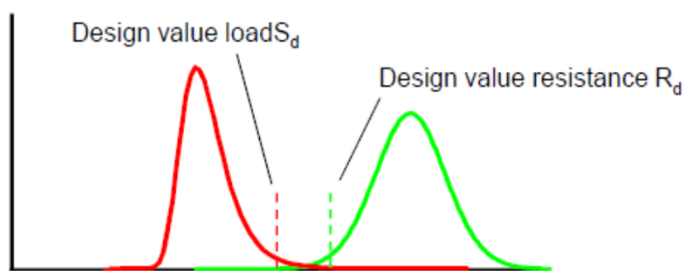


Figure 2.1: Safety principle: resistance (green) should be greater than the load (red). Overlapping area is the probability of failure (Jonkman et al., 2017).

The safety of a flood defence system can be quantified by means of the probability of failure ( $P_f$ ). This is the probability that the load is greater than the resistance. This probability of failure is often expressed in units of time (for example per year) and is given as:

$$P_f = P(Z < 0) \quad (2.2)$$

A probabilistic analysis needs to be made to assess the probability of failure for the different failure mechanisms, and for different elements of the flood defence system. In such an analysis loads and resistances and model uncertainties are characterized by means of probabilistic probability distributions.

As a measure of the safety, one has introduced the target reliability for structures. The target reliability is given by the reliability index  $\beta$  and is directly related to the probability of failure. The target reliability is determined based on the consequences of failure and the working design lifetime. The reliability index ( $\beta$ ) is related to  $P_f$  as follows:

$$P_f = \Phi(-\beta) \quad (2.3)$$

In which  $\Phi$  represents the cumulative normal distribution. The reliability index  $\beta$  gives the distance between  $\mu_z$  (the mean value of  $Z$ ) and  $Z = 0$  in  $\sigma_z$  (standard deviation of  $Z$ ) units as indicated in Figure 2.2.

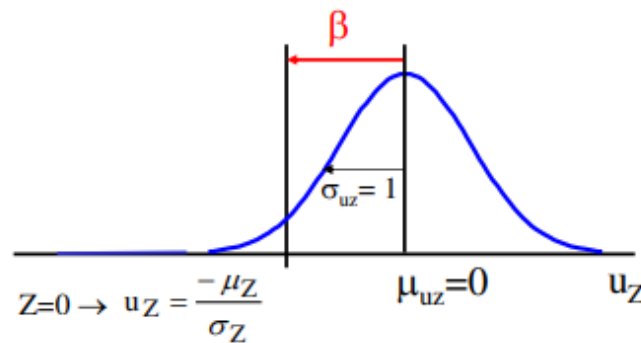


Figure 2.2: Distribution of  $Z = R-S$  and the reliability index (Jonkman et al., 2017)

### 2.1.1. Design methods

In general there are five different methods to calculate the reliability of a structure:

- Level IV (risk-based)
- Level III (probabilistic)
- Level II (approximation)
- Level I (semi-probabilistic)
- Level 0 (deterministic)

A short overview of the different methods is given below.

#### Level IV

In this method the calculations are based on the concept of risk. In general risk can be described as the probability of failure multiplied with the consequences of a failure. Using this method different designs can be compared on an economic basis taking into account uncertainty, costs and benefits. However, this way of designing is quite expensive and time-consuming and is mainly used for structures with large economical and societal risks

#### Level III

In this method the probability of failure is calculated exactly using analytical formulations, numerical integration or most often a Monte Carlo simulation. A Monte Carlo simulation is a sampling method that simulates a given situation numerous times and counts how many time failure occurs. The results are used to determine the probability of failure of the structure.

Another full probabilistic method can be found in the use of a Bayesian Network. This is a theory in the field of statistics based on the Bayesian interpretation of probability where probability expresses a degree of belief in an event. This was first described by Thomas Bayes in 1763.

### Level II

Using a level II analysis the failure probability of the structure is still explicitly calculated, but the problem is simplified by using approximations of the random variables and the limit state functions. This results in less computational effort while the degree of accuracy is almost the same as for a level III analysis. For complicated limit state functions and non-normally distributed random variables the method becomes less accurate.

### Level I

A level I method uses a semi-probabilistic approach. The variables whose probabilistic distributions have to be taken into account are represented by a characteristic value that corresponds to a low percentile in case of a strength parameter or a high percentile in case of a load parameter. Additional partial factors are introduced with values that are based on level II calculations.

### Level 0

In this most basic calculation method, a deterministic mean value for the strength and load is taken, which is then multiplied with a global safety factor.

## 2.1.2. Target reliability for construction pits

In order to determine how safe a structure should be, an acceptable level of risk needs to be defined. For standard applications and systems that are frequently constructed, codes are available that define acceptable safety levels. The Eurocode gives standard values for the reliability index for two reference periods, i.e. one year and 50 years (see Table 2.1) specified for three different classes.

Table 2.1: Target values for  $\beta$  in Ultimate Limit State (EN1991-1-7, 2006)

Class	$t_{ref} = 1 \text{ year}$	$t_{ref} = 50 \text{ years}$
RC3/CC3	5.2	4.3
RC2/CC2	4.7	3.8
RC1/CC1	4.2	3.3

However, a construction pit in a waterway is not an ordinary structure and is not built that often. It can be argued that standard values do not suffice and a risk based analysis is needed to determine the accepted failure probability.

### Risk evaluation

Risk is normally viewed in three different aspects; individual risk, societal risk and economic risk. These three categories are briefly introduced:

#### *Individual risk*

Individual risk criteria are intended to ensure that individual people are not exposed to excessive risk. This is the equity principle, ensuring that all individuals have the same protection.

#### *Societal risk*

Societal risk criteria are given with the intention to limit the risk to the society as a whole. The intention is to limit the risks of large scale accidents with many fatalities. Societal risk criteria are particularly important for big accidents or transport activities, which spread their risks over a constantly changing population of passengers and people near to their ports. Compared to fixed installations, transport activities tend to produce relatively high societal risks despite relatively low individual risks (Agency, European Maritime Safety, 2015).

#### *Economic risk*

Economic risk is the financial view on accidents and failures. Cost-benefit criteria define the point at which the benefits of a risk reduction measure just outweigh its costs. This implements the principle of optimization of protection. By systematically evaluating a range of measures, it is possible to show whether the risks are ALARP (As low as reasonable possible).

The whole process can be schematized using Figure 2.3.

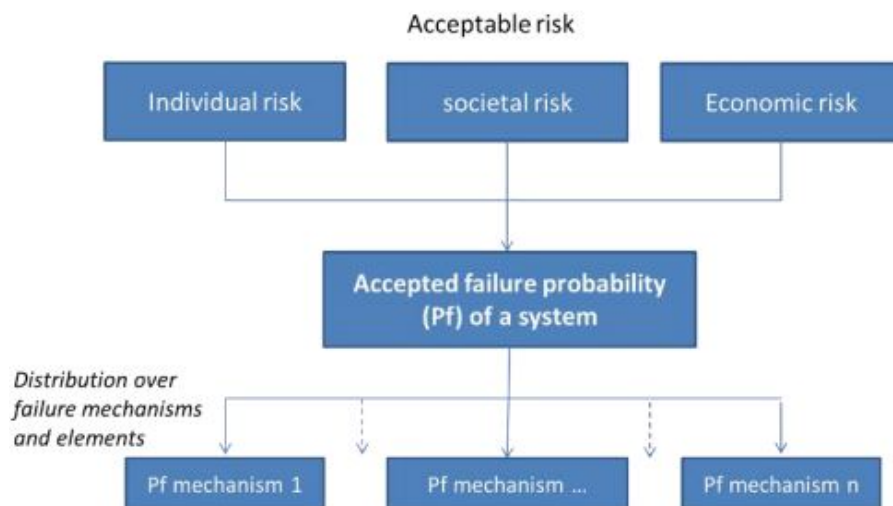


Figure 2.3: Relationship between acceptable risk and failure probability of a system. Adapted from (Jonkman et al., 2017).

### Evaluation

In this thesis the focus will be on the protection of the workers in the construction pit. In this way, the individual risk will be evaluated in order to determine the accepted probability of failure. Furthermore, a level III (probabilistic) method will be used in order to determine the probability of occurrence of forces on the structure.

## 2.2. Loading due to a vessel collision

In order to calculate the probability of failure for each failure mechanism, the loading on the structure and the resistance of the structure should be known. In this section all the different aspects of the loading due to vessel collisions are treated, such as number of collisions, contributing factors and methods to calculate the forcing.

### 2.2.1. Type and number of accidents

A ship collision is always preceded by an accident on the ship itself or at the controlling land based party. Due to better regulations and cooperation between countries in the European Union, accidents are structurally reported and a good overview of the total amount of accidents over the last few years has been achieved (European Maritime Safety Agency, 2017). The total number of accidents reported is almost constant over the last 4 years, as can be seen in Figure 2.4. It is suspected that not all accidents are reported to the national agencies and the total annual incidents rate is estimated at 4000.

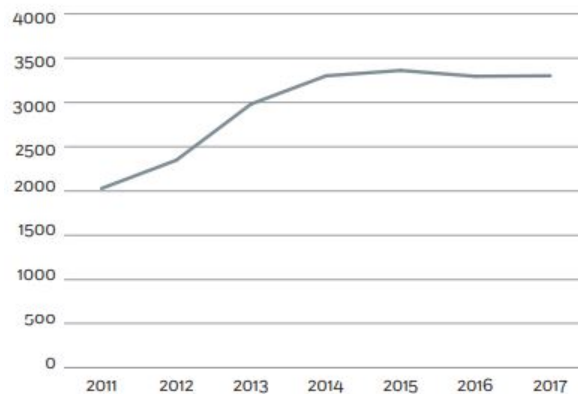


Figure 2.4: Total amount of marine accidents per year reported at EMCIP

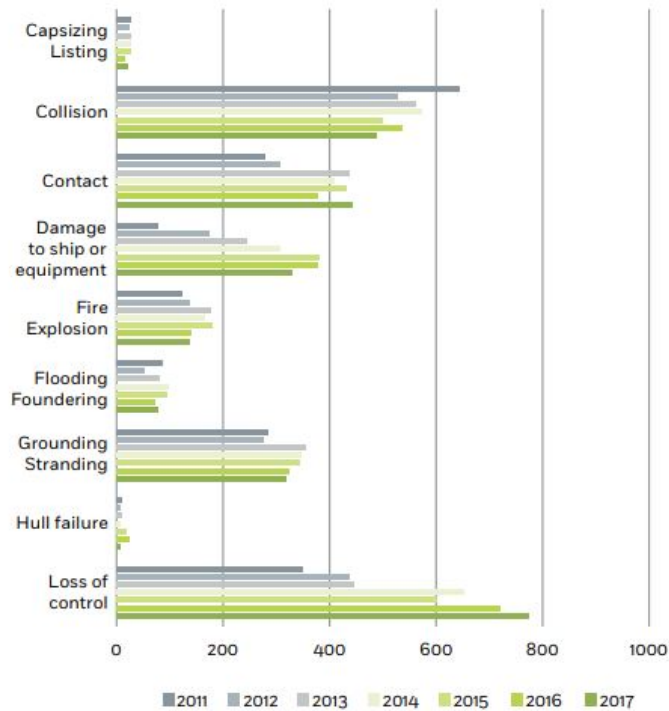


Figure 2.5: Distribution of casualty events with a ship

Taking a look at the type of accidents in Figure 2.5, it can be concluded that collisions and loss of control are the accidents that happen most often. The main part of these accidents (26.2%) take place when a ship is in 'mid-water', which seems logical, as a large part of the operation hours of a vessel will be in this segment.

### 2.2.2. Contributing factors

All accidents are preceded by a type of failure or action. When looking at the main contributing factors, human failure have been reported causing a large proportion of maritime traffic accidents (Hänninen and Kujala, 2012). However, modeling these mechanisms might be challenging as accident occurrence is a result of multiple causes having complex interrelations. Maritime traffic accidents are typically a result of chains of events occurring on many organizational levels while each of these events in an accident chain have normally involved one or more human errors.

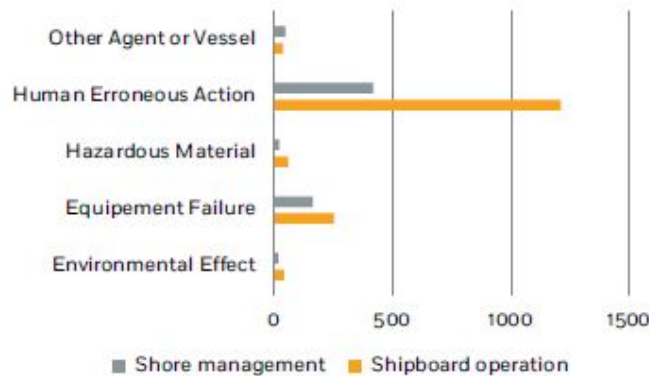


Figure 2.6: Relationship between accidental events and the main contributing factors (European Maritime Safety Agency, 2017)

Figure 2.6 confirms that human failure is the cause of the majority of the accidents in the European Union. A smaller part is related to the mechanical failures and the other causes are almost negligible.

### 2.2.3. Influence parameters in ship collisions

In order to reduce the probability of collision, it is necessary to have an overview of all the factors that play a role and how these can be changed or adapted. Various factors may influence the probability of a collision and these factors can be separated into three main groups (Lutzen, 2001):

- The waterway system including environmental conditions
- The involved vessels
- Human factors

#### The waterway system including environmental conditions

A big influence factor for the waterway system is the traffic. The analysis of the traffic in the region consists of type of vessel, vessel size and intensities. As these factors are more related to the surroundings, like adjacent harbors and cities, these factors are considered to be unchangeable.

Traffic management however, is in principle a mitigation factor. Most of the factors listed in Figure 2.7 are services provided by the harbor authorities in order to improve shipping. These are risk control options which are easily adjustable.

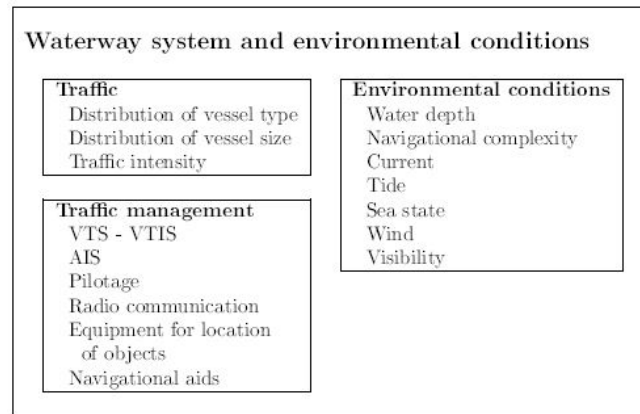


Figure 2.7: Influence of waterway systems on the probability of collision. (Lutzen, 2001)

Environmental conditions also play a role in the ability for safe shipping. These factors depend mostly on geographical location and conditions, which are not easily changed. However, examples exist where man has tried and succeeded in overcoming nature. One of the examples is the wind wall near Rozenburg (The Netherlands), where shipping is improved by taking away the wind for 75%, in order to prevent vessels colliding with a bridge crossing the canal (see Figure 2.8).



Figure 2.8: Wind wall near Rozenburg. Photo by Bart van Damme.

### The involved vessels

The second category is that of the involved vessels. The three main aspects are design, management and instrumentation. As design and instrumentation are directly related to the ship, management is more related to the crew and the shipping company. Guidelines and conventions exist about the education level of the crew, the equipment on-board the vessel and a contingency planning for emergency situations. All parameters mentioned in Figure 2.9 are considered as risk control options, except for the vessel size as this can not be changed easily afterwards.

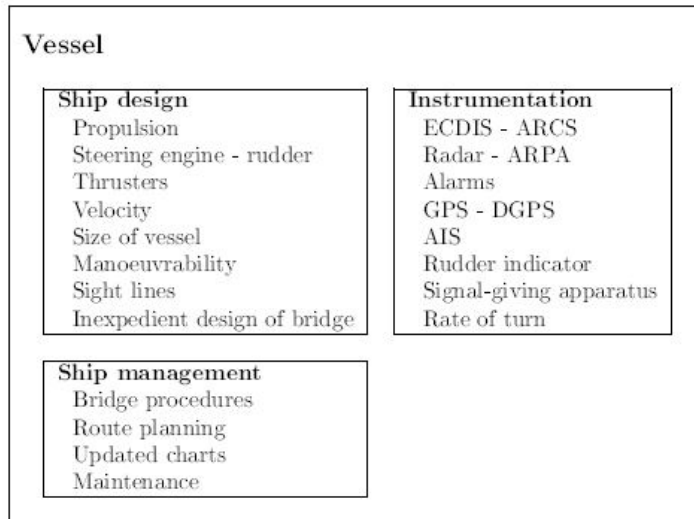


Figure 2.9: Influence of vessel characteristics on the probability of collision. (Lutzen, 2001)

### Human factors

The last category can be considered the most important one. As stated earlier, 60% of the accidents are caused by human failure. Important factors are the duty officer on watch and also the communication on-board the vessel and between the crew. All factors are considered risk control options, because all factors can be mitigated.

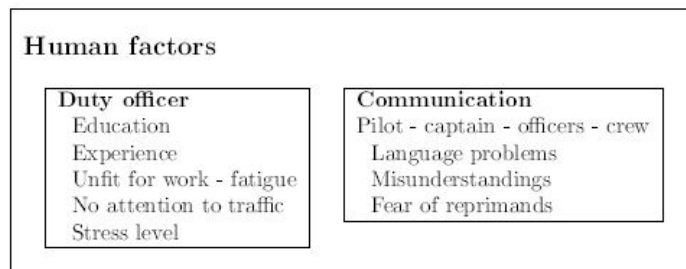


Figure 2.10: Influence of human factors on the probability of collision. (Lutzen, 2001)

### 2.2.4. Determining the collision energy

There are several guidelines that describe the collision process and give rules to calculate the energy that has to be dealt with during a collision. In general the formula given in Equation 2.4 is multiplied with some coefficients, taking into account effects that are known to play a role regarding sailing and berthing vessels.

$$E_{kin} = \frac{1}{2} \cdot m \cdot v^2 \quad (2.4)$$

#### *Hydrodynamic mass coefficient*

The hydrodynamic mass coefficient is introduced to take the water masses into account. When a vessel is sailing, friction and slip stream cause a water body to move with the ship. When a vessel is brought to a stand-still, the water body will work as an extra force on the ship and should therefore be included in the calculation.

Several studies have been done in order to come up with a good way to estimate the volume of water that is affected. Current practice is to add 20% of the ship's mass as hydrodynamic mass, resulting in a  $C_h$  value of 1.2. However, in literature different values can be found for different motions of the ship. As the added mass is dependent on the hull form of the ship and the impact duration, for simplicity reasons Minorksy (1959)



proposed that the added mass should be 0.4 times the ship's mass. In 1971 (Motora et al., 1971) conducted model tests and a hydrodynamic analysis of the added mass coefficient for the sway motion (see Figure 2.11). He found that the coefficient could vary between 0.4 and 1.3. The longer the impact duration, the higher the added mass. So in case of short impact duration, the values proposed by Minorsky could be right. The added mass in forward motion is small compared to the ship's mass. It is found to be 0.02-0.07 (Lutzen, 2001). The added mass for the yaw motion, is found to be 0.21 (Zhang and Pedersen, 1999).

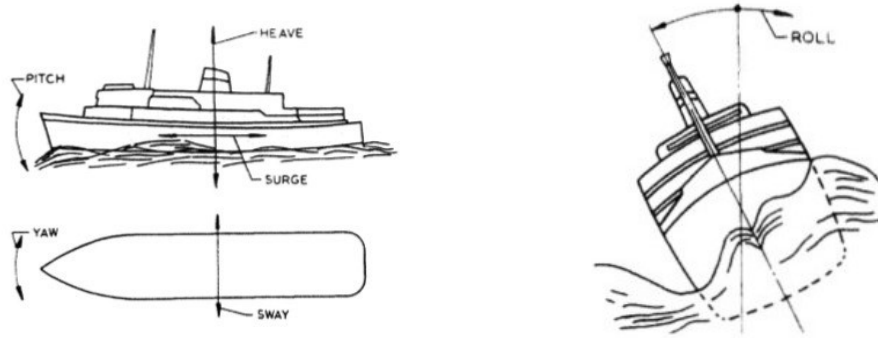


Figure 2.11: Different type of ship motions

#### *Confinement coefficient*

The confinement coefficient is mainly introduced for closed structures like locks or harbors. As this takes into account the increased water pressure when water is confined in between the ship and the structure. For open structures, as discussed in this research, it will not play a role as the water can flow away and very little water will be confined. The values for  $C_c$  will therefore be set to 1.0.

#### *Softness coefficient*

The last coefficient to mention is the softness coefficient. This takes into account the deformability of the ship's hull and the absorption of collision energy by deformation of the hull. For rigid fenders a value of 0.9 is suggested, as the ship's hull will deform in that case.

### CETMEF

The French Institute for Inland and Maritime Waterways (CETMEF) is a technical division of the French Ministry for Sustainable Development. This division provides various services to the government, local authorities and other public entities. One of these services is to provide guidelines for the protection of lock gates against ship collisions, as no legally binding norms for ship collision loads exist. This method proposed by CETMEF is also suggested by the PIANC Working Group 151 and also mentioned in the lecture notes of the course on Port Infrastructure. The method proposed by CETMEF assumes a model in which both vessel and gate are considered deformable and are able to absorb energy. As the method focusses on lock gates, the determination of the collision energy can be universally applied. The studies from CETMEF state that through a dynamic finite element analysis a refined analysis of the collision process may be achieved. However, a first approximation can be given using Equation 2.4 and adding multiple coefficients resulting in the following expression:

$$E_{kin} = C_h \cdot C_c \cdot C_s \cdot \frac{m_s \cdot v_s^2}{2} \quad (2.5)$$

In which:

- $C_h$  = Hydrodynamic mass coefficient [-]
- $C_c$  = Confinement coefficient [-]
- $C_s$  = Ship coefficient [-]

### Eurocode

The Eurocode is the standard code for European countries inside the European Union. In the Eurocode 1 a chapter is devoted to accidental actions, and chapter 4.6 deals with the impact from ship collision (EN1991-1-7, 2006). The detailed determination of the magnitude of the collision energy is treated in the National Annex C of the code. In the code it is stated, that collisions against solid structures in inland waterways should be normally considered as hard impacts, which means that the kinetic energy is being dissipated by elastic or plastic deformation of the ship itself. As in this study the solid structure will be a temporary construction site, the collision will be assumed to be of the soft impact characteristic as protective structures will be present which will be able to take up some of the kinetic energy.

When looking at the formula that the Eurocode proposes, one alteration to the basic equation has been made. According to the Eurocode the hydrodynamic mass, the water body that is moving with the ship, has to be taken into account. In case of bow impact a value of 10% and for side impact a value of 40% is recommended. This changes the basic equation given in Equation 2.4 to the following one:

$$E_{kin} = \frac{1}{2} \cdot (m_s + 0.1 \cdot m_s) \cdot v_s^2 \quad (2.6)$$

The Eurocode gives, in the absence of a dynamic analysis, indicative values of the ship collision forces when handling seagoing vessels. The code also distinguishes between head-on forces ( $F_{dx}$ ) and lateral forces ( $F_{dy}$ ) during a collision, as can be seen in Table 2.2. These forces include the effect of hydrodynamic mass and are based on the calculation showed above.

Table 2.2: Indicative values for dynamic collision force of seagoing vessels

Class of ship	Length (m)	Mass (ton)	Force $F_{dx}$ (kN)	Force $F_{dy}$ (kN)
Small	50	3,000	30,000	15,000
Medium	100	10,000	80,000	40,000
Large	200	40,000	240,000	120,000
Very Large	300	100,000	460,000	230,000

When no dynamic analysis is done for the impacted structure, it is recommended to multiply the values in Table 2.2 with a dynamic amplification factor. For frontal collisions this is 1.3 and 1.7 for lateral impact. For side and stern impacts it is recommended to apply a factor 0.3 to the forces, mainly due to reduced velocities.

### AASHTO

The American Association of State Highway and Transportation Officials (AASHTO) established a code in 1991 to design bridges for vessel collisions. It was their aim to design bridges that were capable of withstanding a collision event of a vessel or barge.

Their method is based on the expression stated in Equation 2.4, the only change is that hydraulic mass is also added into the calculation. As the American system does not use the metric system, the expression in the code is a bit different than used in this report. When transforming it to the metric system, Equation 2.7 remains.

$$E_{kin} = C_h \cdot \frac{1}{2} \cdot m_s \cdot v_s^2 \quad (2.7)$$

The AASHTO gives two extreme values for the hydrodynamic coefficient. Between these values it is possible to interpolate to get a better estimate of the coefficient to be used.

$$C_h = \begin{cases} 1.05 & \text{for underkeel clearance} > 0.5 \cdot \text{draught} \\ 1.25 & \text{for underkeel clearance} < 0.1 \cdot \text{draught} \end{cases} \quad (2.8)$$

### 2.2.5. Vessels under an angle

Collisions of ships with structures are not always head-on. The previous mentioned formulas estimate the total kinetic energy in the moving vessel, but do not take into account the angle of impact and the potential reduction of energy and forces. As the angle of impact ( $\alpha$ ) decreases (taking  $\alpha = 90^\circ$  as head on collision), the probability the force perpendicular to the structure exceeds the maximum friction force on the structure, will increase. When this force exceeds the limit force, the ship will slide along the structure and only a part of the kinetic energy will be transformed into deformation energy. This results in two main situations: sticking or sliding.

When the ship sticks to the structure, an extra component should be considered. As a ship collides under an angle, the velocity vector of the ship will most likely not pass through the point of impact. This will result in a rotational movement around the point of impact and a decrease of impact energy at the structure.

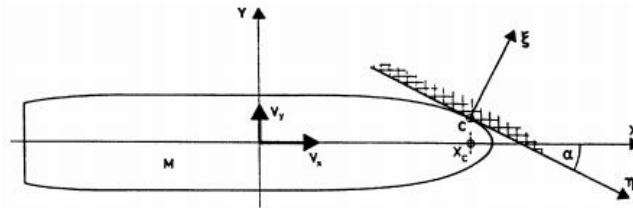


Figure 2.12: Ship impact under an angle (Zhang et al., 2014)

#### Sticking or sliding

The angle of impact at which sliding or sticking occurs, is mainly dependent on the friction coefficient between ship and structure. The Dutch guideline for design of hydraulic structures proposes the use of a friction coefficient  $\mu$  of 0.5, corresponding to a limit values for the sticking case of  $63^\circ$  (ROK, 2017). For further decreasing impact angle, table 2.3 gives reduction factors as a function of the impact angle. This energy is not absorbed by deformation, but will still be present in the vessel as kinetic energy as the vessel will slide along the structure.

Table 2.3: Reduction factors as function of the impact angle (ROK, 2017)

$\alpha^\circ$	60	50	40	30	20	10	5
$\delta$	0.98	0.91	0.82	0.73	0.64	0.48	0.34

For intermediate values of  $\alpha$ , one should interpolate between the values. The lateral force can be calculated as follows:

$$F_{dx} = 3.3 \cdot \sqrt{E_{kin}} + 5.6 \quad (2.9)$$

$$F_{dy} = \delta \cdot F_{dx} \cdot \sin(\alpha) \quad (2.10)$$

And the friction force along the structure becomes:

$$F_R = 0.5 \cdot F_{dy} \quad (2.11)$$

#### Eurocode

The Eurocode states that for angles smaller than 45 degrees ( $\alpha < 45^\circ$ ), a reduction in deformation energy may be applied. The EuroCode suggest to use  $\mu = 0.4$ . and the deformation energy is then given by Equation 2.12.

$$E_{def} = E_{kin} \cdot (1 - \cos(\alpha)) \quad (2.12)$$

In which:

$$\alpha = \text{Berthing angle or angle of impact } [^\circ]$$

### Rotational movement around point of impact

When the ship's velocity vector does not pass through the point of impact, the vessel will also start rotating. The rotation will dissipate energy and result in a lower impact energy at the structure. This effect is already noticed during berthing operations and extensive research has been done in the harbor of Rotterdam (Roubos et al., 2017). To deal with this effect of rotation, the eccentricity coefficient was introduced. This coefficient is defined as stated in Equations 2.13 to 2.17 and presented in Figure 2.13.

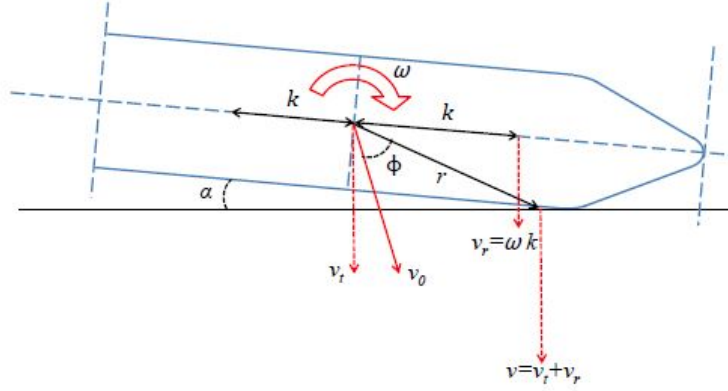


Figure 2.13: Principal of translational and angular velocity during impact.

$$C_E = \frac{k^2 + r^2 \cos^2(\phi)}{k^2 + r^2} + \frac{\omega r}{v} \cdot \frac{2k^2 \sin^2(\phi)}{k^2 + r^2} + \frac{\omega^2 r^2}{v^2} \cdot \frac{k^2}{k^2 + r^2} \text{ (Rotation and translation)} \quad (2.13)$$

$$C_E = \frac{k^2 + r^2 \cos^2(\phi)}{k^2 + r^2} \text{ (Translation)} \quad (2.14)$$

$$C_E = \frac{k^2}{k^2 + r^2} \text{ (Rotation)} \quad (2.15)$$

An estimation of the radius of gyration ( $k$ ) can be obtained using the expression obtained from the OCDI.

$$k = \frac{\sqrt{I}}{L} = \frac{L}{\sqrt{12}} = 0.29 \cdot L \quad (2.16)$$

$$k = L \cdot (0.19 \cdot C_B + 0.11) \quad (2.17)$$

$C_B$  is the blocking coefficient of the ship and can be calculated using Equation 2.18.

$$C_B = \frac{\text{volume of displacement}}{L \cdot B \cdot D} \quad (2.18)$$

In which:

- $C_E$  = Eccentricity coefficient [-]
- $k$  = Radius of gyration of ship [m]
- $r$  = Radius between ship's center of gravity and the impact point [m]
- $v$  = Total translation velocity of center of mass at time of first contact [m/s]
- $\omega$  = Ship's angular velocity at time of first contact with fender [rad/s]
- $\phi$  = Angle between the radius  $r$  and the velocity vector of the ship [°]
- $\alpha$  = Berthing angle [°]
- $L$  = Length of the ship [m]
- $B$  = Beam width of the ship [m]
- $D$  = Draught of the ship [m]

### 2.2.6. Evaluation

The main difference in the calculation methods is the amount of additional factors and how they are calculated. The basic equation for calculation of the kinetic energy is the same in all methods and the coefficient for the additional hydrodynamic mass can be found in every method described. However, the determination of this coefficient is slightly different for each method. More differences arise when looking at ship impact under an angle, as the methods have different approaches to this situation.

In order to compare the different calculations methods, an example calculation will be made with a design vessel for seagoing vessels. In 2016 a new Panama channel opened and a new category of vessels was created, the New-Panamax vessel. This will be the design vessel, as the Nieuwe Waterweg is also dredged to a depth which can accommodate New-Panamax vessels. In Table 2.4 the characteristics of a container vessel are given which are used as input for the calculations.

Table 2.4: Characteristics of a New-Panamax container vessel

Type of Vessel	DWT [t]	Length [m]	Draught [m]	Beam width [m]	Height [m]	Velocity [m/s]
New-Panamax Container	120,000	366	15.2	49	57.91	4.3

For these calculations two scenarios will be examined; the first scenario will be a head-on collision with an angle of impact of  $90^\circ$  and the second scenario a lateral impact under an angle of  $45^\circ$ . In the first scenario the different methods will be used to calculate the total kinetic energy. In the second scenario different methods will be examined to estimate the deformation energy for collisions under an angle.

The results of these example calculations are gathered in Table 2.5 and show the differences in the outcome. For the determination of the total kinetic energy in scenario 1 just small differences can be distinguished. This is due to the fact that the only varying parameter is the added hydraulic mass coefficient, which ranges from 1.1 to 1.25.

Table 2.5: Comparison of the different methods

	Scenario 1 (Head-on) [MJ]	Scenario 2 (Lateral) [MJ]
CETMEF	1331	ROK 819
Eurocode	1220	Eurocode 390
AASHTO	1387	$C_E$ 799

For scenario 2 more significant differences arise and the method proposed by the Eurocode results in a significantly lower value for deformation energy than the two other methods. As the eccentricity coefficient is meant to be used in berthing calculations, it is not clear if this factor can also be used in the calculation of collision energy as the angle of impact is significantly larger than during berthing operations. Nevertheless, the results using this eccentricity factor are quite similar to the values from the ROK.

The resulting force perpendicular to the structure is dependent on the angle of impact and on the friction coefficient as this determines from which angle one deals with a sticking or sliding case.

## 2.3. Resistance of the structure

The design of the pit and the materials used, largely determine the strength of the construction. Construction pits come in various forms and also their strength and force handling can vary. This thesis focuses on construction pits which are made out of 'combination walls'. These walls combine sheet piling with tubular piles, resulting in a combined concept.

### 2.3.1. Temporary construction pits

Construction pits come in different forms and sizes. The most important difference between the different pits is the type of retaining wall used. Several ways exist to construct the retaining wall of an excavation:

#### Sheet piling

Sheet piles are self standing, vertical elements which are coupled using a lock connection. The soil and water pressures are lead into the ground by the 'beam-like' behavior of the sheet piles. The sheet piles will act like an cantilever beam clamped in soil or as a beam supported on two support points; one support in the soil and one where the anchor is placed.

In construction pits the stability of the pit is generally assured by strutting it to the opposite wall. When the distance between the walls is too big or it is not possible to construct the struts, anchoring is used for stability. Anchoring or strutting is used to limit the deformations in the soil surrounding the pit and to lower the economical costs. The vertical sheets will be coupled by use of a wale, spreading the anchor forces over the different sheets (CUR166, 2012).



Figure 2.14: Example of sheet piling. Photo by Swissboring.

#### Combi walls

Combi-walls are made up of primary and secondary elements (combining structural components with a high section modulus interspacing them with components with a lower section modulus, see Figure 2.15). The primary elements can be steel tubular piles, I-sections or built-up boxes uniformly spaced along its length. Their function is to retain earth and water pressures and also as vertical bearing pile for top loads. The secondary elements are, in general, steel sheet piles. The sheet piles mainly retain the water pressures that are acting on the structure and transfer the forces onto the tubular piles.



Figure 2.15: Example of a combi wall in water. Photo by Oriental Steel Pipe.

Combi-walls are applied as big soil retaining structures when constructing hydraulic structures like quay walls, abutments, cofferdams, bridge foundations and construction pits. Combined walls are good solution due to the fact that they have a higher capacity than standard sheet piling walls and also because the fabrication of tubular piles is cost effective. These tubular piles can be welded spirally or longitudinally.

#### Piles

Another solution is to make non ground-displacing pile walls, where piles are made by boring into the ground and mixing grout and cement in order to form concrete piles. These piles will be placed overlapping each other to ensure water tightness. The horizontal bearing capacity is given by the capacity to take up bending moments in the piles, which are then lead into the elastic foundation or to the anchors. To take up bending moments, the piles should be reinforced with reinforcing steel or pre-stressed.

The diameter of drill piles can be up to 2.50 meters. An advantage with respect to sheet piling, is the vertical bearing capacity of a pile wall, which can be considered high in case of a pile wall.



Figure 2.16: Concrete pile wall with heavy top load. Photo by Geotech Rijeka.

#### Diaphragm wall

This solution makes use of the same principle as the previous described method. However, a diaphragm wall has more possibilities as a construction element than the pile wall.

Diaphragm walls are often made of reinforced concrete. The thickness of the walls varies in the range of 0.4 till 1.5 meters and the depth can be up to 120 meters. A diaphragm walls have good horizontal and vertical bearing capacities. Diaphragm walls are often used when constructing parking garages, tunnels and deep cellars.



Figure 2.17: Crane excavating a trench during construction of a diaphragm wall. Photo by GKV Infrastructure Piling Contractors.

### Retaining wall

A often used concept to retain soil is the retaining wall. The retaining function of the wall comes from the weight of the soil on top of the structure. This weight activates a shear resistance between the bottom of the structure and soil underneath it. In weaker soil, the structure is often placed on piles.



Figure 2.18: A simple L-shaped retaining wall. Photo by Marshalls CPM.

Retaining walls are often constructed as L-shaped concrete structures (see Figure 2.18). In this construction method first the soil has to be excavated, after which the structure can be placed. After placing the structure, the soil can be filled up again which will give the stability to the structure. A special variant of retaining walls is used in harbors, where big caisson can be used as retaining walls.

### Cofferdams

A combination sheet piling and retaining walls is the cofferdam. Cofferdams are made up out of sheet piles, connected by anchor bars and then filled with soil or an other material. The retaining function of a cofferdam comes mainly from the weight of the structure, which causes a high resistance against sliding. Cofferdams are often used as breakwater, reinforcing dikes, construction of elevated roads or as retaining walls for making a construction pit in water.



Figure 2.19: A cofferdam with a concrete slab on top. Photo by Dawson Wam.

### Cellular cofferdams

Cellular cofferdams are a variant of normal rectangle cofferdams and are made out of flat steel sheet piles. Due to the shape of the cells, no anchoring is needed. The sheet piling is under tension in their plane (as with a pressurized pipe) and are therefore equipped with strong sheet locks to keep them together. As with normal cofferdams, cellular cofferdams can bridge large level differences.





Figure 2.20: Cellular cofferdam. Photo by C.J. Mahan Construction Company.

### Armored soil

The last option uses the reinforcing effect of placing tension anchors in the soil. Often these anchors are connected with front plates, i.e. concrete slabs, which retain the soil. The structure is built up layer by layer, placing the anchors and front plates and filling up the soil. This structures are often used in dry conditions as the plates are not water tight.



Figure 2.21: The application of a 'terre armee' method to construct a deep excavation. Photo by Noise.

### 2.3.2. Failure of a retaining wall

For a retaining wall, several failure mechanisms are known. In Figure 2.22 these are shown and briefly explained.

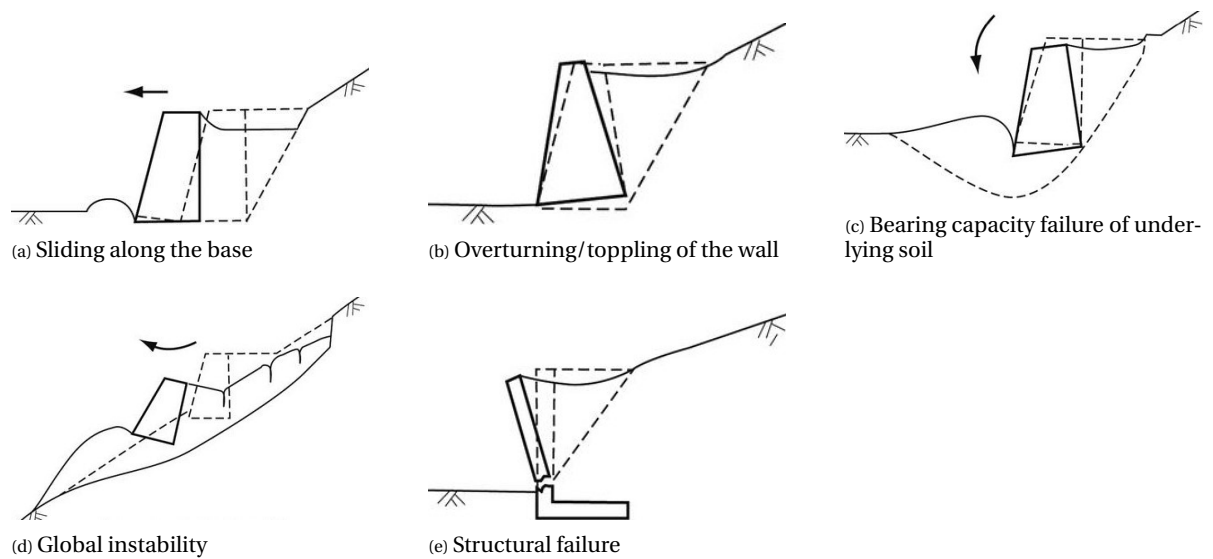


Figure 2.22: Different failure mechanisms of a retaining wall. (Perera, 2018)

### 2.3.3. Failure modes of a combi-wall under collision loading

The focus in this thesis will be on combi-walls. Of the different failure modes listed in Figure 2.22, not all are important for the case of combi-walls. When one assumes that the combi-wall is stable when placed, it is interesting to look into the case of collision loading only. In that specific case, three of the mentioned failure mechanisms are of importance; sliding along the base, overturning/toppling of the wall and structural failure.

#### Sliding along the base

The first failure mechanism that can occur is sliding along the base. In case of a combi-wall, this can also be translated in failure of the horizontal support. In general, construction pits have a concrete floor at the bottom which supports the retaining wall. When the resistance of the floor is not high enough, the horizontal support can fail.

#### Rotational stability

Another failure mechanism that can be discerned for this structure is the rotational failure. As the wall has a large cantilever part which is supported by the concrete floor, the wall or tubes could start rotating around the concrete floor. It should be checked if the passive soil and water pressures are sufficient to withstand the rotating moment at the level of the concrete floor.

#### Structural failure

Structural failure occurs when a high loading is applied on the structure. In case of a vessel collision, a high external load is applied at the top of the structure and high bending moments occur in the structure. Two types of failure can occur:

- Buckling of the tubular elements
- Failure of the interlocking system

Buckling occurs when the bending moment capacity of the tubular piles is reached. This is further treated in Section 2.3.5. The second type of structural failure is the failure of the interlocking. In this type of failure deflection of the piles becomes too large and the interlocking between the sheet piles will fail while tubular piles are still standing. This is described into more detail in Section 6.2.3.

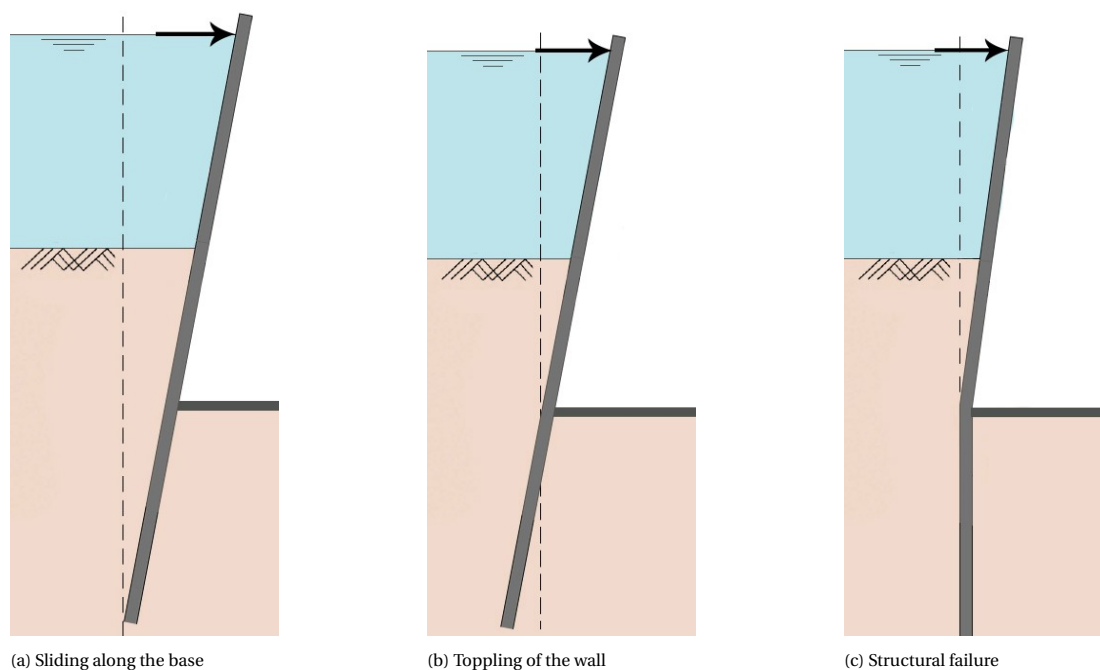


Figure 2.23: Failure modes for a combi-wall under collision loading.

### 2.3.4. Lateral soil pressure

The load on the combi-wall results in displacement of the structure and triggers reaction forces in the soil. The stresses in the soil can be determined as follows (Verruijt and Van Baars, 2007):

$$\sigma'_h = K \cdot \sigma'_v \quad (2.19)$$

In which:

- $\sigma'_h$  = effective horizontal soil stress [kPa]
- $\sigma'_v$  = effective vertical soil stress [kPa]
- $K$  = lateral stress coefficient [-]

The lateral stress coefficient is largely determined by the relative density of the soil, the stress history, plasticity index, over-consolidation ratio (OCR) and other soil properties.

When the soil is in rest and there is no horizontal strain, the lateral stress coefficient is denoted as the neutral earth pressure coefficient  $K_0$ . Positive horizontal strain is defined as active soil pressure and the related coefficient is  $K_a$ . Passive soil pressure results in a negative strain and a higher coefficient,  $K_p$ .

The neutral earth pressure coefficient  $K_0$  can be given as a function of the internal friction angle ( $\phi'$ ):

$$K_0 = 1 - \sin(\phi') \quad (2.20)$$

The active and passive earth coefficients are given as follows (Rankine, 1856):

$$K_a = \frac{1 - \sin(\phi')}{1 + \sin(\phi')} \quad (2.21)$$

$$K_p = \frac{1 + \sin(\phi')}{1 - \sin(\phi')} \quad (2.22)$$

These coefficients are quite conservative and simple in their approach of the soil pressure. When a more accurate estimate of the soil resistance is required, a non-linear soil model can be helpful.

#### Nonlinear soil pressures

In a more realistic model the soil pressure is modeled as non-linear with the depth. The soil pressure is a nonlinear function depending on a set of different factors. The p-y curves analysis is a numerical model that simulates the soil resistance as predefined nonlinear springs (see Figure 2.24).

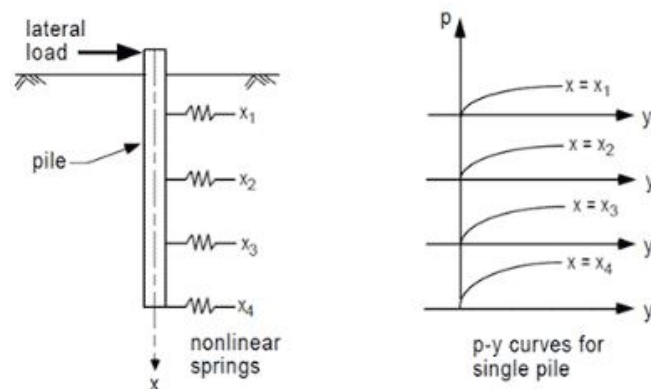


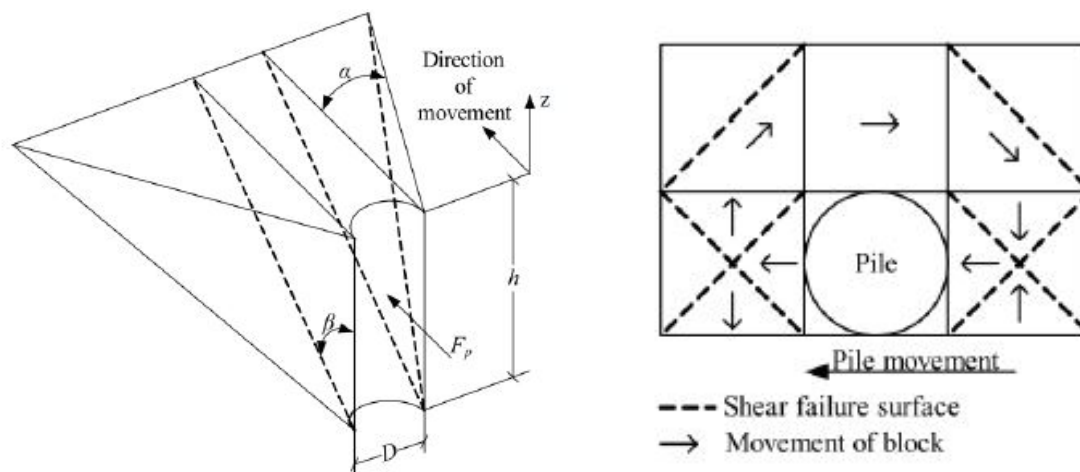
Figure 2.24: Single pile model (Brown, D.A.; Turner, J.P.; Castelli, R.J., 2010)

The soil is represented by a series of nonlinear p-y curves that vary with depth and soil type. The p-y curve for a certain depth may depend on many factors, such as:

- Soil type
- Type of loading
- Foundation diameter and cross-sectional shape
- Coefficient of friction between foundation and soil
- Depth below ground surface
- Foundation construction methods
- Group interaction effects

Over the years several tests have been done to estimate the p-y curves. The original p-y curves are developed by Reese et al. (1974) from the results of tests at Mustang Island on two 0.6m diameter piles embedded in a deposit of submerged, dense, fine sand. For other soil types, other p-y curves have been derived.

At shallow depths a wedge will form in front of the pile assuming that the Mohr-Coulomb failure theory is valid. Reese et al. (1974) uses the wedge shown in Figure 2.25a to analytically calculate the passive ultimate resistance at shallow depths. By using this failure mode a smooth pile is assumed and therefore no tangential forces occur at the pile surface. The active force is also computed from Rankine's failure mode, using the minimum coefficient of active earth pressure.



(a) Small depths

(b) Large depths

Figure 2.25: Soil failure modes according to Reese et al. (1974).

At deep depths the sand will, in contrast to shallow depths, flow around the pile and a static failure mode as sketched in Figure 2.25b is used to calculate the ultimate resistance. The values found with the p-y curves consider a fully mobilised passive lateral soil pressure. Therefore they still result in upper boundaries for the real soil pressure.

### 2.3.5. Local buckling

An important failure mode for tubular piles is the occurrence of local buckling, as already mentioned in Chapter 2. In this section the reader is given a more elaborated review of this phenomenon.

The classification of a cross-section depends on the width to thickness ratio of the parts subject to compression. For the slender cross-sections in class 4, the maximum stress is determined by local buckling and the stress in the outer fiber is lower than the yield stress  $f_y$ . In other words, combi-walls with classification 4 reach the Ultimate Limit State (ULS) before they start yielding (see Figure 2.26).

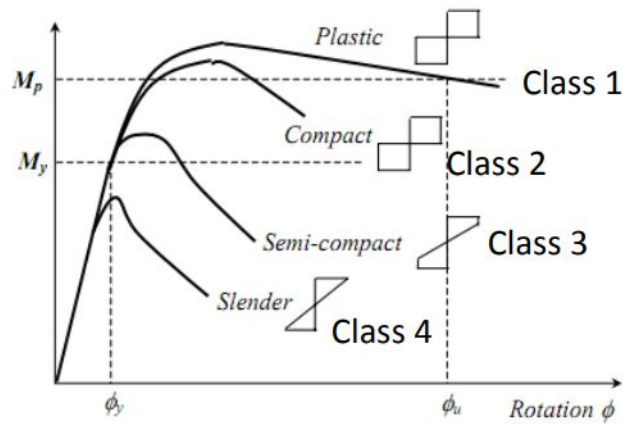


Figure 2.26: Different cross-section classes.

The cross-section class is determined by the following equation (EN1991-1-1, 2005):

$$\frac{D}{t \cdot \epsilon^2} \quad (2.23)$$

In which:

$$\begin{aligned} D &= \text{Diameter of the pile} \\ t &= \text{thickness of the pile} \\ \epsilon^2 &= \frac{235}{f_y} \end{aligned}$$

According to EN 1993-5 the steel tubes used as primary elements in combined walls, should be evaluated according to EN1993-1-1 when they are categorized in cross-sections classes 1-3 and according to EN1993-1-6 when categorized as class 4. The four cross-section classes are defined as:

Table 2.6: Classification of cross-sections (EN1991-1-1, 2005).

Class	Limits	Characteristics
1 - Plastic	$\frac{D}{t} < 50 \epsilon^2$	- Full plastic moment allowed - Section is able to develop a plastic hinge - Plastic redistribution allowed
2 - Compact	$\frac{D}{t} < 70 \epsilon^2$	- Full plastic moment allowed
3 - Semi-compact	$\frac{D}{t} < 90 \epsilon^2$	- Full elastic moment allowed (Yield limit in outer fiber)
4 - Slender	$\frac{D}{t} > 90 \epsilon^2$	- Limited effectiveness, buckling stress (Below yield limit) allowed in outer fiber - Refer to EN 1993-1-6

Winkel et al. (2017) already stated that the EN 1993-1-6 shell buckling rules are over-conservative and may lead to economical unfavourable designs. The Eurocode EN 1993-1-6 has been updated in 2017 and a method has been added for pure bending of the primary tubular piles. This method is less conservative compared to the earlier version of EN 1993-1-6. However, because of the significant influence of the membrane force of the intermediate sheet piling, in this thesis the CUR211E will be used, since this method includes the membrane forces in the checking of the tubular section.

For the analysis of the different cross-sections, several methods exist. In Figure 2.27 an overview is given for the different classes. As can be seen for the Slender cross-sections (Class 4) two different methods exist. The 'reduced cross-section' or 'effective width' method and the 'reduced stress' method.

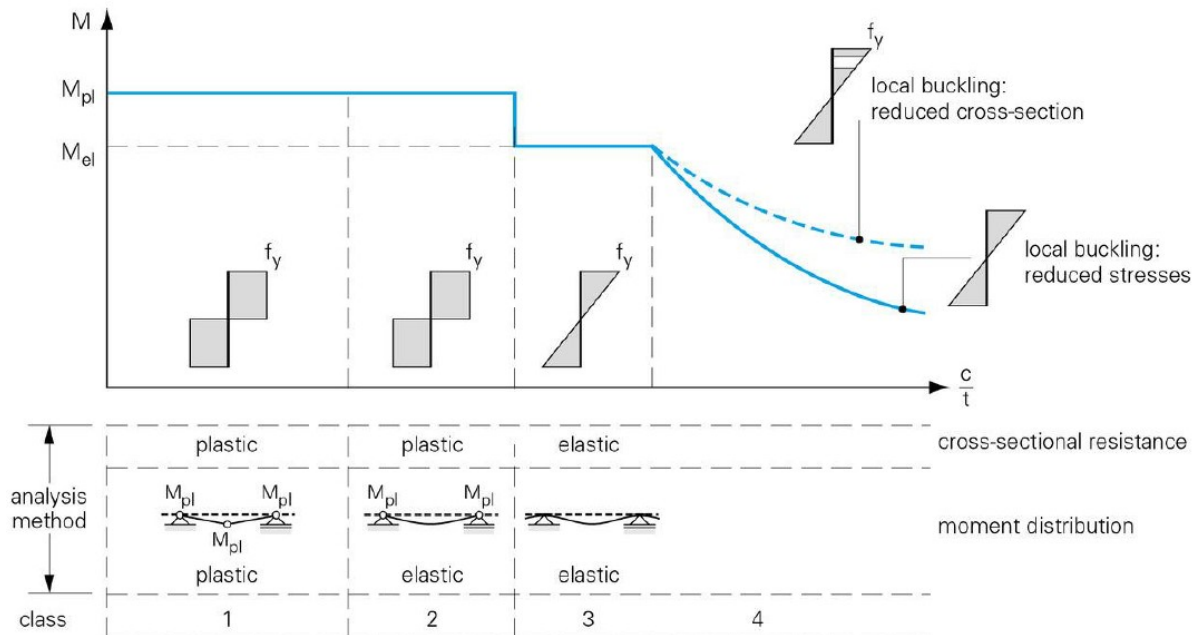


Figure 2.27: Cross-section classes and analysis methods. (Lecture slides Steel Structures 2)

### Stress bases method

When applying the local stress criterion (as given by the EN1993-1-6 (2005)) local buckling calculations lead to conservative designs. By applying this criterion, all the parameters that influence the local buckling behavior are taken into account by applying a reduction on the local buckling stress. This approach has restrictive effect on the tubes, in which a part of the shell yields before local buckling (Kostis, 2016).

### Strain based method

The CUR211 (2014) recommends to use the method based on the critical strain criterion from Gresnigt (1987). The critical strain criterion is a safe lower bound of measured critical strains (with estimated 5% probability of a lower value).

$$\begin{aligned} \epsilon_{cr} &= 0.25 \cdot \frac{t}{r} - 0.0025 & \text{for } \frac{D}{t} < 120 \\ \epsilon_{cr} &= 0.10 \cdot \frac{t}{r} & \text{for } \frac{D}{t} > 120 \end{aligned} \quad (2.24)$$

In which:

$\epsilon_{cr}$  = critical strain  
 $r$  = radius of the pile

In case of pure bending the position of the yield strain is indicated with the angle of plasticity rate  $\theta$ , starting for plastic strain in the outer fibre, and approaching 0 for the full plastic moment.

$$\begin{aligned} \sin \theta &= 1/\mu & \text{for } \epsilon_{cr} > \epsilon_y \\ \theta &= \pi/2 & \text{for } \epsilon_{cr} < \epsilon_y \end{aligned} \quad (2.25)$$

The bending moment as a function of the plasticity rate can be calculated with (CUR211, 2014):

$$M_R = \frac{1}{2} \cdot \left( \frac{\theta}{\sin\theta} + \cos\theta \right) \cdot M_{pl;d} \quad \text{for } \epsilon_{cr} > \epsilon_y$$

$$M_R = \mu \cdot M_{el;d} \quad \text{for } \epsilon_{cr} < \epsilon_y$$
(2.26)

In which:

$$M_{pl;d} = \frac{D^2 \cdot t \cdot f_y}{y_{M0}}$$

$$M_{el;d} = \frac{\pi}{4} \cdot \frac{D^2 \cdot t \cdot f_y}{y_{M0}}$$

$$y_{M0} = 1.0$$

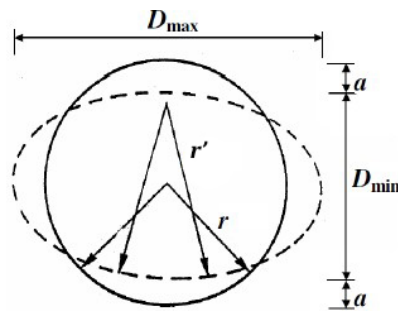
The resistance against local buckling is mainly determined by the ability of the tube to maintain its circular shape. Cross-sections with large  $D/t$  ratios tend to adopt an oval shape that creates a 'flat' top portion, with a virtually larger radius, which increases the susceptibility to buckling. Moreover, the load capacity is influenced by the presence of residual stresses, the stress-strain relation of the steel, effects of non-linear geometric behaviour, the presence of soil fill and external tension forces (Winkel et al., 2017; Gresnigt, 1987).

### 2.3.6. Bending moment resistance tubular pile

To check whether local buckling occurs, the cross-section at the location of the concrete floor is checked for its bending moment. This is the location with the highest bending moment and therefore the biggest compressive strains in the pile. The class of the pile can be determined using Formula 2.23. When piles are classified as slender (Class 4), the piles do not reach their yield stress before buckling. The critical strain criterion can be calculated using Formula 2.24.

$$\epsilon_{cr} = 0.25 \cdot \frac{t}{r'} - 0.0025 \quad \text{for } \frac{D}{t} < 120$$

The radius in the calculation is the increased radius due to ovalisation and can be calculated with the following formula (CUR211, 2014):



$$r' = \frac{r}{1 - 3a/r}$$
(2.27)

Figure 2.28: Radius  $r'$  in an ovalised cross-section. (EN1993-4-3, 2009)

This will lead to a lower critical strain and consequently a lower theoretical bending moment as can be evaluated with Equations 2.24 and 2.26. The bending moment shall be further reduced with the factors  $g$  and  $\beta_c$  to account for the effect of ovalizing bending stresses and deformations respectively.

$$M_{Rd} = g \cdot \beta_g \cdot \beta_s \cdot M_R$$
(2.28)

In which:

$$g = \frac{c_1}{6} + \frac{2}{3}$$

$$c_1 = \sqrt{4 - 2 \cdot \sqrt{3} \cdot \frac{m_{eff;Sd}}{m_{pl;Rd}}}$$

$$\beta_g = 1 - \frac{2a}{3r}$$

The parameter  $\beta_s$  is meant to account for the fact that local buckling in the elastic area tends to cause sudden failure, without deformation capacity. This is dependent on the ratio between the critical strain and yield strain ( $\mu$ ) which is defined in Equation . Recommendations have been made, although some room for national authorities is left to deviate from the recommended values.

$$\mu = \frac{\epsilon_{cr}}{\epsilon_y} \quad (2.29)$$

Now the  $\beta_s$  can be defined as follows:

$$\begin{aligned} \beta_s &= 0.75 && \text{for } \mu \leq 1 \\ \beta_s &= 0.625 + 0.125 \mu && \text{for } 1 \leq \mu \leq 3 \\ \beta_s &= 1.0 && \text{for } \mu \geq 3 \end{aligned}$$

### 2.3.7. Out-of-roundness

Tubular piles tend to not be perfectly round and this will reduce the critical strain. For piles in combi-walls four causes of out-of-roundness can be distinguished.

#### Production process of the pile

During the production process of the tubular piles, an initial out-of-roundness can appear. This is categorized by the EN1991-1-1 (2005) in classes A to C, giving an indication of the quality of the production process. The out-of-roundness parameter is given as:

$$U_r = \frac{D_{max} - D_{min}}{D_{nom}} \quad (2.30)$$

with the following data:

Table 2.7: Recommended values for  $U_r$  (EN1991-1-1, 2005)

Class	$D \leq 0.50\text{m}$	$0.50\text{m} < D < 1.25\text{m}$	$1.25 < D$
A - Excellent	0.014	$0.007 + 0.0093(1.25-D)$	0.007
B - High	0.020	$0.010 + 0.0133(1.25-D)$	0.010
C - Normal	0.030	$0.015 + 0.0200(1.25-D)$	0.015

The parameters given in Equation 2.30 are defined as given in Figure 2.29.

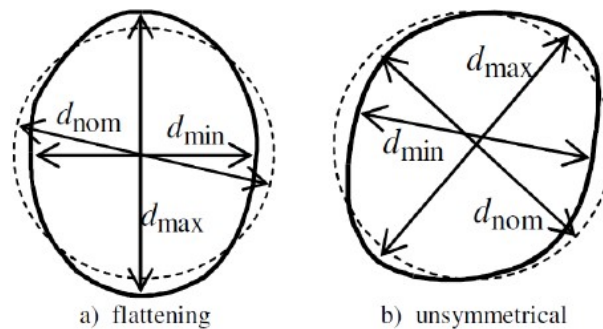
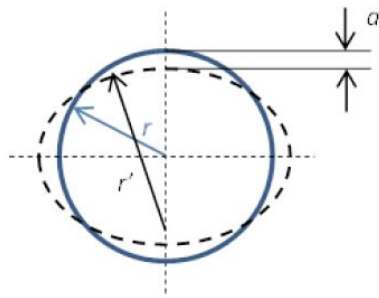


Figure 2.29: Measurement of diameters for assessment of out-of-roundness (EN1993-1-6, 2005).

The ovalisation deformation (a) at one side, as defined in Figure 2.30, can be calculated with Formula 2.31.





$$a = \frac{1}{4} U_r D \quad (2.31)$$

Figure 2.30: Ovalisation due to initial out-of-roundness.

### Tensile forces introduced by the secondary members

After placing the primary elements, the secondary elements are placed between them by driving them into the ground. These elements are connected with so-called interlocks, delivering the forces from the secondary elements to the primary elements.

### Pile drift

In theory the primary elements are driven vertically into the ground. In practice, however, this is never completely true. The piles often have a vertical aberration (pile drift) as well as a horizontal displacement due to the tolerances in the framework used to place them. In Figure 2.31 the possible situations are presented and the most unfavorable pile in this figure is pile number 5. Due to the aberration of piles 4 and 6, the tension forces on pile 5 will work on both sides and cause ovalisation of the tube. The horizontal displacement is assumed to be 20 mm due to some tolerances in the pile frame and the pile drift is estimated to be 0.5% due to tolerances in the vertical pile stand (BAAK, 2019).

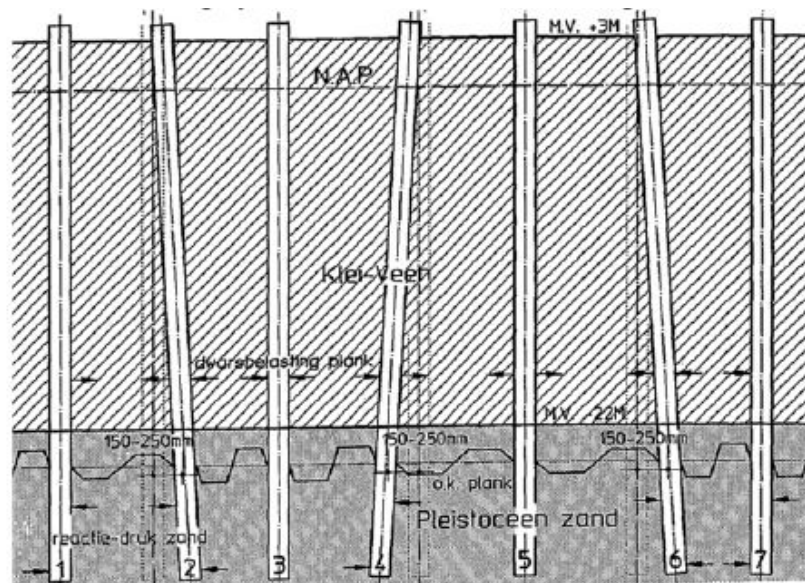


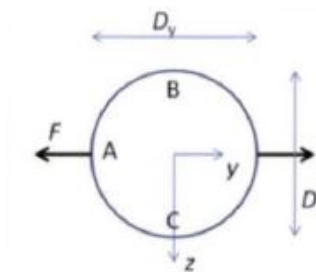
Figure 2.31: Possibilities of a aberration in the piles.

### Water pressures

In addition to the forces from aberration of the sheet piles, there are forces due to the water pressure. In the current case, above the underwater concrete floor this pressure exists only on one side of the wall, resulting in a deformed sheet pile. Beneath the underwater concrete floor, the pressures on both sides of the sheet piling are equal, and cancel each other out.

### Ovalisation

After determining the tensile forces due to pile drift and water pressures, the ovalisation can be calculated. Ovalisation due to forces from the secondary elements can be schematized by Figure 2.32. The change in ovalisation is given by  $\Delta D_z$  and described by Formula 2.32 (CUR211, 2014).

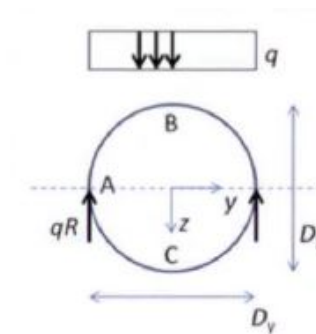


$$\Delta D_z = -\left(\frac{2}{\pi} - \frac{1}{2}\right) \cdot \frac{FR^3}{EI} \quad (2.32)$$

Figure 2.32: Case with tensile forces from secondary members (CUR211, 2014).

### Outside soil pressure

The soil pressures on the tube wall result in ovalisation of the walls. The water pressures acts on the pile and the sheetpiles directly and perpendicular. The perpendicular pressures on the tube wall do not cause ovalisation (CUR211, 2014). The ovalisation due to soil pressures can be calculated by the formula given in Equation 2.33.



$$\Delta D_z = -\frac{1}{12} \cdot \frac{qr^4}{EI} \quad (2.33)$$

Figure 2.33: Case with soil pressure on one side (CUR211, 2014).

### Brazier effect

Ovalisation as a second order effect of the tube's overall curvature has been studied by (Gresnigt, 1987) and is called the 'Brazier effect'. The formula for the ovalisation as a consequence of imposed curvature of the tube is:

$$a = \frac{\kappa^2 \cdot r^5}{t^2} \quad (2.34)$$

In which:

$$\kappa = \frac{M_{Ed}}{EI}$$

For curvature with meridional stresses beyond the yield limit this formula changes into:

$$a = \frac{\frac{\sigma_y}{E} \cdot \kappa \cdot r^4}{t^2} \quad (2.35)$$

## 2.4. Conclusion

The safety of a construction pit can be expressed by the difference between the loading and resistance of the pit. Out of the several design methods that are proposed, a level IV/III probabilistic method will be used in order to assess the safety of the pit. The required safety level for the construction pit can be calculated using the individual risk criteria, resulting in a limit value for the probability of failure. This value can then be translated to a reliability index for the pit.

The safety of the pit is of importance for the protection of the workers in the construction pit. As this risk only concerns a small amount of people and the location is fixed, the societal risk can be neglected. As for this study, the economic aspects are disregarded, the only risk left is the individual risk which will be evaluated in order to determine the accepted probability of failure.

Different approaches are proposed in order to estimate the collision force. It is found that the method stated in the Eurocode gives a good estimation for head-on collisions, but does not cover vessels colliding under an angle. For vessels colliding under an angle, three different methods are described. From the analysis it becomes clear that the method proposed by the ROK is the best applicable and suitable in case of ship collisions.

The construction pit will be made of combi-walls, and this type of structure has several failing mechanisms. Four different failure mechanisms are treated. As slender piles are subjective to local buckling failure, this is treated into detail. However, because of the significant influence of the membrane force of the intermediate sheet piling, in this thesis the CUR211E will be used, since this method includes the membrane forces in the checking of the tubular section.



## Case description - Blankenburg Connection

*This chapter provides the reader with additional information and details on the case. In Section 3.1 the Blankenburg Connection was introduced and a description of the basic situation was given. In Section 3.2 the details and dimensions of the case are given. In Section 3.3 the different collision scenarios are given, after which in Section 3.4 the possible consequences are listed. The chapter finalizes with the conclusion in Section 3.5.*

### 3.1. Project description

Despite the investments in roads and public transport in the recent years, it appears that the accessibility by road of the Rotterdam region, even with low economical growth, will face severe problems in 2020 (Rijkswaterstaat, 2015). To improve the accessibility of Rotterdam and the harbor in particular, it was decided to construct the Blankenburg connection (A24). This highway will connect the A20 and the A15 located west of the city of Rotterdam and it will increase the reliability of the road network around the city.



Figure 3.1: Location of the Blankenburg connection near Rotterdam. Image taken from [www.landenwater.nl](http://www.landenwater.nl).

The project covers the construction of several kilometers of highway, two tunnels, multiple bridges and connections. The total budget for the project amounts up to 1.1 billion euros, which makes it one of the bigger project in the Netherlands at the moment.

In Figure 3.2 the profile of the connection is shown, showing the two tunnels and the junctions with the A15 and the A20. The Hollandtunnel will be constructed as a 'cut-and-cover tunnel' made on land, while the Maasdelatunnel will be crossing the Scheur and an 'immersed tunnel' concept is used.

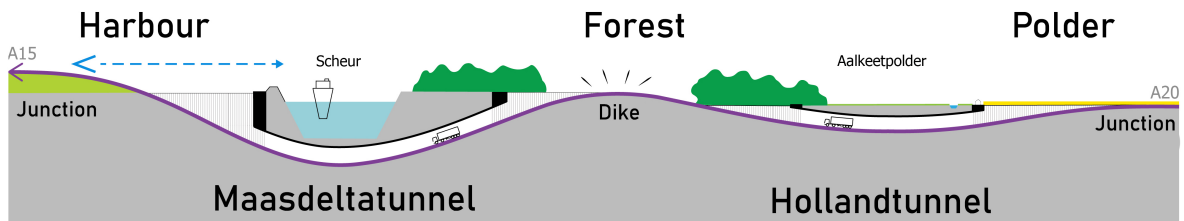


Figure 3.2: Blankenburg connection. Image adapted from wUrck.

### 3.1.1. Construction method

As can be seen in Figure 3.1 the new highway will have to cross a river, the Scheur to be exact. A waterway acts as a natural barrier and can be quite a challenge for engineers. In the case of the Blankenburg connection it is chosen to build a tunnel, the Maasdelatunnel, using the immersed tunnel construction method. This method consist of one or multiple tunnel elements which are built in a dry dock. After completion of the element, it is temporarily sealed off and floated to the project location where it is immersed into a dredged trench. Examples of tunnels built using this method can be found everywhere in the world, the first of which was completed in 1930 (Tunnel, 2018).



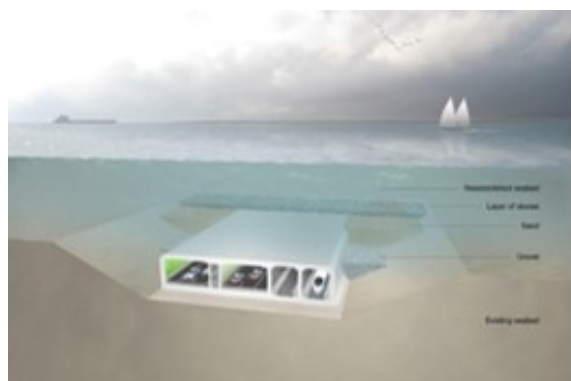
(a) Construction of the tunnel element. Photo by Doka.



(b) Transportation of the tunnel element. Photo by DIMCO.



(c) Immersion of the tunnel element. Image by RambolGroup.



(d) Finishing of the tunnel. Image by RambolGroup

Figure 3.3: The construction of an immersed tunnel.

In order to minimize the number of tunnel elements which have to be immersed, BAAK has decided to extend the construction pits from the banks towards the edge of the shipping lane. In this way, the distance between the banks will decrease, resulting in a lower amount of tunnel elements to be immersed (see Figure 3.4). The tunnel will exist of 2 elements each 200 meters long, one constructed on each side of the Scheur. After construction of the elements, the construction pits are flooded and the elements will be floated to their final location where they are immersed.

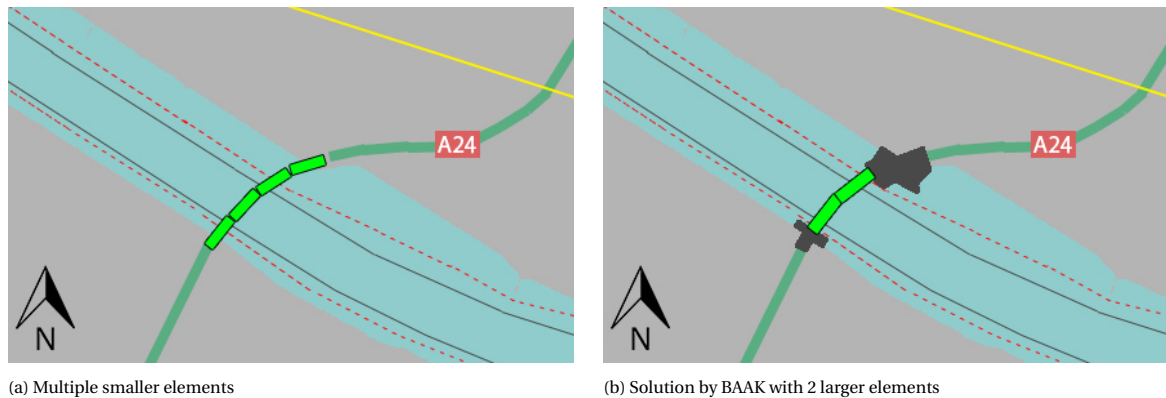


Figure 3.4: Different tunnel element sizing

In Figure 3.5 an artist impression of the construction method is given. The element that will be floated to the middle of the Scheur is given in gray, whereas the tunnel itself is indicated in brown. As can be seen from this figure, the element is built on top of the tunnel.

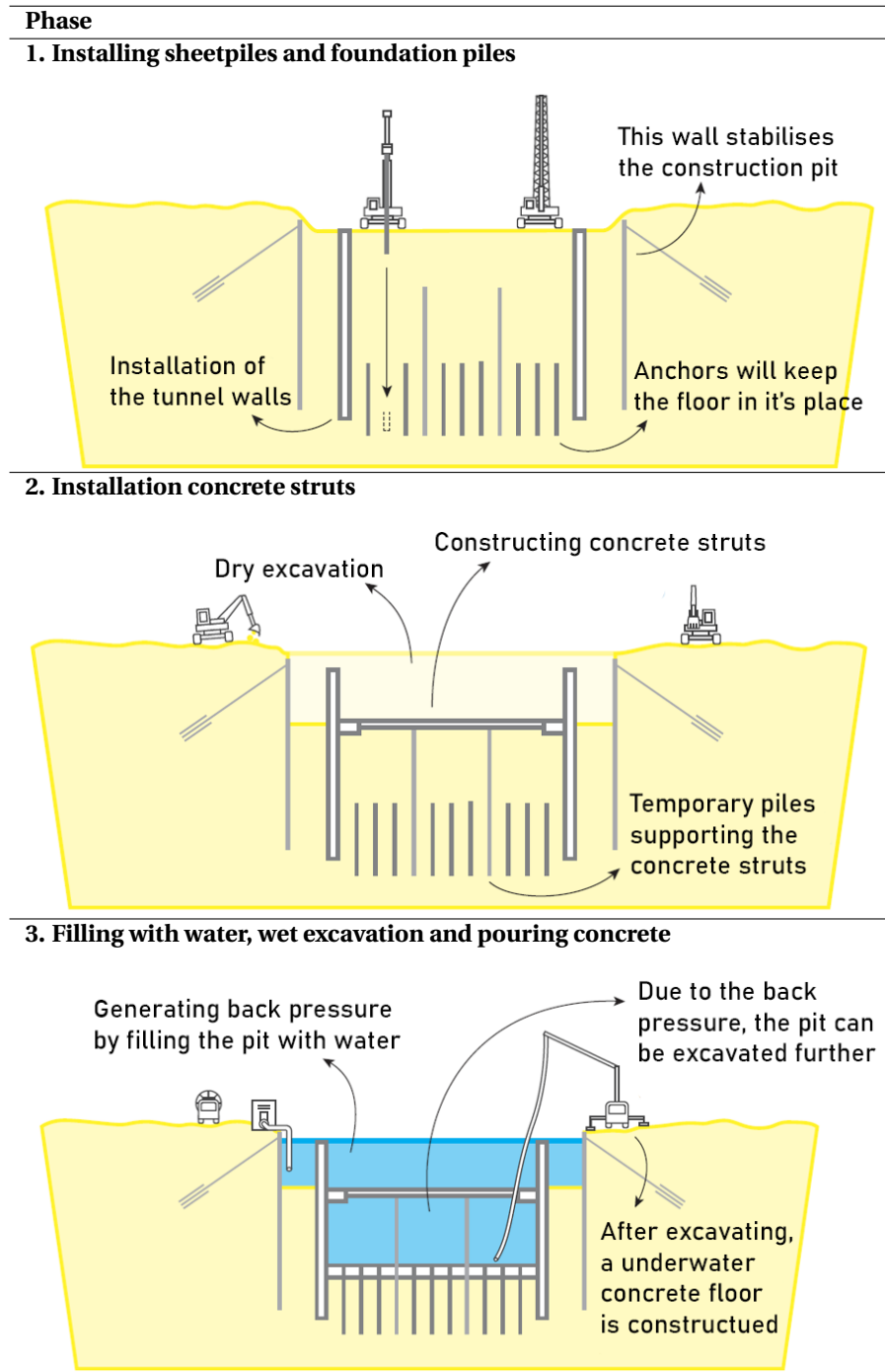


Figure 3.5: Construction of the cofferdams on the North side with the tunnel placement indicated. Adapted from BAAK.

### 3.1.2. Project phases

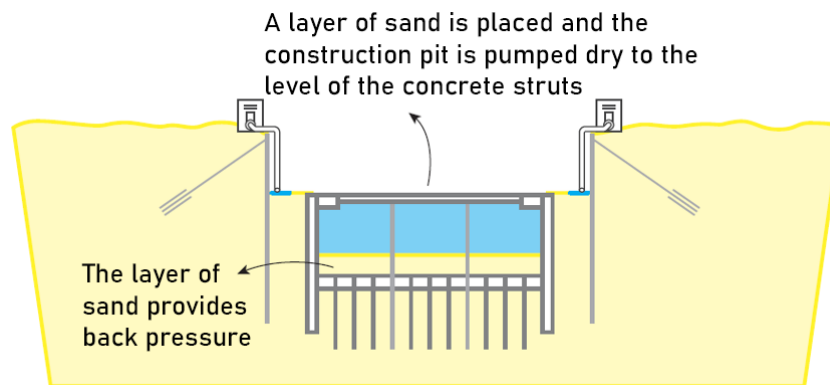
The total project duration is planned to be 6 years, in which several phases or situations can be discerned. In these phases the consequences of a ship collision will be different, depending on the lay-out of the structure. In Table 3.1 the different phases are given.

Table 3.1: The different phases of the project. Images adapted from BAAK.

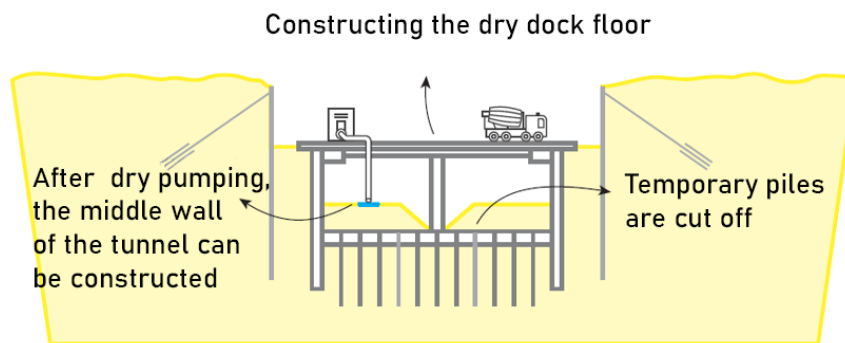




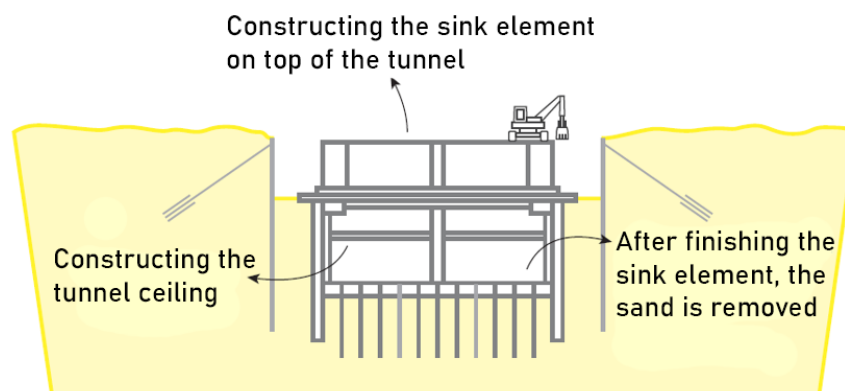
#### 4. Dry pumping



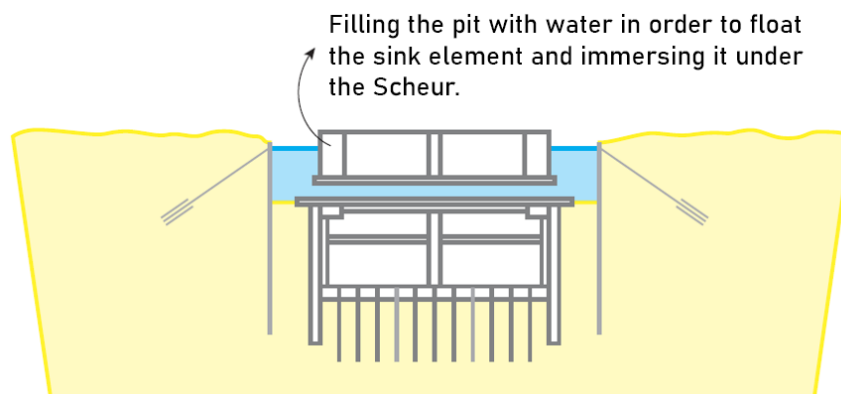
#### 5. Construction of dry dock floor and dry pumping



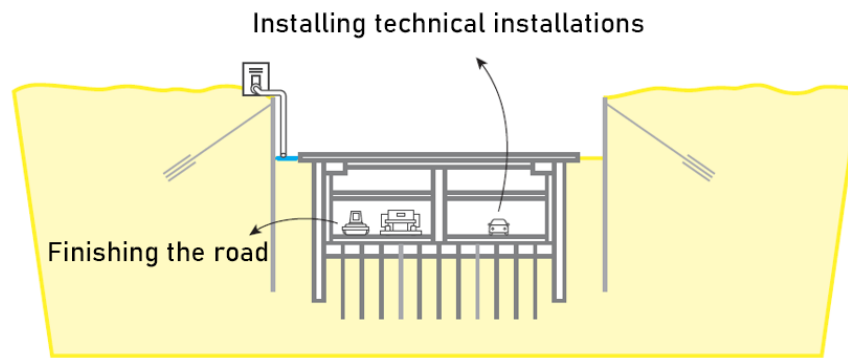
#### 6. Construction of the tunnel element and finishing ramp



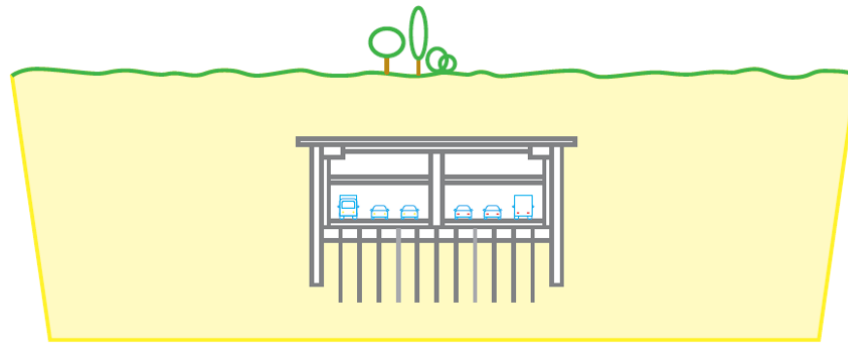
#### 7. Immersion of the tunnel element



---

**8. Finishing tunnel**

---

**9. Tunnel is ready for usage**

### 3.2. Construction site

In order to construct the tunnel and its elements, two construction sites will be made. One located at the south side of the channel and one at the north side. As can be seen in Figure 3.6, these sites are partly located into the water.

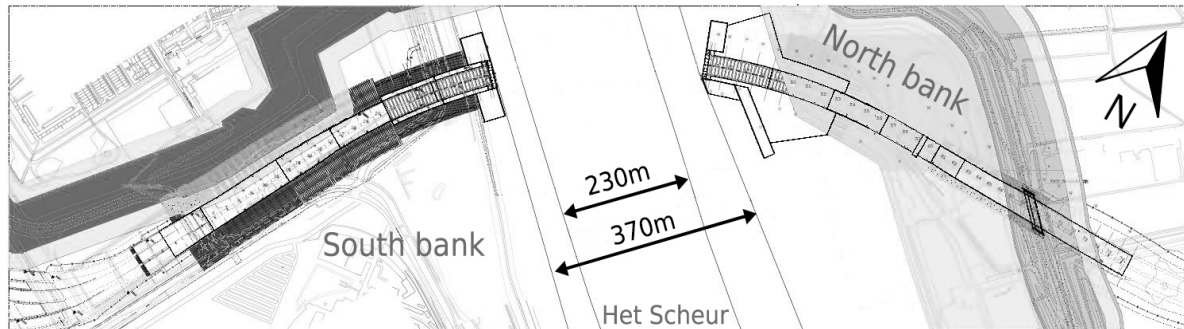


Figure 3.6: Location of the construction sites in the Scheur

In the design by BAAK the construction pit is used twice. First the permanent part of the tunnel will be constructed using a cut-and-cover method. Above the part of the tunnel that is siding the river, a temporary dry dock floor is constructed at which the tunnel element will be realized. This element will later in the process be floated into the channel and then immersed into position (see Figure 3.7 for clarification).

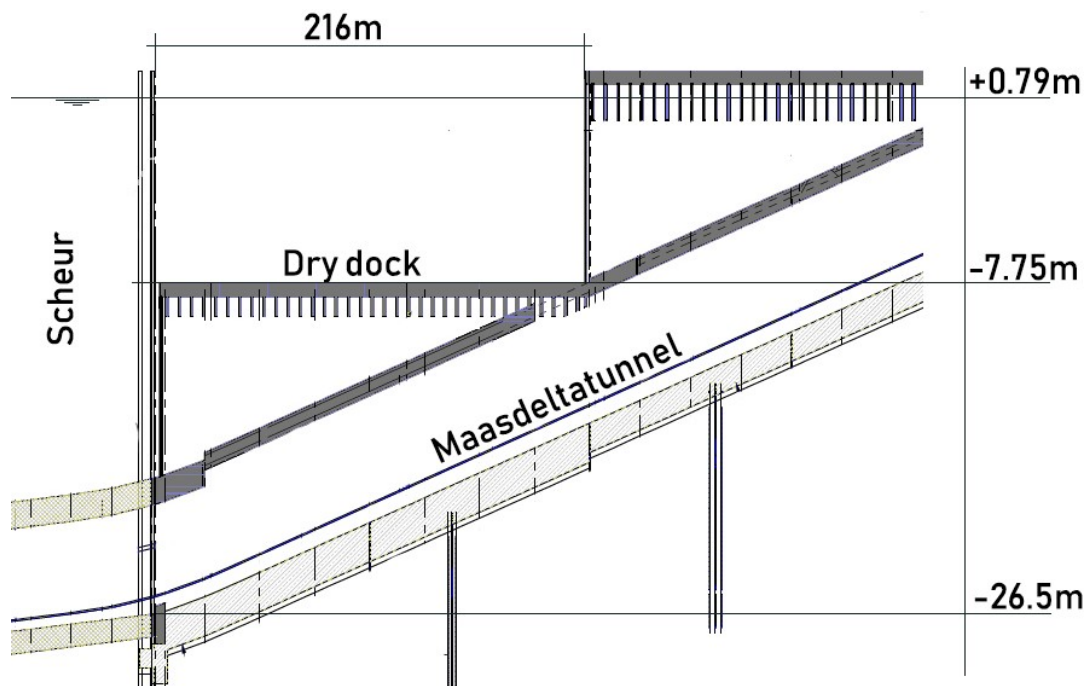


Figure 3.7: Construction principle of the Maasdeltatunnel with a dry dock constructed inside the construction pit (North side). Figure adapted from BAAK and not to scale.

Both the construction sites, at the south and at the north bank, will consist of multiple cofferdams and combi-walls. An overview of the site located at the south side is given in Figure 3.8. The construction site at the north bank is a little bit different in size and orientation, but the construction principle is the same.

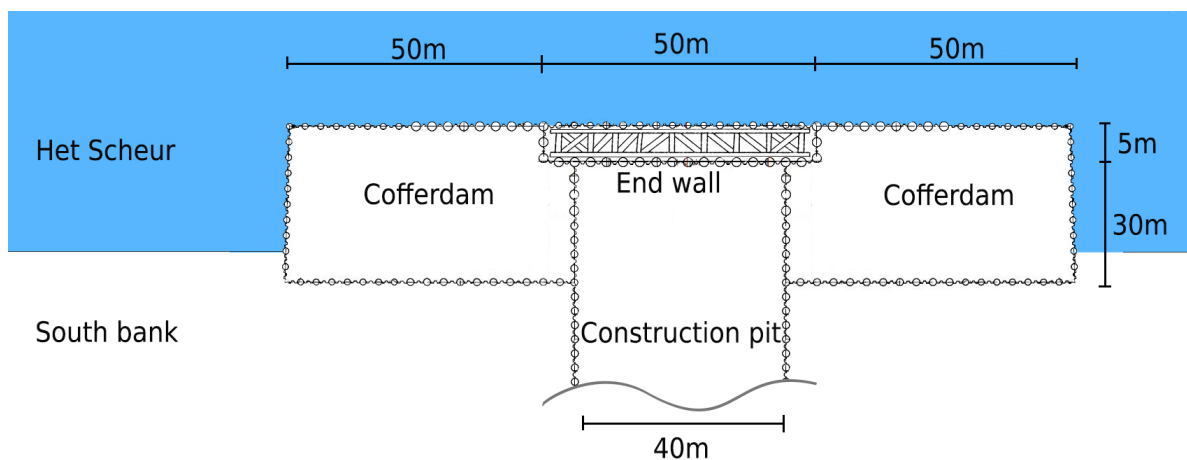


Figure 3.8: Plan view of the construction site at the south bank.

### 3.2.1. Components of the construction pit

The design in Figure 3.8 consist of a framework, multiple cofferdams, combi-walls and an end-wall consisting of a double combi-wall. The underlying concepts for these design choices are important to understand the design. Therefore the different components and their function will be described briefly.

#### Cofferdams

Cofferdams are temporary enclosures constructed in a water body to be able to drain the enclosed area. Cofferdams are often filled with sand and drained. The main function of the cofferdams on both sides of the construction pit is to provide stability and water tightness. When excavating the pit and draining the water, the walls of the pit should be able to withstand the soil and water pressures acting on the walls. As this particular pit is quite deep, it might come in handy to drain the cofferdams as well, so that the inside walls only have a soil pressure.

A second function of these dams is collision protection. The cofferdams extend a distance of approximately 30 meters into the channel and the chance that a vessel collides with the structure is real. The cofferdams will be filled with granular material and will therefore act as rigid structure, protecting the sides of the construction pit.

Besides these primary functions, the cofferdams also provide space for equipment, cranes and (un-)loading of material. The functions of these cofferdams can be summarized as follows:

- Stability of the soil surrounding the pit
- Protecting the sides of the construction pit from collision
- Storage and placing of equipment

### Double end-wall and framework

The end wall in the design made by BAAK consists of a double combi wall, as can be seen in Figures 3.8 and 3.9. The reason why there is no cofferdam in this place, is because of the 'gate' function of this part of the construction. The end wall has to be easy to remove as the tunnel element will be floated out trough this opening.



Figure 3.9: Construction of the end wall including framework. Photos by BAAK.

During construction of the tunnel, the main function of this wall is retaining water and soil pressures. As the construction pit will be excavated to a depth of 26.5 meters, the walls should be able to retain the forces from the water and soil column. The second wall is placed in order to be able to inspect the inner wall on both sides regarding water tightness.

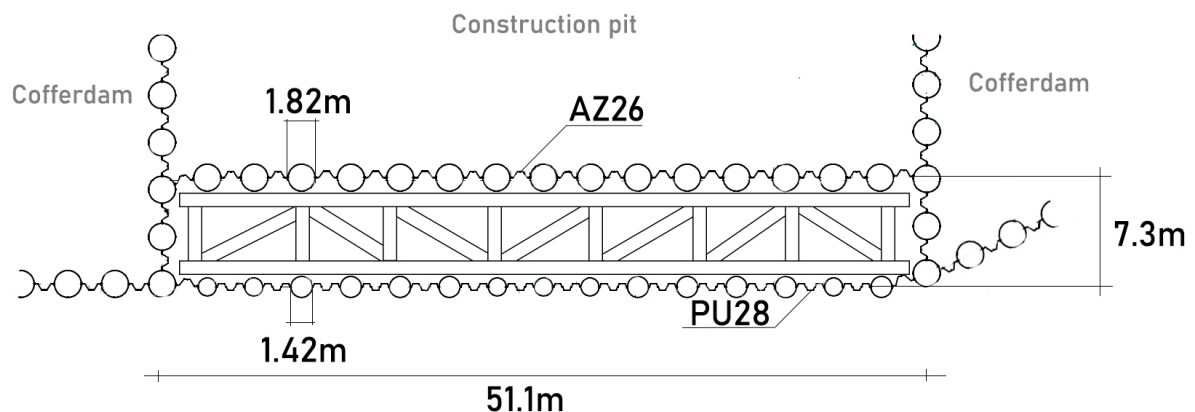


Figure 3.10: Dimensions of the end wall at the north side of the Scheur. Adapted from BAAK.

Additionally, the end-wall has a protective function against colliding vessels. The end-wall is parallel to the shipping lane and therefore the chance it gets hit is lower than for the cofferdams. However, the construction is less rigid and failure may result in severe consequences. A second wall is placed behind the primary one, to prevent the pit from flooding when a minor collision occurs. The framework which is present in the design, is intended to give stability to the outer combi wall. Through this framework the forces are led into the structure and forces are distributed. This is mainly intended in the case of high loads, as will occur during a collision.

The functions of this end-wall can then be summarized as follows:

- Retain water and soil
- Protect construction site from vessels
- Protect construction site from flooding
- Provide a bridge to each cofferdam

### 3.2.2. Design of the end-wall

The end-wall is made of heavy tubular piles with different diameters. The outer combi-wall is made up out of tubular piles with a diameter of 1.42 meters, connecting them with PU28 sheet piling. The inner wall is made out of tubular piles with a diameter of 1.82 meters. The sheet piles connecting them are of the AZ26 type.

The main difference between these two types of sheet piling is the allowance of stress free deformation. AZ26 profiles are able to rotate in the interlocking as the hinges are not aligned in the same plane (Figure 3.11). In the case of PU28 sheet piling, all the locks are aligned and stress free rotation of the sheet piles is not possible (Figure 3.12).

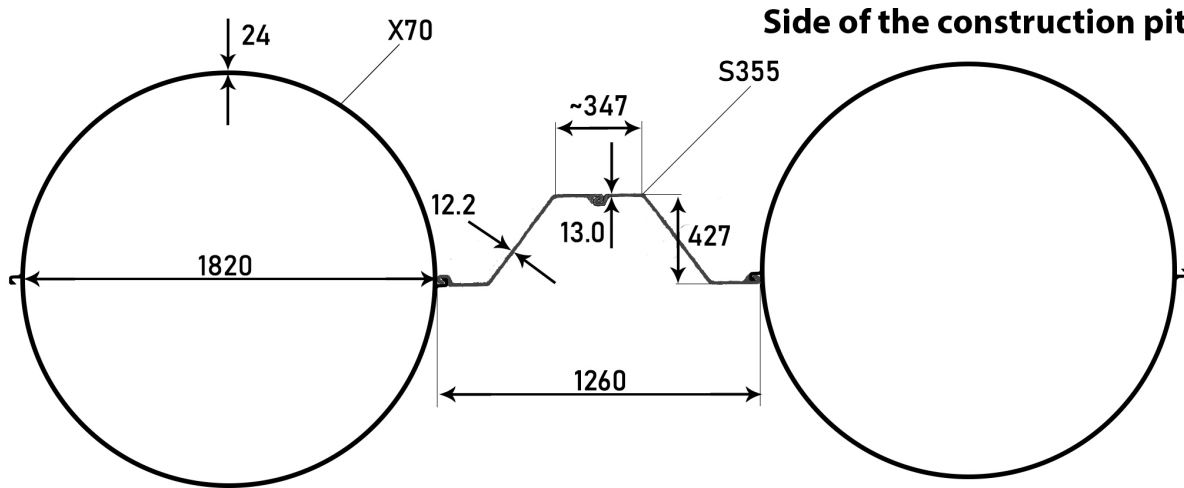


Figure 3.11: Combi wall of tubular piles with AZ26 sheet piling.

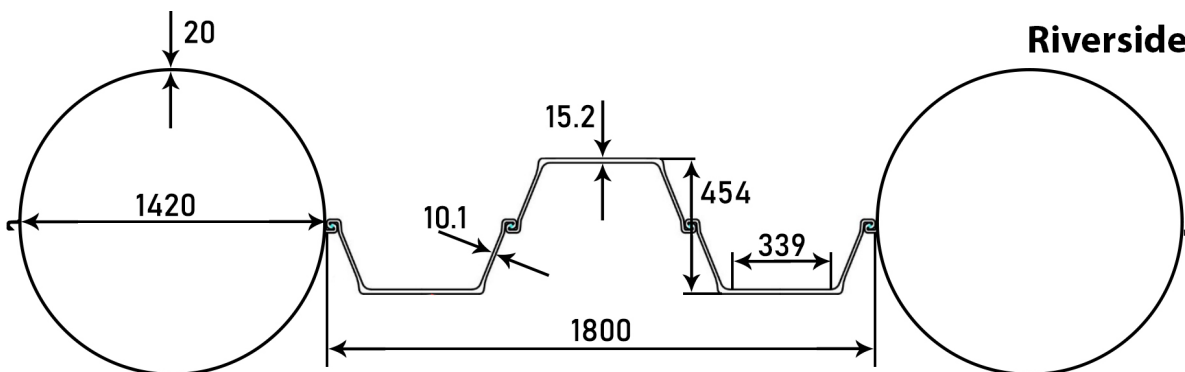


Figure 3.12: Combi wall of tubular piles with PU28 sheet piling.

For further details about the combi-walls and interlocking, see Chapter 6.

### 3.3. Collision scenarios

For the case of the Maasdelatunnel it is unknown what the probability of a collision is. A couple of different scenarios in which the end-wall is struck by a vessel will be described in order to give some insight into the problem and the range of possible collisions.

#### Evasive maneuver

A ship has to perform an evasive maneuver in order to prevent collision with another ship and is unable to change its course in time to prevent collision with the structure. In such cases the captain of the ship will most likely try to decrease the velocity and the angle of impact will be small, see Figure 3.13 for an illustration of the situation.

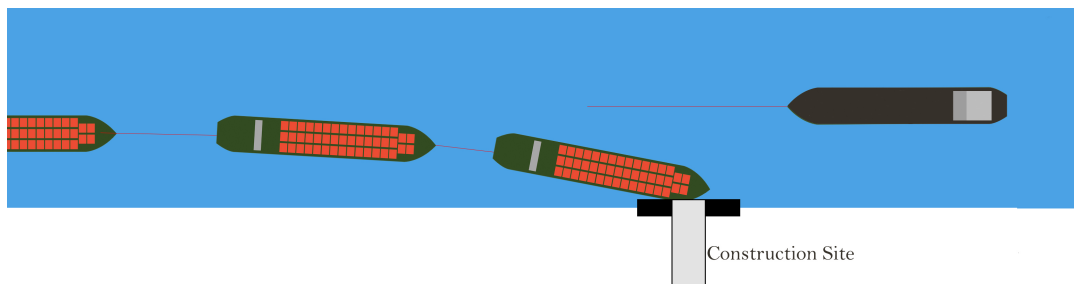


Figure 3.13: Scenario 1 - Evasive maneuver

#### Traffic intensity

In this scenario the traffic situation or intensity is such that a ship does not have enough space to maneuver. This can be caused by different aspects, such as the velocity, the maneuverability, weather circumstances, level of experience of the navigator, underkeel clearance and several other factors. The ship will collide sideways to the structure, as can be seen in Figure 3.14.

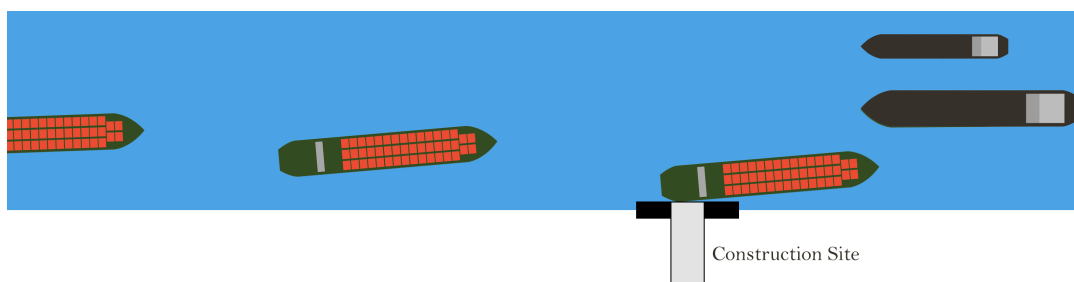


Figure 3.14: Scenario 2 - Traffic intensity

#### Tug assistance

This scenario is only valid for the bigger and seagoing ships. Inland going ships usually don't need tug assistance. When a ship with tug assistance loses one of the tugs, the ship can drift out of course and hit the structure. The velocities will be low and the impact will be partly sideways to the structure.

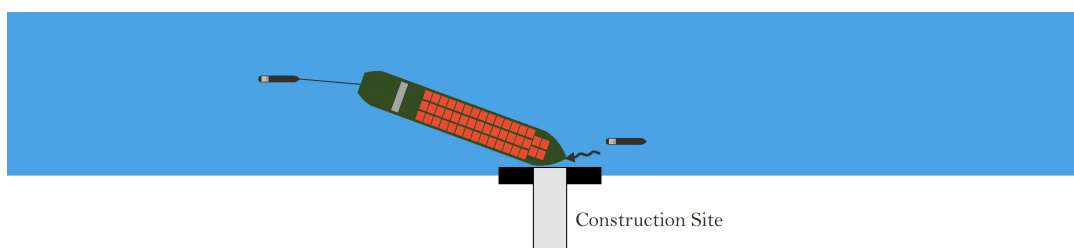


Figure 3.15: Scenario 3 - Tug assistance

### Human failure

Due to the fact that the captain of the ship is not present, not paying attention or sleeping, the ship wanders off course and hits the structure. This is less likely to happen with seagoing ships, as there are usually more people on the bridge who can intervene and correct mistakes from other crew members. For inland going ships this is often not the case and the captain could fall asleep and lose control of the ship.

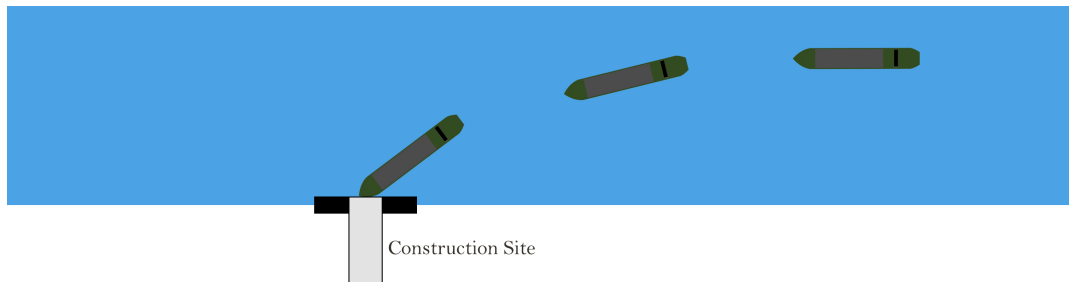


Figure 3.16: Scenario 4 - Human failure

### Local bathymetry and conditions

Due to the presence of the construction site and the dredging or dumping of material, the bathymetry may be influenced in such a way that ships experience unexpected currents. In combination with local winds, this could lead to collision with the structure, as can be seen in Figure 3.17.

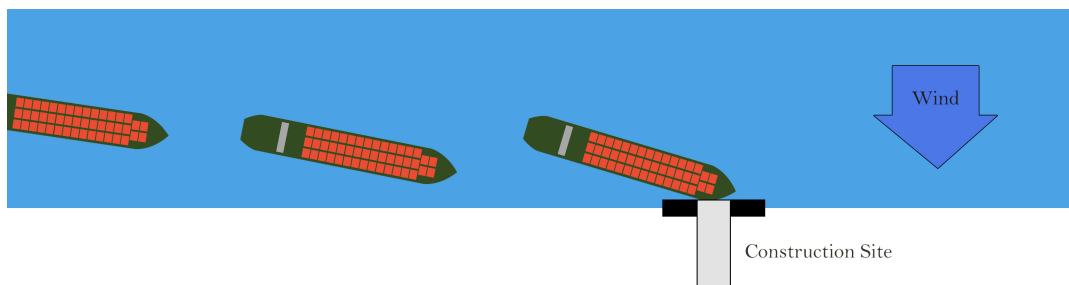


Figure 3.17: Scenario 5 - Local bathymetry and conditions

### Technical problem or error

A ship has technical problem or error and drifts off course. In this scenario it is assumed that the event of rudder failure and engine failure will not happen at the same time. This will result in two sub scenarios, one in which the velocity will be normal and the angle of impact small, and one in which the velocity will be low and the angle of impact big.

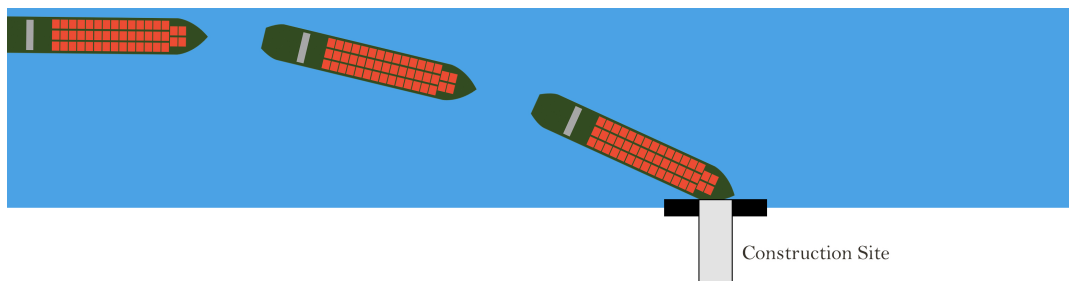


Figure 3.18: Scenario 6 - Technical problem or error



### 3.4. Consequences of a ship collision

The consequences of a ship collision can be related to the different phases of the project, as the direct consequences are, for example, dependent on the amount of work done and the amount of workers present at the construction site. For a detailed description of the project phases, see Section 3.1.2. In Table 3.2 the phases of the project are classified into three different consequences classes: Minor, Medium and Major. The classification is briefly explained in the table.

Table 3.2: Consequences of failure of a ship collision.

Classification	Phases (#)	Description of the consequences
Minor	<p>① Installation of the tunnel walls. This wall stabilises the construction pit. Anchors will keep the floor in its place.</p> <p>② Dry excavation. Constructing concrete struts. Temporary piles supporting the concrete struts.</p> <p>③ Generating back pressure by filling the pit with water. Due to the back pressure, the pit can be excavated further. After excavating, an underwater concrete floor is constructed.</p> <p>④ Installing technical installations. Finishing the road.</p> <p>⑤</p> <p>⑥</p> <p>⑦</p> <p>⑧</p> <p>⑨</p>	<p>During these phases there will be water on both sides of the end-wall or most of the construction works are already finished. No workers are working below the waterline and the consequences of a collision and possible failure of the end-wall during these phases, are therefore mainly deformation of the already build structure, the colliding vessel and potentially some injuries of workers working on the vessel or on top of the structure.</p>
Medium	<p>④ A layer of sand is placed and the construction pit is pumped dry to the level of the concrete struts. The layer of sand provides back pressure.</p> <p>⑦ Filling the pit with water in order to float the sink element and immersing it under the Scheur.</p>	<p>During these phases no workers will be present in the construction pit. However, the financial consequences can be big, as the tunnel element can be hit and damaged, and repairs may be expensive.</p>
Major	<p>⑤ After dry pumping the middle wall of the tunnel can be constructed. Constructing the dry dock floor. Temporary piles are cut off.</p> <p>⑥ Constructing the sink element on top of the tunnel. Constructing the tunnel ceiling. After finishing the sink element, the sand is removed.</p>	<p>After dredging and draining the pit, the construction of the tunnel element on the bottom of the pit can start. In these phases several workers will work at a level of approximately -26m NAP and at the dry dock floor. When the end-wall fails during this phase, it is assumed that the workers will have not enough time to get themselves to safety, as the pit will be flooded in a small amount of time. The consequences are deformation of the vessel and structure, loss of equipment and above all: loss of human life.</p>

### 3.5. Conclusion

During the construction of the Maasdeltatunnel a construction pit will be made which is partly located in the Scheur (see Figure 3.5). Vessels sailing by might hit the structure which then can endanger the safety of the construction pit, leading to unacceptable consequences. However, several parameters and aspects are still unknown and should be assessed.

The first aspect that is unknown is the probability of a vessel collision at the Scheur. From the scenarios it becomes clear that there are several causes that can lead to a collision on the structure. Out of historical data an estimate of the probability can be made, giving a general number for the probability of a collision. However, the influence of different parameters (i.e. pilot presence) is still unknown, making it difficult for the company to decide which measures to implement in order to reduce the probability of a collision.

Based on the classification of the different phases in consequences classes, the governing phases (5 & 6) are taken as a basis for this thesis.

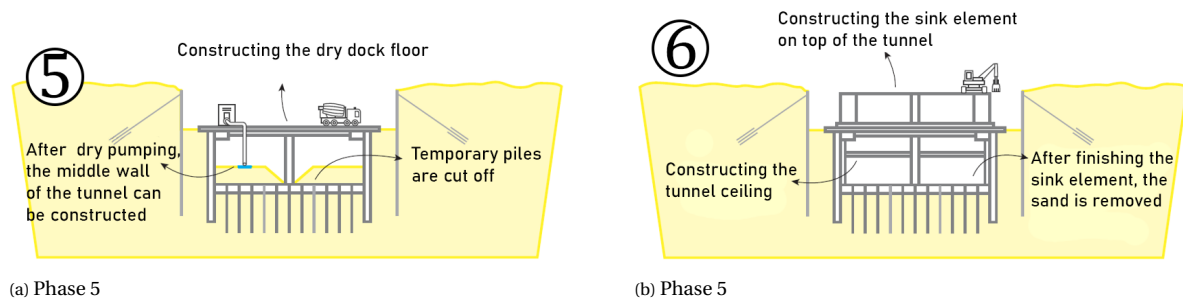


Figure 3.19: Governing construction phases.

Finally, in the design by BAAK a double end-wall is constructed at the head of the construction pit, see Figure 3.20. The second wall is considered as a sacrificial wall in order to withstand potential ship collisions. As the probability of the collision and the magnitude of the force are unknown or uncertain, it is uncertain if the double end-wall is a conservative design or the perfect solution.

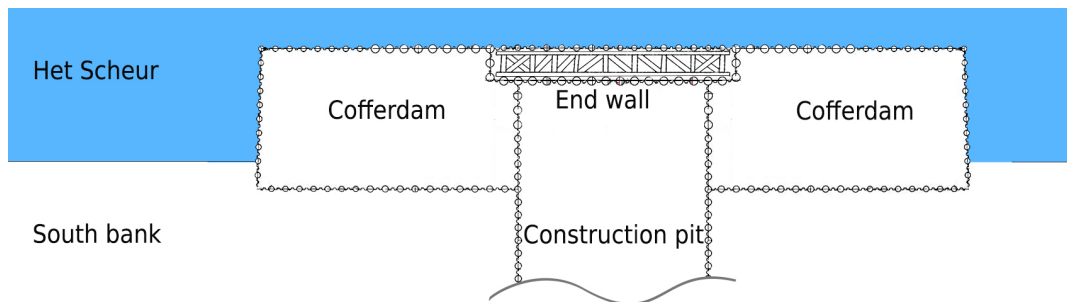


Figure 3.20: Design by BAAK of the construction pit at the South bank.

# 4

## The probability of a collision

*In this chapter the probability of a collision is described using a Bayesian belief network. In Section 4.1 the existing models are introduced and described after which in Section 4.2 the new model is constructed. In Section 4.3 the results of the model are presented and compared with historical data. Section 4.4 closes the chapter with some conclusions.*

### 4.1. Bayesian networks

A method to include all the parameters described in Section 2.2.3, is the use of a Bayesian Network. In a Bayesian Network one defines nodes (events) and edges (relations), which are conditionally dependent on each other. Often this is an acyclic directed graph (DAG), which means that the 'parent' node only influence the 'child' node and not the other way around.

The popularity of Bayesian Networks as a method to describe complex events, has increased over the last decade. However, before a Bayesian Network can be defined, first some basic concepts of probability theory have to be introduced. These definitions are adapted from [Koller and Friedman \(2009\)](#) and are given in Appendix B.

#### 4.1.1. Collision model for the Scheur

When looking at human failure regarding ship collisions, a whole set of parameters is of influence on the final event. All these parameters can be represented by nodes in the network, having a (conditional) probability of occurrence. In order to say something about the underlying relationships between parameters, data analysis should be done or experts should be consulted.

For the Finnish Gulf multiple studies and data analyses have been carried out, and several models, all employing the Bayesian network, have been produced that give insight in the conditional probabilities of several parameters. The network created in this study is based on the data obtained for the Finnish Gulf and the Baltic Sea (based on the work of [Hänninen and Kujala \(2012\)](#), [DNV \(2005\)](#) and [Mazaheri et al. \(2016\)](#)). However, it should be noted that the Finnish Gulf and the Baltic Sea are different from the Scheur in several ways. Therefore, in the next sections the parameters are studied and adapted to make the model appropriate for conditions at the Scheur.

#### 4.1.2. Existing collision models

During the last three decades, several techniques have been developed for the quantitative study of human reliability. In the 1980s, techniques were developed to model systems by means of binary trees, which did not allow for the representation of the context in which human actions occur. Thus, these techniques cannot model the representation of individuals, their interrelationships, and the dynamics of a system. These issues made the improvement of methods for Human Reliability Analysis (HRA) a pressing need ([Martins and Maturana, 2013](#)).

In 2005 the Det Norske Veritas did a Formal Safety Assessment in order to estimate the cost-effectiveness of Electronic Chart Display and Information System (ECDIS) as a risk control option to reduce the grounding risk for vessels in the Finnish Gulf (DNV, 2005). The model, a Bayesian network, is based on parameters determined for large seagoing passenger vessels in earlier work and a extensive model with 69 nodes and 107 edges is presented.

Another model was made by Hänninen and Kujala (2012). This model describes the collision risk for vessel-vessel collisions in the Finnish Gulf and determines the influence of the different parameters on the model. Even though a collision with a static object is somewhat different, the actions on the vessel and the human interactions described by the model can be the same.

Based on the work of DNV (2005), another model was constructed by Mazaheri et al. (2016) in order to estimate the grounding of vessels in the Finnish Gulf even better. Most risk models for ship-grounding accidents use accident statistics and expert opinions as a basis for their model. The major issue with such kind of models is their limitation in supporting the process of risk-management with respect to grounding accidents, since they do not reflect the reality to the extent required (Mazaheri et al., 2016).

Also in other domains one can find Bayesian Networks being used as a tool to describe human interactions and failures. Wang et al. (2013) made use of a Bayesian Network to estimate the fatalities when a collision occurs, Ancel et al. (2015) gives some insight in the aviation and de Oña et al. (2011) uses a network to describe traffic injury severity. In Table 4.1 six different kinds of Bayesian Networks are listed and the amount of nodes, edges and their domain is given.

Table 4.1: Existing BBN models for ship-grounding accidents detected in the literature analysis and comparable BBN models in other domains.

Source	Nodes	Edges	Domain
Mazaheri et al. (2016)	33	49	Transportation/maritime/grounding
DNV (2005)	69	107	Transportation/maritime/grounding
Hänninen and Kujala (2012)	75	136	Transportation/maritime/collision
Wang et al. (2013)	16	27	Transportation/maritime/collision-fatalities
Ancel et al. (2015)	62	85	Transportation/aviation
de Oña et al. (2011)	18	30	Transportation/road

In this thesis the works of Mazaheri et al. (2016), DNV (2005) and Hänninen and Kujala (2012) are used to construct a new Bayesian Network for the case of the Blankenburg Connection.

#### 4.1.3. Overview of the existing model

The structure which will be used in this thesis as basis for the model, is the model structure used by Mazaheri in 2016. This model gives results in the same order of magnitude as the other models, is quite easy to use and is based on the other studies as well. The model is constructed of 32 nodes, describing the processes that are assumed to have influence on the probability of a collision.

The factors in this model can be listed as follows:

- Adequate alarm
- Authority gradient
- Being of course
- Bridge design
- BRM
- Collision
- Communication, cooperation, monitoring
- Competence
- Cumulated tasks
- Detection
- Incapacitated
- Lack of training
- Location
- Loss of control
- Maintenance routine
- Manning
- Metreological condtions
- Navigation method
- Navigational Error
- Pilot presence

- Pilot vigilance
- Safety culture
- Season
- Signal quality
- Situational awareness
- Sudden Situational Change
- Technical Failure
- Technical Redundancy
- Traffic distribution
- Type of Ship
- Visibility
- Voyage preparation
- VTS
- Waterway complexity

Now it is important to determine which parameters will have to be changed when looking at the Scheur conditions. Also, it should be checked if some parameters that are relevant for the Scheur should be added to the model.

#### Model structure

The complete Bayesian Belief Model which is constructed by Mahazeri is calculated using software called GeNIe, developed by BayesFusion. The model and its mutual relations are given in Figure 4.1.

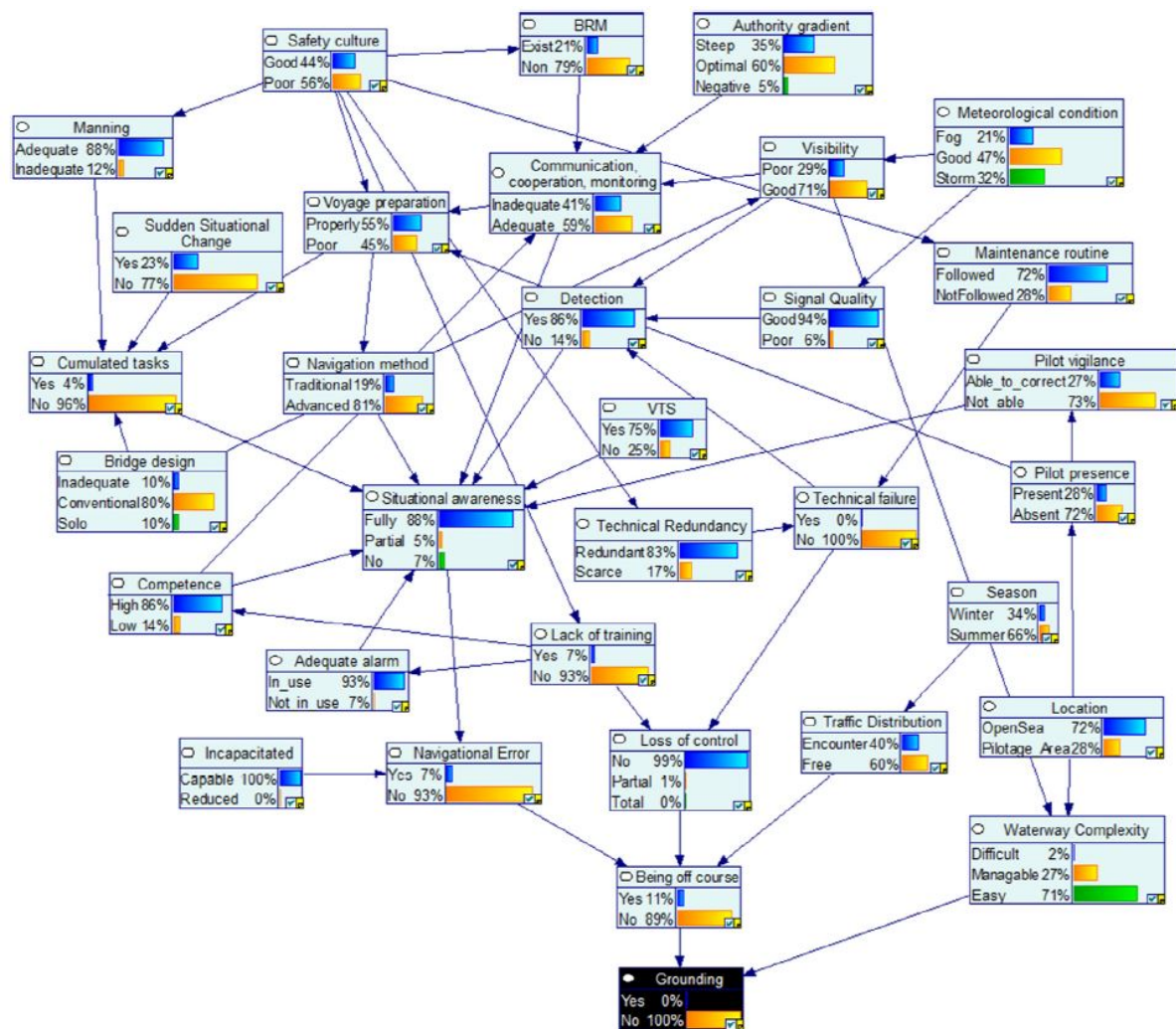


Figure 4.1: Bayesian belief network for ship grounding in the Finnish Gulf (Mazaheri et al., 2016)

#### 4.1.4. Adaptations to implement the model at the Scheur

In order to use the model, it should be adapted to the local conditions at the Scheur. To do so, it is important to map out all the similarities and differences between the two Bayesian Networks.

### Collision (or grounding)

One difference that immediately stands out, is the end node of the system. In the existing model the final node is the event of grounding and this is similar to the case of the Blankenburg Connection, in which the collision with the structure is of interest. Although this may seem to be a significant difference, it can be argued that placing a temporary construction in a water body, can be compared to sand banks and rocks in a sea.

One of the causes in the event of groundings is, that the crew of a vessel is often unaware of their precise location and the neighborhood of sand banks and rocks. Due to the lack of knowledge and wrong interpretation of systems, this can result in groundings. When comparing this to the situation in the Scheur, one could say that placing temporary structures in the river may result in a similar situation in which the crew could be unaware of the new situation. As the width and depth of the channel is now limited, a collision event is assumed to be similar to a grounding event on one of the banks.

### Waterway complexity

Another difference is the dimensions of the water body on which the vessel is sailing. The Finnish Gulf is a narrow sea, but in comparison with the Scheur, still a very large and broad sea. However, groundings often occur near the shore and in approach channels to harbors, such that a comparison is not completely off (see Figure 4.2). Therefore the node called 'Waterway Complexity' in Mazaheri's model should be reviewed and the Scheur should be classified as one of the states given in the model (Difficult/Manageable/Easy) based on the Waterway Complexity Index (WCI) (Mazaheri et al., 2015).

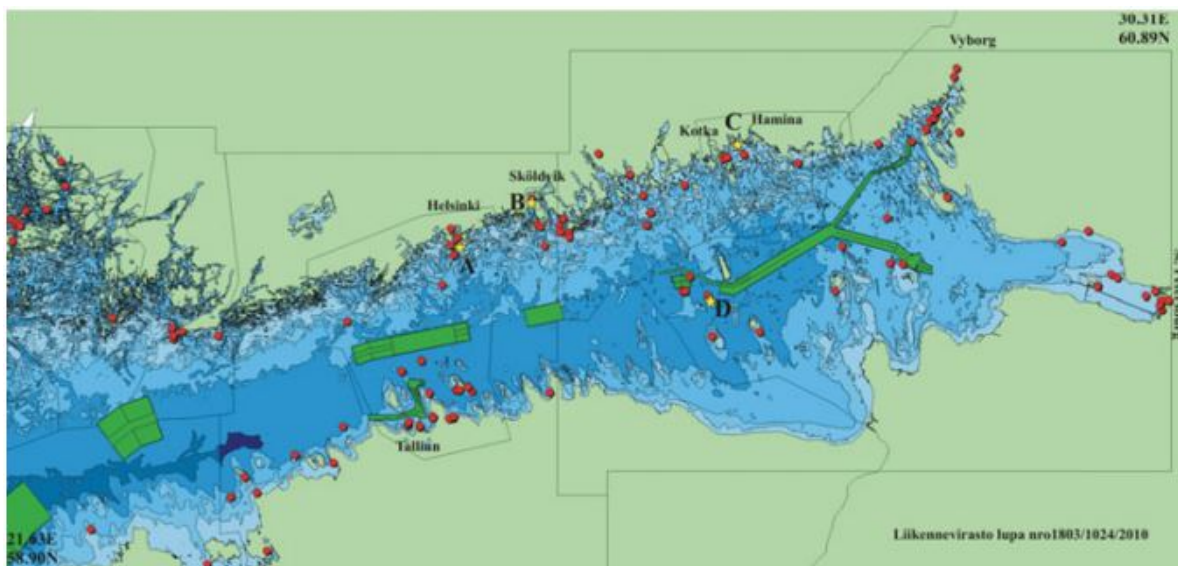


Figure 4.2: Grounding accidents happening in the Gulf of Finland (1989–2010) shown in red dots (Mazaheri et al., 2015)

### Type of vessel

A third difference can be found in the type of vessels reviewed. In the case of Mazaheri, only sea-going vessels were taken into account. However, at the Scheur a large proportion of the fleet are inland going vessels. Besides the difference in size and weight, inland going vessels often have different regimes and systems on board resulting in higher probabilities of collision for these types of vessels.

### Meteorological conditions

Due to the location of the Finnish Gulf the weather conditions are different from the conditions in The Netherlands. The Gulf of Finland is often frozen in winter time, which affects the amount of shipping and the probability of encountering traffic. As the Scheur is located in a different climate area and is also the entrance channel of the port of Rotterdam, it is assumed that this will be kept open at all times. The conditional probabilities of the node should be adapted to the relevant values based on appropriate data.

### Pilot presence

In the model for the Finnish Gulf the presence of a pilot is dependent on the location of the vessel. However, in the port area of Rotterdam, seagoing vessels can not call on the port without a pilot (although there are some exemptions). On the other hand, inland going vessels calling port in Rotterdam do not use pilot guidance. So the presence of a pilot on-board a vessel at the Scheur, is not dependent on the location, but rather on the vessel type.

### Assumptions in adapting the model:

- The structure of the model is kept the same.
- Parameters relating to human (inter)actions at the Scheur are the same as in the Finnish Gulf.
- Parameters related to the surroundings, weather, waterway and ship distribution are adapted to the Scheur conditions using data and engineering judgment.

## 4.2. Setting up the new model

After discerning the points on which to adapt the model of the Finnish Gulf to also fit the Scheur, the model for the Scheur can be constructed. The nodes and conditional probabilities that will have to change in this new model require some background and explanation. The rest of the nodes are described in Appendix C and will be treated into detail.

### 4.2.1. Waterway complexity

In order to rank the Scheur in the same way as the waterways in the research of Mazaheri et al. (2015), there are two options. The first option is to rely on expert opinions (local pilots) and to rate the waterway in the same way they did in the research. The pilots mainly based their judgment on:

- Ship draught and size in relation to the available space.
- The need for reduction of ship speed under certain circumstances, e.g. in the presence of two-way traffic.
- Width of the waterway, especially when two-way traffic is allowed.
- Number of turns and the magnitude of course alteration.
- The width of the waterway immediately following the turn.
- Fairway marking, especially in the areas which require increased attention of a pilot, e.g. due to significant course alteration.

As local Dutch pilots may rate the waterway different from the Finnish pilots, the ratings will be difficult to compare. Therefore this option is discarded and an estimate of the WCI is made based on statistics. For both waterways the number of grounding events are known and the frequency of grounding/collision can be compared.

#### Actual accidents at the Nieuwe Waterweg

The port of Rotterdam keeps record of all accidents on the water around the port. In the case of the Nieuwe Waterweg, data is available for the period of 2012-2017 and a total of 329 accidents are registered. These accidents occurred in a 24km long stretch of the Nieuwe Waterweg (including the Scheur), close to the construction site. Approximately 184,000 vessels pass by the project location every year.

Filtering the data with respect to groundings and collision with objects, as these are the type of accidents which are relevant for the Blankenburg case, 67 accidents remain. Taking into account the number of passages and the length of the waterway, the frequency of a ship collision/grounding on the Nieuwe Waterweg/Scheur (per year, per passage) becomes:

$$f_{pass,Scheur} = \frac{67}{6 \cdot 184,000 \cdot 24} = 2.529 \cdot 10^{-6} [1/year/km] \quad (4.1)$$

#### Groundings at the Finnish Gulf

In the case of the Finnish Gulf, vessel groundings for the period of 1989-2010 are registered by the HELCOM institute. Mazaheri et al. (2015) looked at the different waterways which were part of the research and calculated the frequency of a grounding event for the different waterways (see Table 4.2).

Table 4.2: Grounding frequency of the studied waterways– WCI scaled from 0 (the most difficult) to 1 (the easiest) (Mazaheri et al., 2015).

Fairway	WCI	No. of groundings (1989-2010)	Ship Transits in 2010	$f_{gr}$
Kotka	0.75	4	6226	2.92 E-5
Sköldvik	0.76	5	3632	6.26 E-5
Helsinki-West	0.74	1	4887	0.93 E-5
Helsinki-South	0.53	5	5119	4.44 E-5
Hamina	0.64	4	3473	5.24 E-5

When comparing the frequency of grounding/collision at the Scheur with the frequencies in the Finnish Gulf, the value is comparable with the values found for Sköldvik. This waterway is rated as the easiest waterway in the research of Mazaheri et al. (2015). For the new model, it is assumed that the waterway complexity will be the same as for Sköldvik.



### 4.2.2. Type of vessels

To take into account the fact that at the Scheur one is dealing with a mixed fleet, an extra node is added to the model. This node describes the probability that a vessel is a seagoing or inland going vessel. The vessel type directly influences the presence of a pilot, as inland going vessels do not use pilots.

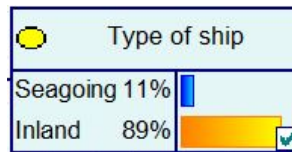


Figure 4.3: 'Type of ship' node in the model.

The probability for this node is based on the data provided by the Port of Rotterdam.

### 4.2.3. Meteorological conditions

The node 'Meteorological conditions' is adapted to the conditions in the Netherlands using data from [Port of Rotterdam \(2012\)](#). In this publication of the Port of Rotterdam several parameters are described using measured data. Two parameters will be adapted to the local conditions, which are the 'Wind' and 'Fog' parameter. On top of that, the node will be uncoupled from the 'Traffic distribution' node, as the meteorological conditions are assumed to have no influence on the vessel distribution at the Scheur.

The four different seasons are defined as follows:

Spring : March, April, May

Summer : June, July, August

Autumn : September, October, November

Winter : December, January, February

For the wind Figure 4.4 is used and it is assumed that a wind of > 4bft will be considered as 'Windy'.

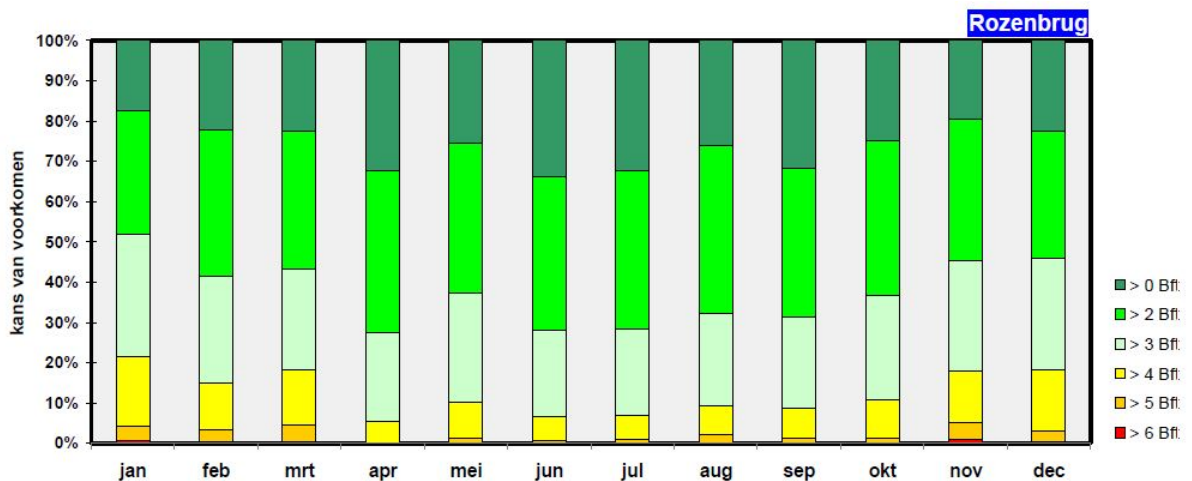


Figure 4.4: The distribution of wind near Rozenbrug.

When looking at the occurrence of fog, Figure 4.5 is used and it is assumed to be 'Fog/Misty' when sight is less than 2000 meters.

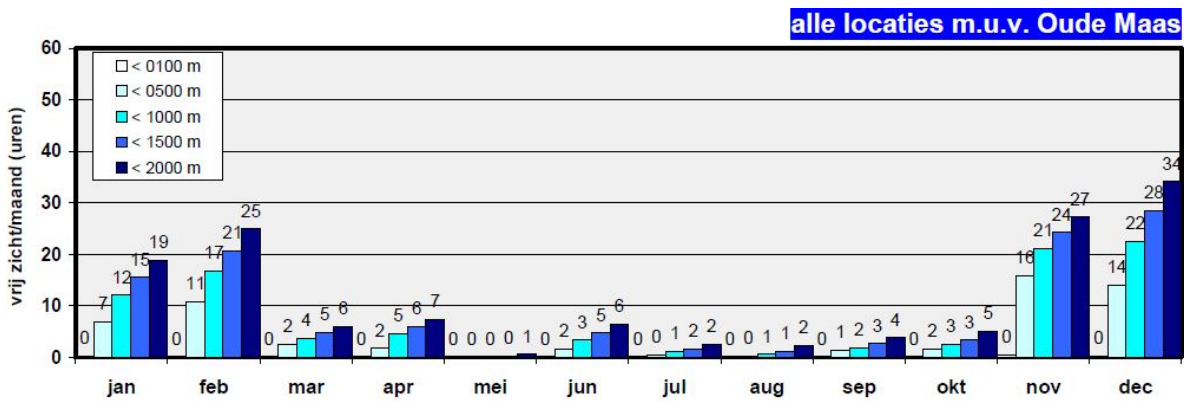


Figure 4.5: Amount of hours with limited sight at the waters around the Port of Rotterdam.

This will result in the node given in Figure 4.6.

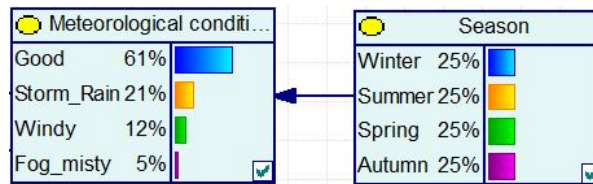


Figure 4.6: The 'Meteorological conditions' node in the model.

#### 4.2.4. Pilot presence

The last node that has to be adapted is the presence of a pilot onboard of a vessel. Out of data from Lood-swezen (2018) it becomes clear that 98% of the seagoing vessels is making use of a pilot. Inland going vessels do not use pilots, which makes the conditional probability for this node as given in Figure 4.7.

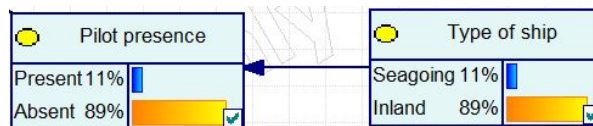


Figure 4.7: 'Pilot presence' node connected with the 'Type of ship' in the model.

### 4.2.5. Scheur Model

With the adaptations implemented the Scheur model looks as follows:

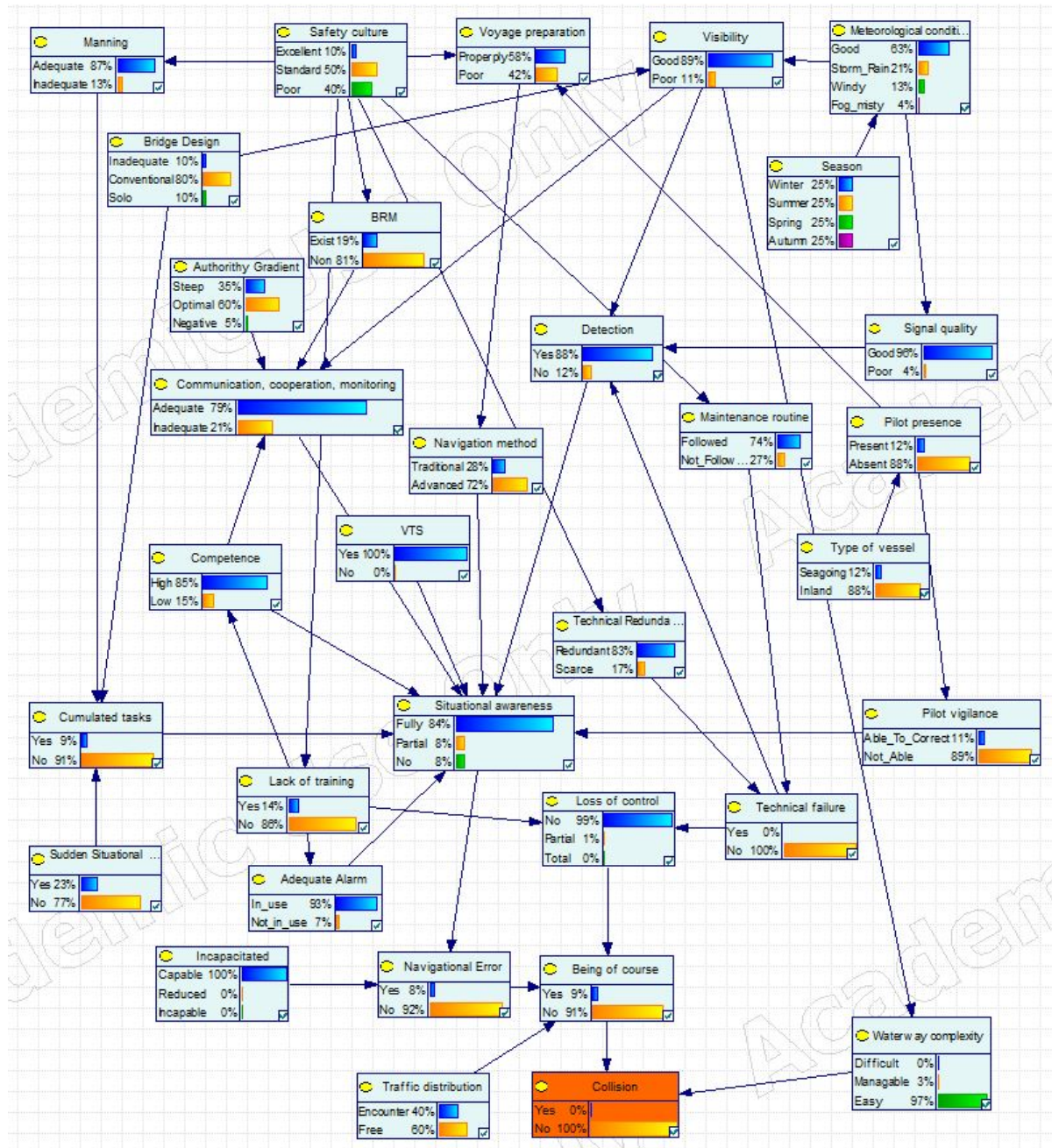


Figure 4.8: Bayesian belief network for ship collision at the Scheur

### 4.3. Probability of a collision according to the model

The probability of a collision given by the model can be calculated by setting the 'Collision' node to 'Yes' and calculating the probability (see Figure 4.9). This is called 'Setting Evidence' and the software is then able to calculate the probability of this event, given the other nodes.

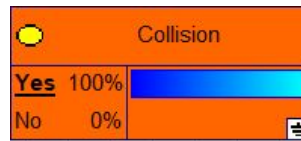


Figure 4.9: Setting the evidence of the model

The frequency of a collision given the model in Figure 4.1, is calculated to be:

$P_{collision,scheur}$	= 6.552 E-05 [1/year]
$P_{collision,projectLocation}$	= 2.730 E-06 [1/year/km]

#### 4.3.1. Comparison with historical collision data

In order to validate the model, the outcome of the model can be compared to the earlier mentioned frequency of collision for the Scheur see Equation 4.1. When comparing these values, one can see that the value from the model is about 10% higher than the one out of the data. The model seems to be overestimating the actual frequency collision, which can be viewed as a conservative value.

##### Distribution along the Scheur

The calculated relative frequency and the probability from the model are estimates for the whole Scheur/Nieuwe Waterweg. When assuming that 'collision' events within 1 kilometer of the project location result in a loading on the structure, the frequency at the location can be calculated.

Method	Prob/year/km
$P_{pass,model}$	= 2.730 E-06
$P_{pass,Scheur}$	= 2.529 E-06

Using Figure 4.10 the average amount of collisions per kilometer can be calculated. The Blankenburg construction site is located at kilometer 1017 which has 15 recorded accidents. The mean ( $\mu$ ) for this distribution is 13.12, which put the Blankenburg site just above average. If it is assumed that accidents are equally distributed over the total length of 24 kilometers, a reasonable value will be found for the Blankenburg location. For other locations this may differ and this approach is not applicable.

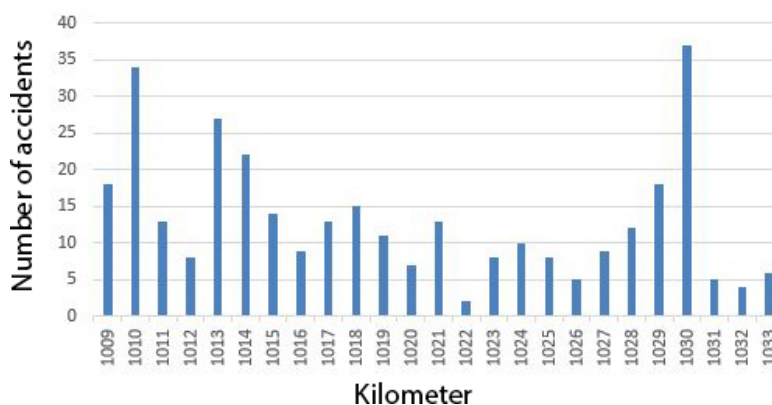


Figure 4.10: Number of accidents per kilometer at the Nieuwe Maas/Scheur/Nieuwe Waterweg.

### 4.3.2. Influence of the different parameters

All the nodes in the system have a certain influence on the outcome of the system. The nodes that positioned further away from the end node, the collision node, will have a smaller influence on the actual event than the nodes closer to the end node. In order to give some insight on how big the influence of the different parameters are, each parameter is evaluated.

One can manually adapt the nodes by giving them a preset state and then calculate the probability. In this way, all nodes can be evaluated in their 'best' and 'worst' state. This will result in a  $\Delta P_{collision}$  for each parameter and the possibility to rank the parameters to their influence (see Table 4.3).

Table 4.3: Influence of the different states of nodes on the probability of a collision. Ordered by the amount of influence.

Node	Best state	Worst state	$\Delta P_{Collision}$
Being of course	No	Yes	4.17E-04
Navigational Error	No	Yes	3.21E-04
Incapacitated	Capable	Incapable	1.18E-04
Loss of control	No	Total	1.17E-04
Situational awareness	Fully	No	8.06E-05
Waterway complexity	Easy	Difficult	4.71E-05
Traffic distribution	Free	Encounter	2.28E-05
Technical Failure	No	Yes	1.29E-05
Competence	High	Low	9.71E-06
Detection	Yes	No	9.44E-06
Visibility	Good	Poor	7.67E-06
Lack of training	No	Yes	7.53E-06
Metreological condntions	Good	Fog/Misty	7.21E-06
Pilot vigilance	Able to correct	Not able to correct	6.58E-06
Pilot presence	Yes	No	5.94E-06
Type of Ship	Seagoing	Inland going	5.82E-06
VTS	Yes	No	5.01E-06
Cumulated tasks	No	Yes	4.94E-06
Adequate alarm	In use	Not in use	4.25E-06
Signal quality	Good	Poor	4.21E-06
Navigation method	Advanced	Traditional	3.34E-06
Communication, cooperation, monitoring	Adequate	Inadequate	3.32E-06
Manning	Adequate	Inadequate	2.70E-06
Safety culture	Excellent	Poor	1.89E-06
Voyage preparation	Properly	Poor	1.65E-06
Season	Summer	Winter	8.30E-07
BRM	Exist	Non	7.53E-07
Bridge design	Conventional	Inadequate	5.16E-07
Technical Redundancy	Redundant	Scarce	5.10E-07
Maintenance routine	Followed	Not followed	3.99E-07
Authority Gradient	Optimal	Negative	2.43E-07
Sudden Situational Change	No	Yes	2.36E-07

### Reducing the probability of collision

Out of a perspective of the construction company, it is interesting to look at which parameters can be changed and which measures give the highest reduction in probability. In order to do so, Table 4.4 is composed, giving the maximum positive effect when changing a node. For some nodes the probability of the worst state is already low and improving the conditions only results in a minor reduction of the collision probability (i.e. technical failure). Out of the table room for improvement can be quantified for each parameter.

Table 4.4: Maximum effect when changing a node for the better.

<b>Node</b>	<b>Positive Difference</b>
Being of course	3.58E-05
Navigational Error	2.65E-05
Situational awareness	1.05E-05
Traffic distribution	9.12E-06
Pilot vigilance	5.86E-06
Pilot presence	5.22E-06
Type of Ship	5.10E-06
Competence	1.50E-06
Safety culture	1.13E-06
Detection	1.11E-06
Lack of training	1.03E-06
Metreological condtions	9.28E-07
Navigation method	9.27E-07
Visibility	8.81E-07
Waterway complexity	7.88E-07
Communication, cooperation, monitoring	7.07E-07
Voyage preparation	6.89E-07
BRM	6.10E-07
Loss of control	6.03E-07
Season	4.33E-07
Cumulated tasks	4.25E-07
Manning	3.54E-07
Adequate alarm	3.00E-07
Signal quality	1.77E-07
Maintenance routine	1.06E-07
Bridge design	9.20E-08
Technical Redundancy	8.67E-08
Authority Gradient	5.48E-08
Sudden Situational Change	5.44E-08
Incapacitated	3.70E-09
Technical Failure	3.50E-11
VTS	5.00E-12

### Proposed measures

As a owner of a project, it is interesting to look at the nodes in which measures can be taken to decrease the probability of a collision. As the nodes are ordered by the amount of influence on the final node of 'Collision', it can easily be seen which nodes can be effectively changed. From Table 4.4 four nodes are considered in which measures could be taken which may lead to a lowered probability.

Table 4.5: Proposed measures for nodes which can be adapted by the project owner.

<b>Node</b>	<b>Measure</b>
Traffic distribution	Impose an in- and outgoing window for all vessels in order to prevent vessel encounters near the structure
Pilot vigilance	Additional training of pilots
Pilot presence	Require all vessels to use pilots
Detection	Placing markers and signals to improve detection of the structure

#### 4.4. Conclusion

In this chapter the use of a Bayesian Network is used as a method to take into account all the different parameters influencing the probability of collision. When comparing the outcome of the model with the value based on the data available for the Scheur, it can be concluded that the probability of the model has the same order of magnitude as the actual data. A small difference can be noticed, which is probably explained by the fact that not all incidents are being reported to the Port authorities. This is a known phenomenon in shipping and it is estimated that approximately 20% of all marine incidents is not reported ([European Maritime Safety Agency, 2017](#)).

In the constructed model the presence of the construction pit at the side of the waterway does not influence the outcome of the model. The complete structure is located outside of the shipping channel, so no real constraints are present. However, captains and pilots may be influenced due to the presence of the structure and the activity of construction works. The influence on the decision-making and difficulty of navigating is unknown and further research is recommended.

The probability of a collision at the project location is determined to be:

$$\underline{P_{Collision} = 2.730 \text{ E-06 [1/year/km]}}$$

The table listing the influence of the different parameters, makes it visible what kind of measures can be taken in order to decrease the collision probability. As not all parameters can be adapted that easily in practice, a selection is made of parameters based on the adaptability from the perspective of the project owner. Four measures are proposed, when in case the probability of a collision is too high and should be decreased.

Table 4.6: Proposed measures for nodes which can be adapted by the project owner.

Node	Measure
Traffic distribution	Impose an in- and outgoing window for all vessels in order to prevent vessel encounters near the structure
Pilot vigilance	Additional training of pilots
Pilot presence	Require all vessels to use pilots
Detection	Placing markers and signals to improve detection of the structure

The model used in this chapter is not a complete one and is only adapted on several points to the conditions on the Scheur. Several additional parameters can be included in the model, to better represent the actions and decisions on a vessel. However, the basis for these parameters should be checked and their influence on the probability should be assessed.



# 5

## The magnitude of the collision force

*In this chapter a probabilistic model is used to determine the frequency of occurrence of impact loads on the structure. In Section 5.1 the model is explained and constructed. In the following section the different input parameters are discussed, after which in Section 5.3 the limitations of the model are discussed. Section 5.4 gives an overview of the model and a calculation example. The results of the model are given in Section 5.5. The chapter is closed off with the conclusions in Section 5.6.*

### 5.1. Model set-up

According to the information in Chapter 2 the main cause of collision is human failure. In Chapter 4 this aspect is treated into further detail, giving a probability of collision for the vessels on the Scheur. Now that the probability is known, the next step is to determine the magnitude of the collision.

In order to determine the magnitude of the force, a model is created. To set-up the model a basic situation is chosen, as can be seen in Figure 5.1. A vessel is sailing in the Scheur approaching the project location. A certain event takes place (described in Chapter 4) and the vessel collides with the structure. Multiple parameters should be assessed to come up with the final force on the structure. One could think of vessel velocity, location in the waterway, weight of the vessel and turning radius.

To account for all the different values and combinations between parameters, it is chosen to use a Monte Carlo simulation. In this way the model is run several hundreds of times, in order to sample the outcomes.



Figure 5.1: Sketch of the basic situation.

### 5.1.1. Magnitude of the force

The force that acts on the structure can be described using the formula proposed by [Joustra and Pater \(1993\)](#). Although the formula is limited to values of  $E_{kin}$  up to 50 MNm and deformations of 4 meters (as it is not tested for other values), it is assumed in this thesis to be valid for all cases.

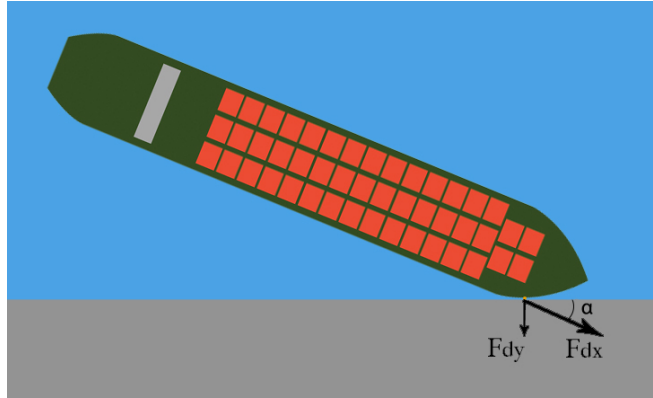


Figure 5.2: Definitions concerning a colliding vessel

First the kinetic energy of the vessel should be calculated, which can be described by Equation 5.1. An elaborated discussion on the different methods to describe the amount of kinetic energy and which parameters are applicable in this case, was discussed in Section 2.2.4.

$$E_{kin} = \frac{1}{2} \cdot C_h \cdot m_s \cdot v_s^2 \quad (5.1)$$

After calculating the kinetic energy of the vessel, this energy can be translated into a force in the direction of the vessel ( $F_{dx}$ ). This can be done using Formula 5.2.

$$F_{dx} = 3.3 \cdot \sqrt{E_{kin}} + 5.6 \quad (5.2)$$

Due to several different reasons, the vessel will not always collide head-on at the structure. The force perpendicular to the structure ( $F_y$ ) can be calculated by the formula given by the [ROK \(2017\)](#) and is given in 5.3. In this formula a reduction coefficient ( $\delta$ ) is introduced

$$F_{dy} = \delta \cdot F_{dx} \cdot \sin(\alpha) \quad (5.3)$$

The reduction coefficient comes into play for vessels colliding under an angle. It is assumed that vessels that come in under an angle, will also start sliding along the structure. In this way a part of the energy, calculated with Equation 5.1, is kept within the vessel as velocity along the structure. When the angle of impact ( $\alpha$ ) becomes smaller, the reduction increases. See Figure 5.2 for the visualization.

$$\delta = 0.1789 \cdot \alpha^{0.4163} \quad (5.4)$$

A force that is acting under angle could normally be translated in two smaller forces which act parallel and perpendicular to the structure. However, in this case the vessel is assumed to be sliding along the structure, which means that only a part of the force  $F_{dx}$  should be taken into account. In this case the force parallel to the structure is not calculated using geometry of the forces, but with Equation 5.5.

$$F_R = 0.5 \cdot F_{dy} \quad (5.5)$$

## 5.2. Input parameters

Important for the probabilistic calculation are the input parameters. In Figure 5.3 several of them are indicated.

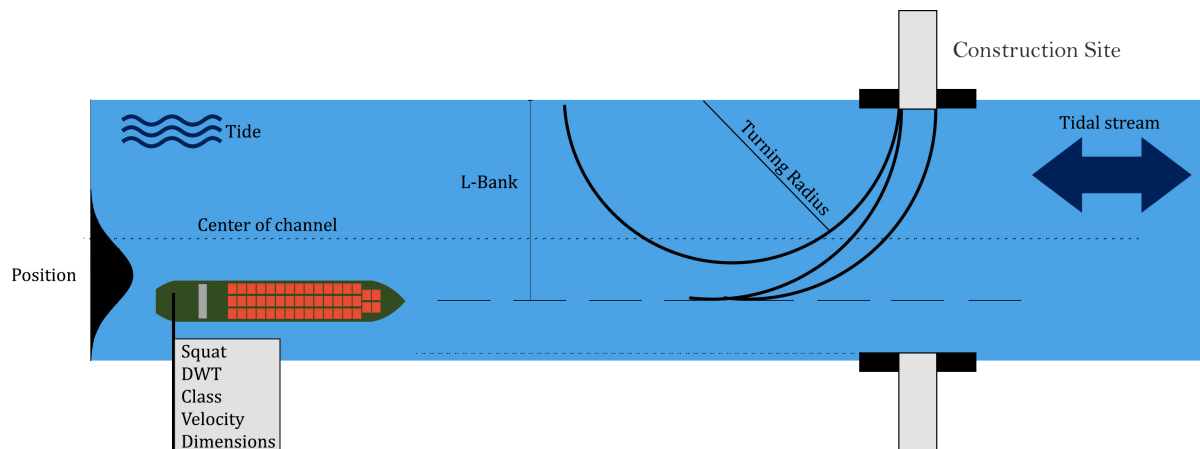


Figure 5.3: Different input parameters influencing the collision energy.

### 5.2.1. Classification and number of vessels

At the project location of the Blankenburg, the fleet is a mixed fleet of seagoing and inland going vessels. The port of Rotterdam keeps record of all vessels passing by and the numbers for this specific location are given in Tables 5.1 and 5.3 divided into the different DWT classes. As dredging took place in the summer van 2018, the situation after dredging is the current situation.

Table 5.1: Amount of seagoing vessels per DWT class per year at project location. Data provided by the Port of Rotterdam.

DWT1	DWT2	DWT3	DWT4	DWT5	DWT6	DWT7	Situation
461	532	1,759	16,946	2,234	975	41	Before dredging
460	481	1,644	16,648	2,153	1,014	39	During dredging
461	532	1,759	16,946	2,234	1,025	47	After dredging - Current situation

Seagoing vessels are categorized in classes based on their Dead Weight Tonnage (DWT), which is the weight carrying capacity of a vessel. Seagoing vessels are categorized into 7 different categories ranging from 0 to 190.000 DWT. The classification is given in Table 5.2.

Table 5.2: Dead Weight Tonnage per DWT-Class

DWT1	DWT2	DWT3	DWT4	DWT5	DWT6	DWT7
< 750	750-1,500	1,500-2,500	2,500-15,000	15,000-50,000	50,000-110,000	110,000-190,000

Whereas seagoing vessel are classified according to DWT, inland vessels are divided into CEMT classes (EN1991-1-7, 2006). However, for modeling purposes it is convenient to just use one classification. Hence, in this approach, the inland going vessels are brought under the seagoing vessel classification as shown in Table 5.3. Two additional categories are distinguished in this table, namely 'DWT1 Other' and 'DWT4 Dredging'. The additional DWT1 category described the amount of pleasure yachts and small boats, which are different from commercial shipping. Dredging vessels are also indicated as a separate group because of their low velocity and dredging activities at the Scheur.

Table 5.3: Amount of inland going vessels per DWT class per year at the project location. Data provided by the Port of Rotterdam.

DWT1	DWT2	DWT3	DWT4	DWT1 Other	DWT4 Dredging	Situation
0-III	III-IVa	IV, Va	$\geq Va$	0-III	$\geq Va$	(CEMT-class)
13,988	12,822	16,319	57,116	58,607	-	Before dredging
12,922	11,846	15,076	52,766	58,507	668	During dredging
13,988	12,822	19,083	57,235	58,607	100	After dredging - Current situation

The total amount of vessels per vessel class can be calculated and is shown in Table 5.4. With an average of 500 vessels per day, it can be concluded that the Scheur is busy waterway.

Table 5.4: Total amount of seagoing and inland going vessels per DWT class per year at the project location.

DWT1	DWT2	DWT3	DWT4	DWT5	DWT6	DWT7	Total
73,056	13,354	20,842	74,181	2,234	1,025	47	184,739

Based on the recorded amount of vessels at the location of the Blankenburg connection, the relative frequency of each class can be calculated (see Figure 5.4) which is used in the model as an input parameter.

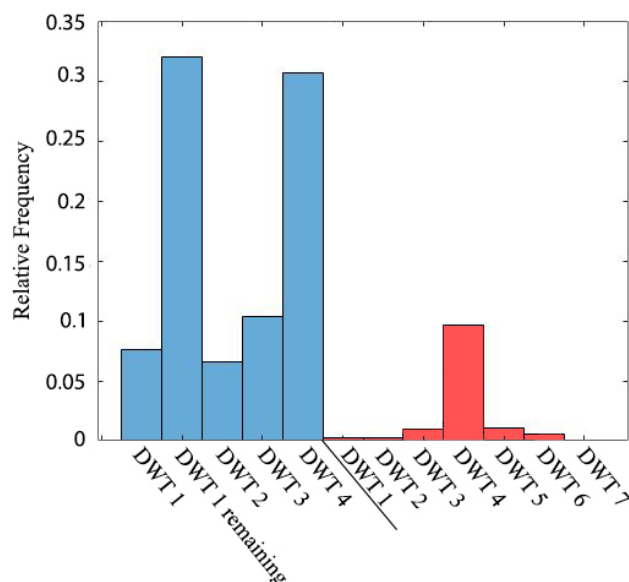


Figure 5.4: Relative frequency of vessel class based on actual data. Blue indicating the inland vessels, red the seagoing vessels.

### 5.2.2. Dead weight tonnage of the vessels

The dead weight tonnage of a vessel is an important factor when regarding collisions. As no specific information is available or could be found regarding the loading percentage of vessels, it is assumed in this thesis that vessels are fully loaded. An analysis was done on 1313 vessels visiting the harbor of Rotterdam this year (data obtained on three different days), and no clear distribution for the different vessel classes could be discerned. Therefore it will be assumed that the dead weight tonnage is uniformly distributed within a vessel class. In Figure 5.5 the distribution of the DWT is given for the DWT4 class.

### 5.2.3. Vessel dimensions

The dimensions of a vessel are important in the case of a ship collision. The width of the vessel is of influence on the area of impact, the length and draught influences the turning radius of the vessel and the draught also determines the width of the channel were the vessel can sail.

An analysis has been done on vessel data obtained from EAU (2015) and these results are compared with the analysis on the 1313 vessels having visited the Port of Rotterdam this year. From this analysis it can be

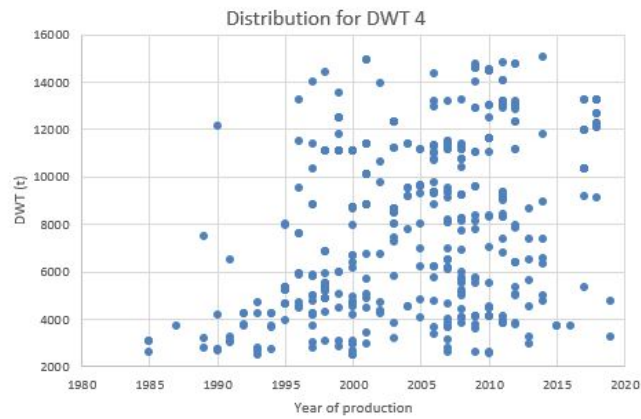
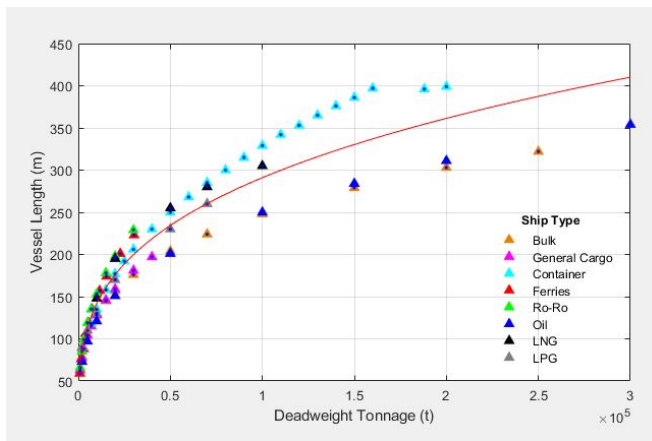


Figure 5.5: Distribution of dead weight within a vessel class.

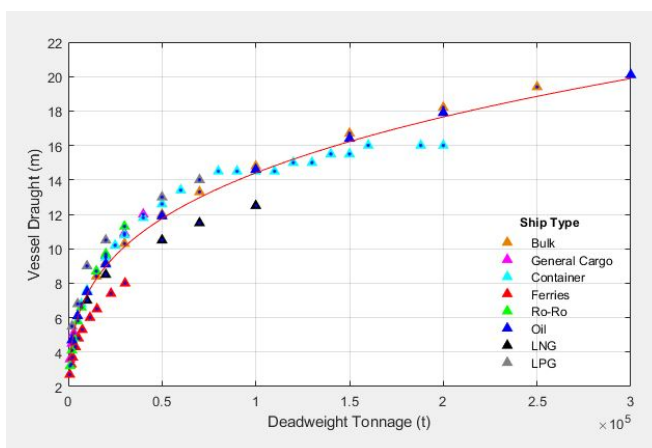
concluded that the dimensions of a vessel are highly correlated with the DWT of a vessel. Based on the DWT of the ship, the length, width and draught can be estimated using Equations 5.6 to 5.8.



$$L_{vessel} = 7.9839 \cdot DWT^{0.3123} \quad (5.6)$$

Correlation coefficient = 0.8378

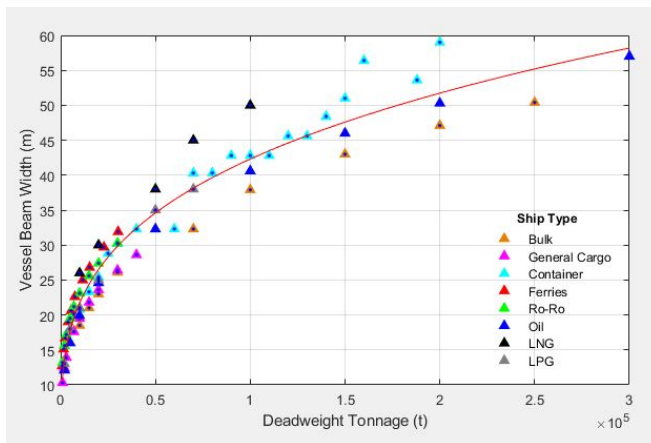
Figure 5.6: Correlation between DWT and vessel length



$$D_{vessel} = 0.4907 \cdot DWT^{0.2935} \quad (5.7)$$

Correlation coefficient = 0.8862

Figure 5.7: Correlation between DWT and vessel draught



$$B_{vessel} = 1.497 \cdot DWT^{0.2902} \quad (5.8)$$

Correlation coefficient = 0.8902

Figure 5.8: Correlation between DWT and vessel beam width

### 5.2.4. Vessel velocity

The velocity is an important parameter in the calculation of the kinetic energy of the vessel, which is decisive for the collision force. In this case the velocity of the vessel is based on a representative value coupled to the DWT of the vessel (Havenbedrijf Rotterdam, 2015). The velocity of the vessel is an empirical estimation which is given by BAAK and presented in Figure 5.10. These values only differ slightly from the average values found by MARIN (2017) for the total area of the Port of Rotterdam. It is therefore assumed that these values are a good estimation of the vessel velocity.

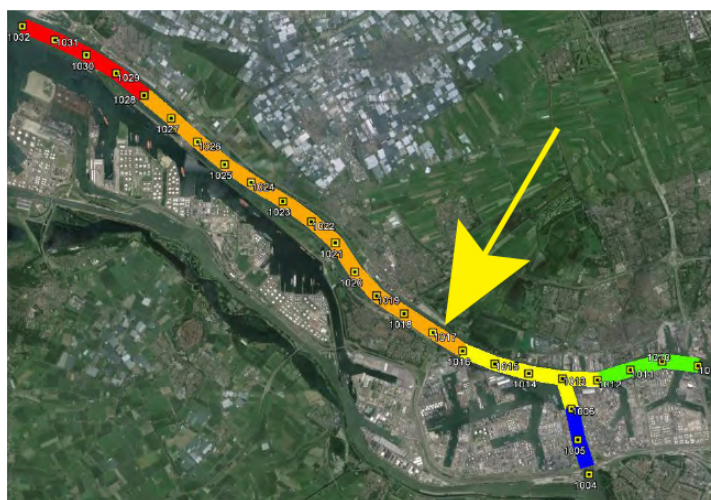


Figure 5.9: Area of application (Havenbedrijf Rotterdam, 2015)

	DWT1 < 750	DWT2 750- 1.500	DWT3 1.500- 2.500	DWT4 2.500- 15.000	DWT5 15.000- 50.000	DWT6 50.000- 110.000	DWT7 110.000- 190.000
1028-1032	8.0	8.0	8.0	8.0	8.0	8.0	8.0
1016-1028	8.0	8.0	8.0	8.0	7.5	7.5	7.5
1012-1016	8.0	8.0	8.0	8.0	7.0	7.0	6.5
1009-1012	7.5	7.5	7.5	7.5	6.0	6.0	5.5
1004-1006	7.0	7.0	7.0	7.0	3.0	3.0	3.0

Figure 5.10: Estimated velocity of sea-going vessels (knots) (Havenbedrijf Rotterdam, 2015).

### 5.2.5. Water level

When navigating in shallow and confined waterways, such as the Scheur, variations in water level are a navigation safety issue. As the project location is close to the sea, the water level variation is mainly caused by tide. A second contributing factor is the squat generated by the ship.

#### Tide

The tide is of importance for this calculation as the draught/depth ratio influences the navigability of the vessel. The tide at the location of the Blankenburg connection ranges from -0.5 meters till a maximum of 1.5 meters, see Figure 5.11.

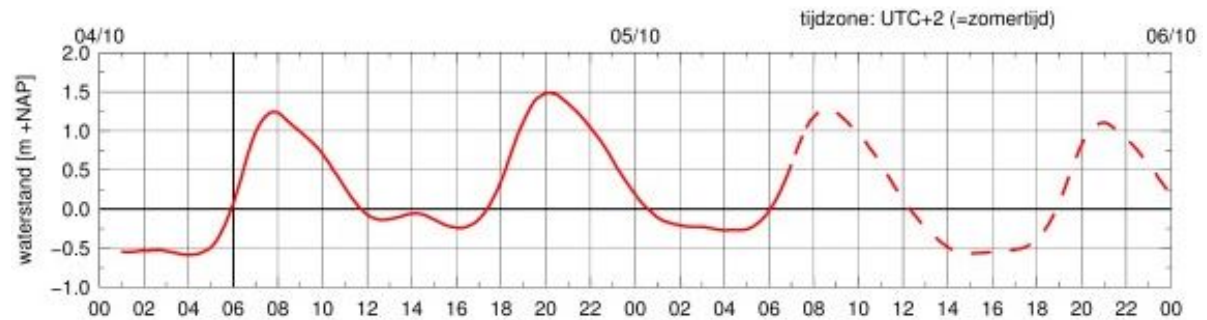


Figure 5.11: Tidal fluctuations at the project location for 4 and 5 October 2019.

In the model the tide will be approximated using a sinus function with a mean value of 0.5 meters. Per simulation a new random x-value for the tide is taken, which corresponds with an y-value on the graph showed in Figure 5.12.

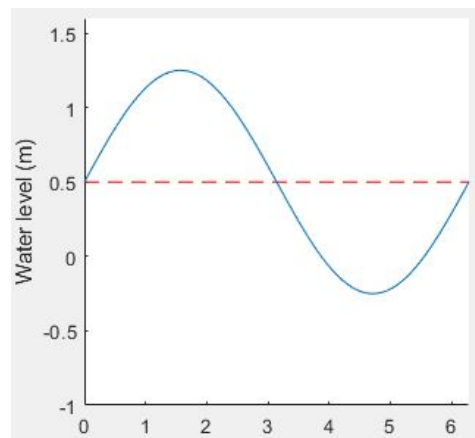


Figure 5.12: Model approximation of the tide at the project location.

### Tidal stream

Directly related to the tide is the tidal stream. With the incoming tide the water level rises and the velocity and the direction of the water inside the Scheur will change, see Figure 5.13. The amplitude of the tidal stream is about 0.75 m/s with a mean around 0.35 m/s.

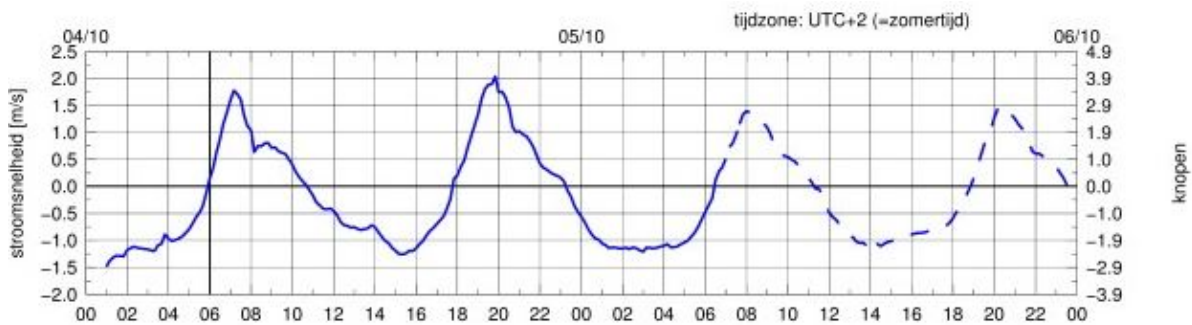


Figure 5.13: Tidal stream fluctuations at the project location for 4 and 5 October 2019.

For the model the tidal stream is approximated using again a sinus function. The tidal stream will be considered as direct consequence of the tide, as tidal lag is neglected in this model. In this way the random x-value generated in the tide calculation, is used again to estimate the tidal stream. In this manner the direct link between the two phenomena is ensured.

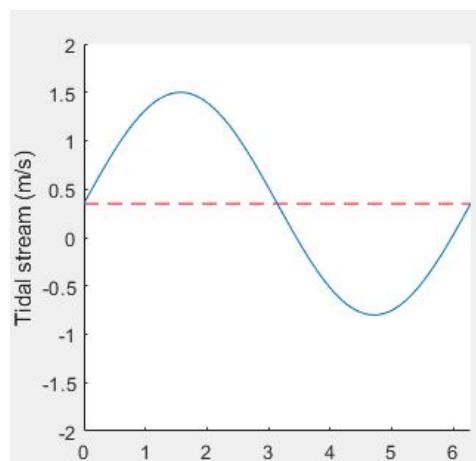


Figure 5.14: Model approximation of the tidal stream at the project location.



### Squat

As the Scheur is a relatively narrow channel, the influences of squat can not be neglected. Due to the squat effect the vessel will drop a bit further into the water, hindering the maneuverability of the ship (see Figure 5.15).

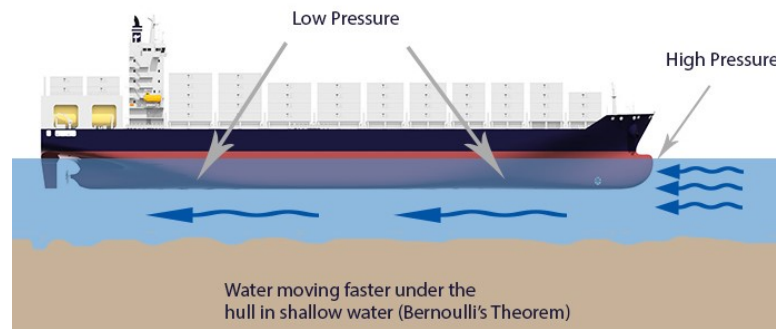


Figure 5.15: Squat effect on vessels in shallow waters.

To calculate the effect of squat in this situation, the method of preservation of energy is used (Verheij, H.J.; Stolker, C.; Groenveld, R., 2008). The amount of squat ( $z$ ) experienced by the vessel is given by Equation 5.9.

$$z = \alpha \cdot \frac{(V'_s + U_r)^2}{2 \cdot g} - \frac{V_s'^2}{2 \cdot g} \quad (5.9)$$

In which:

- $z$  = squat [m]
- $\alpha$  = correction factor for non-uniform distribution of  $U_r$  [-]
- $V'_s$  = Vessel velocity with respect to the water [m/s]
- $U_r$  = actual return current with respect to the banks [m/s]
- $g$  = gravitational constant [ $m/s^2$ ]

#### 5.2.6. Turning circle

The turning circle is an important factor in the calculation of the impact force. As the Scheur is a narrow channel, vessels with a large turning circle will not be able to hit the structure head-on (which is the least favorable situation).

As a head-on collision would result in the highest impact loads, the model assumes that all vessels will turn with their minimal turning radius. In other words, the rudder of the vessel is changed to its ultimate position.

Furthermore, based on literature it becomes clear that navigational ability of vessels is decreasing in shallow water (Reynolds, 1976). In deep water vessels can turn with a radius of 3 times the length of the vessel. In shallow water the turning radius increases to approximately 5 times the length of the ship. This is due to the fact that the water can not escape that easily and a certain amount of blockage occurs, increasing the turning radius of the vessel. Shallow water is assumed for a depth/draught ( $S$ ) ratio lower than 3.0 (Consultants, The Øresund Link, 1994).

Table 5.5: Influence of the depth on the turning radius

S (depth/draught)	Turning radius
$> 3$	$3 \cdot L$
$2 < S < 3$	$4 \cdot L$
$S < 2$	$5 \cdot L$

### 5.2.7. Position of the vessel

The impact force on the structure is further influenced by the position of the ship in shipping channel. The position determines the distance to the structure and therefore also the completion of the vessels' turn. As the Scheur is a two-way shipping channel, the location of the ship in the channel is assumed to be normally (Gaussian) distributed on one side of the channel.

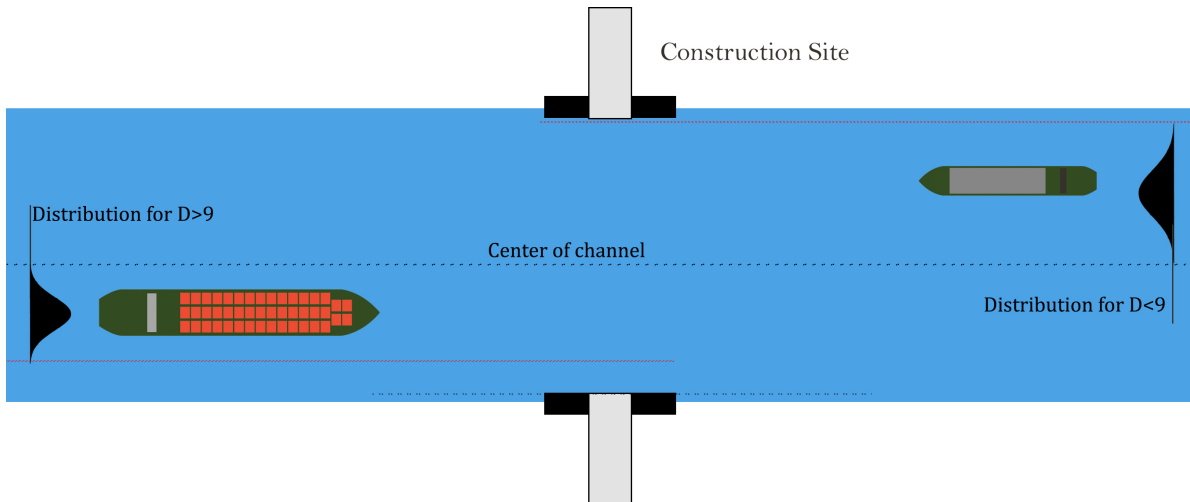


Figure 5.16: The location of the vessel is assumed to be Gaussian distributed.

Another aspect that should be taken into account is that vessels with a draught bigger than 9.0m, will have to use the dredged channel which has a limited width of 230 meters. The location will still be assumed to be normally distributed over half the channel width (see also Figure 5.16).

Table 5.6: Dependence of the width of the shipping lane on the draught of the vessel.

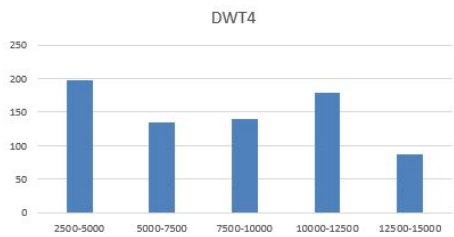
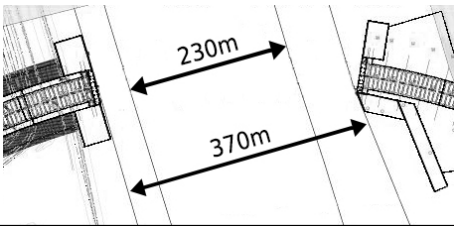
Draught	Shipping lane	Width	Depth
$D > 9.0$	Dredged channel	230 m	16.2 m
$D < 9$	Complete channel	370 m	10.0 m

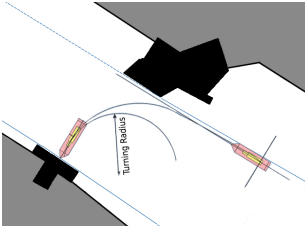
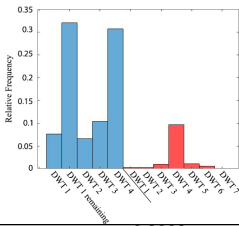
Last aspect on the position of the vessel is the fact that the vessel can either sail upstream or downstream. This is especially important for the velocity of the vessel, as the tidal stream should be added to vessel velocity. Of lesser importance is the influence on the squat of the vessel.

As vessels go to and from the harbor, it is determined that that half of the vessels will go upstream and the other half downstream.

## 5.2.8. Overview of the input parameters

Table 5.7: Overview of the input parameters for the probabilistic model.

Parameter (A-Z)	Type	Resource	Graphic/Equation
Dead weight tonnage of the vessel (DWT)	Stochastic	Based on analysis done on 1313 vessels visiting the Port of Rotterdam. Assumed to be uniformly distributed within vessel class.	
Dimensions of the channel	Deterministic	Data provided by BAAK	
Draught of the vessel	Deterministic	Data analysis on data from <a href="#">EAU (2015)</a> and 1313 vessels visiting the Port of Rotterdam	$D_{vessel} = 0.4907 \cdot DWT^{0.2935}$
Friction Coefficient	Deterministic	Based on <a href="#">ROK (2017)</a> . Reduction may be applied for impact angles smaller than 63 degrees.	$\delta = 0.1789 \cdot AoI^{0.4163}$
Length of the vessel	Deterministic	Data analysis on data from <a href="#">EAU (2015)</a> and 1313 vessels visiting the Port of Rotterdam	$L_{vessel} = 7.9839 \cdot DWT^{0.3123}$
Position of the vessel	Stochastic	Assumed to be normally distributed over the channel based on <a href="#">Consultants, The Øresund Link (1994)</a>	$LOC = \text{normrnd}(LOC_{Mean}, LOC_{SD})$ <i>with</i> $LOC_{Mean}$ = mean value $LOC_{SD}$ = Standard deviation
Squat	Deterministic	Calculation method out of <a href="#">Verheij, H.J.;Stolker, C.;Groenveld, R. (2008)</a>	$z = \alpha \cdot \frac{(V'_s + U_r)^2}{2 \cdot g} - \frac{V'_s{}^2}{2 \cdot g}$
Tidal stream	Stochastic	Data from <a href="#">NV, Havenbedrijf Rotterdam (2019)</a> and a assumed sinusoidal behavior.	$TidalStream = \beta + TS \cdot \sin(\theta)$ <i>with</i> $\beta = 0.35\text{m}$ $TS = 1.15\text{m}$
Tide	Stochastic	Data from <a href="#">NV, Havenbedrijf Rotterdam (2019)</a> and a assumed sinusoidal behavior.	$Tide = \beta + TA \cdot \sin(\theta)$ <i>with</i> $\beta = 0.50\text{m}$ $TA = 0.75\text{m}$

Turning circle	Deterministic	Based on Reynolds (1976) and Consultants, The Øresund Link (1994)																																																	
Upstream / Downstream	Stochastic	Based on engineering judgment	$P(Upstream) = P(Downstream) = 0.5$																																																
Velocity of the vessel	Deterministic	Data from Havenbedrijf Rotterdam (2015) and MARIN (2017)	<table border="1" data-bbox="922 544 1377 685"> <thead> <tr> <th></th> <th>DWT1 &lt; 750</th> <th>DWT2 750- 1.500</th> <th>DWT3 1.500- 2.500</th> <th>DWT4 2.500- 15.000</th> <th>DWT5 15.000- 50.000</th> <th>DWT6 50.000- 110.000</th> <th>DWT7 110.000- 190.000</th> </tr> </thead> <tbody> <tr> <td>1028-1034</td> <td>8.0</td> <td>8.0</td> <td>8.0</td> <td>8.0</td> <td>8.0</td> <td>8.0</td> <td>8.0</td> </tr> <tr> <td>1016-1028</td> <td>8.0</td> <td>8.0</td> <td>8.0</td> <td>8.0</td> <td>7.5</td> <td>7.5</td> <td>7.5</td> </tr> <tr> <td>1012-1016</td> <td>8.0</td> <td>8.0</td> <td>8.0</td> <td>8.0</td> <td>7.0</td> <td>7.0</td> <td>6.5</td> </tr> <tr> <td>1009-1012</td> <td>7.5</td> <td>7.5</td> <td>7.5</td> <td>7.5</td> <td>6.0</td> <td>6.0</td> <td>5.5</td> </tr> <tr> <td>1004-1008</td> <td>7.0</td> <td>7.0</td> <td>7.0</td> <td>7.0</td> <td>3.0</td> <td>3.0</td> <td>3.0</td> </tr> </tbody> </table>		DWT1 < 750	DWT2 750- 1.500	DWT3 1.500- 2.500	DWT4 2.500- 15.000	DWT5 15.000- 50.000	DWT6 50.000- 110.000	DWT7 110.000- 190.000	1028-1034	8.0	8.0	8.0	8.0	8.0	8.0	8.0	1016-1028	8.0	8.0	8.0	8.0	7.5	7.5	7.5	1012-1016	8.0	8.0	8.0	8.0	7.0	7.0	6.5	1009-1012	7.5	7.5	7.5	7.5	6.0	6.0	5.5	1004-1008	7.0	7.0	7.0	7.0	3.0	3.0	3.0
	DWT1 < 750	DWT2 750- 1.500	DWT3 1.500- 2.500	DWT4 2.500- 15.000	DWT5 15.000- 50.000	DWT6 50.000- 110.000	DWT7 110.000- 190.000																																												
1028-1034	8.0	8.0	8.0	8.0	8.0	8.0	8.0																																												
1016-1028	8.0	8.0	8.0	8.0	7.5	7.5	7.5																																												
1012-1016	8.0	8.0	8.0	8.0	7.0	7.0	6.5																																												
1009-1012	7.5	7.5	7.5	7.5	6.0	6.0	5.5																																												
1004-1008	7.0	7.0	7.0	7.0	3.0	3.0	3.0																																												
Vessel classification	Stochastic	Relative frequency based on data provided by Port of Rotterdam																																																	
Width of the vessel	Deterministic	Data analysis on data from EAU (2015) and 1313 vessels visiting the Port of Rotterdam	$B_{vessel} = 1.497 \cdot DWT^{0.2902}$																																																

### 5.3. Model limitations

The model is not a complete representation of the reality. Some limitations or assumptions have been made and will be briefly explained.

#### Turning radius

In this model it is assumed that all vessels will start turning with a minimal turning radius which is dependent on the length and draught of the vessel. It is further assumed that the vessel can fail either way of the channel, so either to starboard or to port side. This gives a 50% chance of failing to port and 50% chance of failing to starboard. The side to which the vessel will be turning is of importance, as the distance to each bank will differ depending on the location. When a vessel completes a 90 degrees turn, it is assumed that the vessel will collide with the structure head-on, so the maximum angle of impact is set to 90 degrees.

#### Vessel velocity

No accurate data could be found on the velocity of vessels in the Scheur. Based on estimation done by [Havenbedrijf Rotterdam \(2015\)](#) the velocity of the vessels is found. The velocity is an important factor in the calculation, as it is squared in the calculation of the kinetic energy. So it could be worth investing into research to better estimate the velocity of the vessels.

#### Orientation of the pit on the North bank

In the original case of the Blankenburg connection the construction pit on the north bank is constructed under an angle of approximately 30 degrees with the waterway. In Chapter 7 the influence of placing the pit under an angle is reviewed, but in first instance the construction pits are assumed to be perpendicular to the waterway. In this way there is no difference between the two banks, only the discharge of the river can influence the loading on the structure.

### 5.4. Model overview

The model used in the calculations is visualized in Figure 5.17. The steps are indicated in different colors, which are explained in the legend added to the figure.

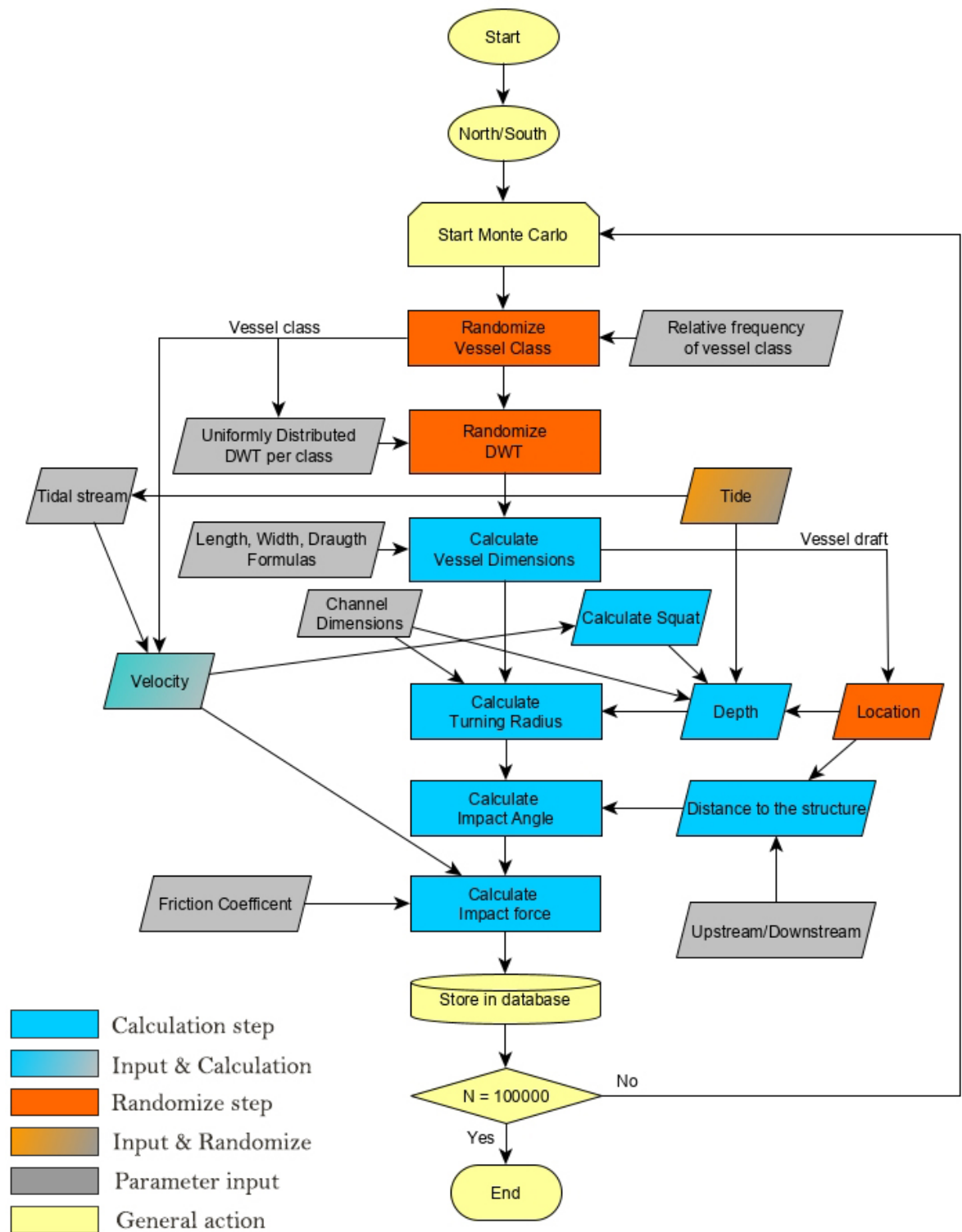


Figure 5.17: Flow chart of the calculation process



## 5.5. Results

After calculating the impact force on the structure for 50,000 times using a Monte Carlo simulation, a probability density plot can be made. As the the case of the Blankenburg has a structure on both the south and the north side, the model is run two times to calculate the forces on both sides of the river.

### North side

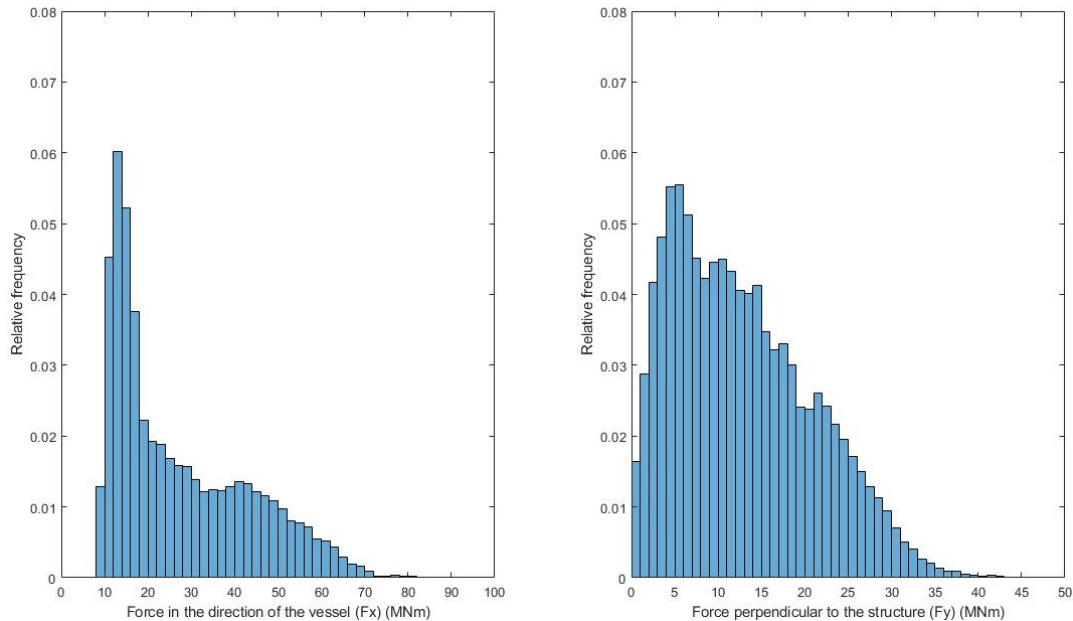


Figure 5.19: Forces on the structure on the North side of the Scheur

### South side

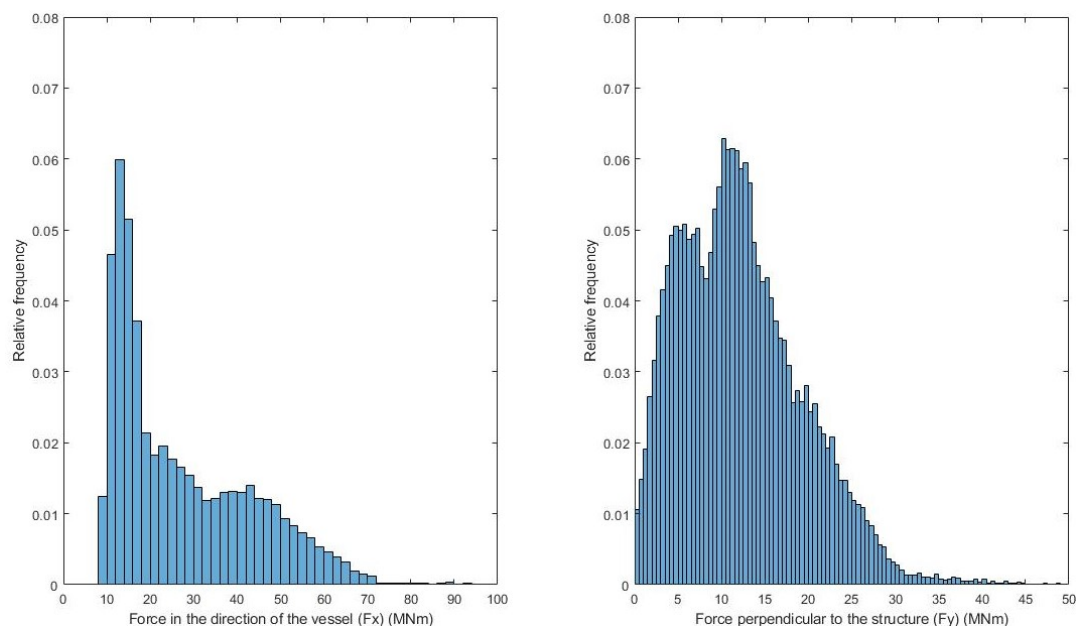


Figure 5.20: Forces on the structure on the South side of the Scheur

From these figures it becomes clear that the north and south side of the Scheur differ slightly in the occurrence of impact forces. This is due to the fact that the tidal stream that is present in the Scheur affects the velocity of the vessel and in that, the magnitude of the impact force.



When plotting the force in the direction of the vessel against the force on the structure, the correlation between the two parameters becomes visible. The results are shown in Figure 5.21. The orange line in the figure is the zero reduction line.

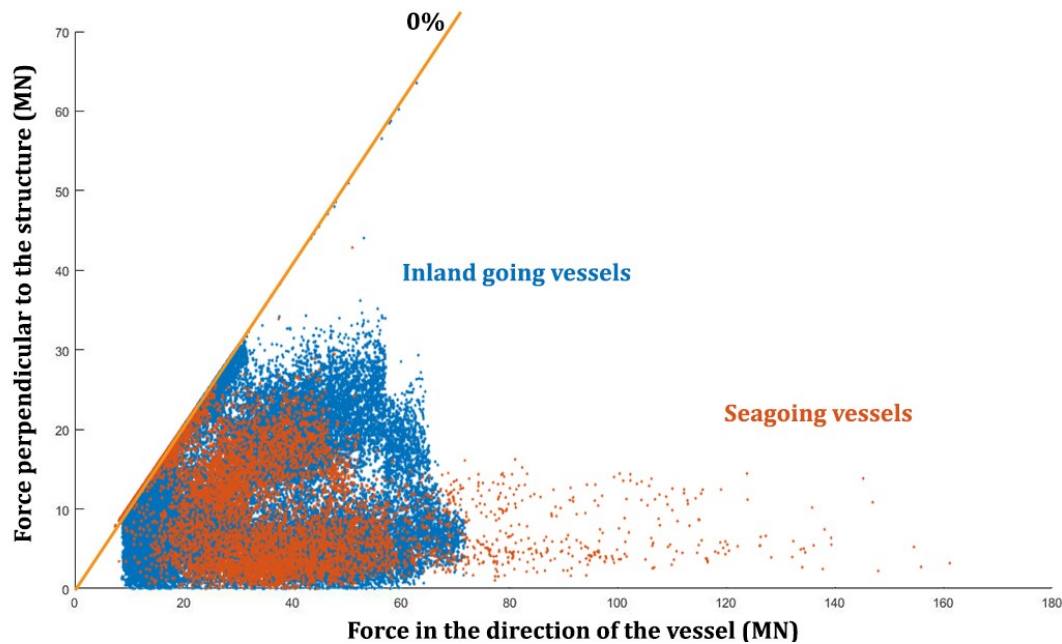


Figure 5.21: Correlation between  $F_{dx}$  and  $F_{dy}$  for the South side.

The zero percentage line is a boundary condition for the system. No additional energy is put into the system after collision so points above this line are not possible, as a point above this line would have a higher force on the structure than there is energy present in the vessel.

Drawing additional conclusions on the basis of this figure is difficult, as no clear correlation between the two parameters is found.

#### Characteristic vessel

As can be seen in Subsection 5.2, the fleet at the Scheur is composed of different vessel types and classes. For the probabilistic calculation all the vessels are taken into one big group. However, from a project owner perspective it is interesting to determine which type of vessel is normative, as possible mitigation measures can be different for seagoing or inland going vessels.

Table 5.8: Vessel classes and the 95% characteristic impact force.

Inland going vessels			Seagoing vessels		
Vessel Class	Rel. Freq.	95% Force [MN]	Vessel Class	Rel. Freq.	95% Force [MN]
-	-	-	-	-	-
DWT 1	0.076	16.42	DWT 1	0.0025	15.33
DWT 1 Rem.	0.317	16.44	DWT 2	0.0029	17.73
DWT 2	0.069	21.78	DWT 3	0.0095	20.87
★ DWT 3	0.103	26.86	DWT 4	0.0917	16.00
★ DWT 4	0.310	20.72	DWT 5	0.0121	13.56
			DWT 6	0.0055	12.73
			DWT 7	0.0003	13.00

From Table 5.8 it becomes clear that the biggest seagoing vessels do not result in the highest forces on the structure. Inland going vessels of class 3 and 4 are governing, which may come across as unnatural, as these are not the biggest vessels. However, due to their relatively small length, inland going vessels tend to hit the structure head-on more often.

## 5.6. Conclusion

The forces on the structure are determined using a Monte Carlo simulation of the model. In this way a probability density function for the magnitude of the force is generated, giving insight in the occurrence of forces on the structure.

From the results it can be concluded that there is a small difference in magnitude of forcing between the North and South side of the channel. The reason for this is a combination of the velocity of the vessel and the impact angle. A vessel sailing downstream is accelerated, as where a vessel sailing upstream is slowed down. This is important, as vessels sailing downstream can hit the structure on the South side with a higher angle of impact, resulting in a higher collision load. Turning the construction pit on the south side to face more to the downstream vessels, could be feasible when looking at the magnitude of the force.

For the safety assessment of the construction pit, the force perpendicular to the end-wall is of interest. This force is calculated using a reduction coefficient based on the amount of friction between the vessel and the structure, and the angle of impact. The amount of reduction decreases with an increasing angle of impact. As in general seagoing vessels are bigger than inland going vessels, the length of the seagoing vessels limits the possibility to hit the structure head-on. The kinetic energy stored inside the vessel is bigger, however, the forcing on the structure is lower. Therefore, it can be concluded that inland vessels are governing in this case; in relative frequency but also in the magnitude of forcing.

## Resistance of the structure

In Chapter 2 the theoretical background of collisions and combi-walls is treated. In combination with the information about the Blankenburg case in Chapter 3, the proposed design by BAAK can now be checked for the collision case. In Section 6.1 the different variants are discussed. This is followed by the strength calculations for the double end-wall, after which in Section 6.3 the single end-wall is treated. The conclusions based on this chapter are given in Section 6.4

### 6.1. Variants of the structure

The existing design by BAAK exists of a double combi-wall connected with a frame, as can be seen in 6.1a. The question in this thesis (see Chapter 1) is whether a single combi-wall would also suffice to withstand the collision forces imposed by a colliding vessel. In this way a variant on the original design is created, which is showed in Figure 6.1b.

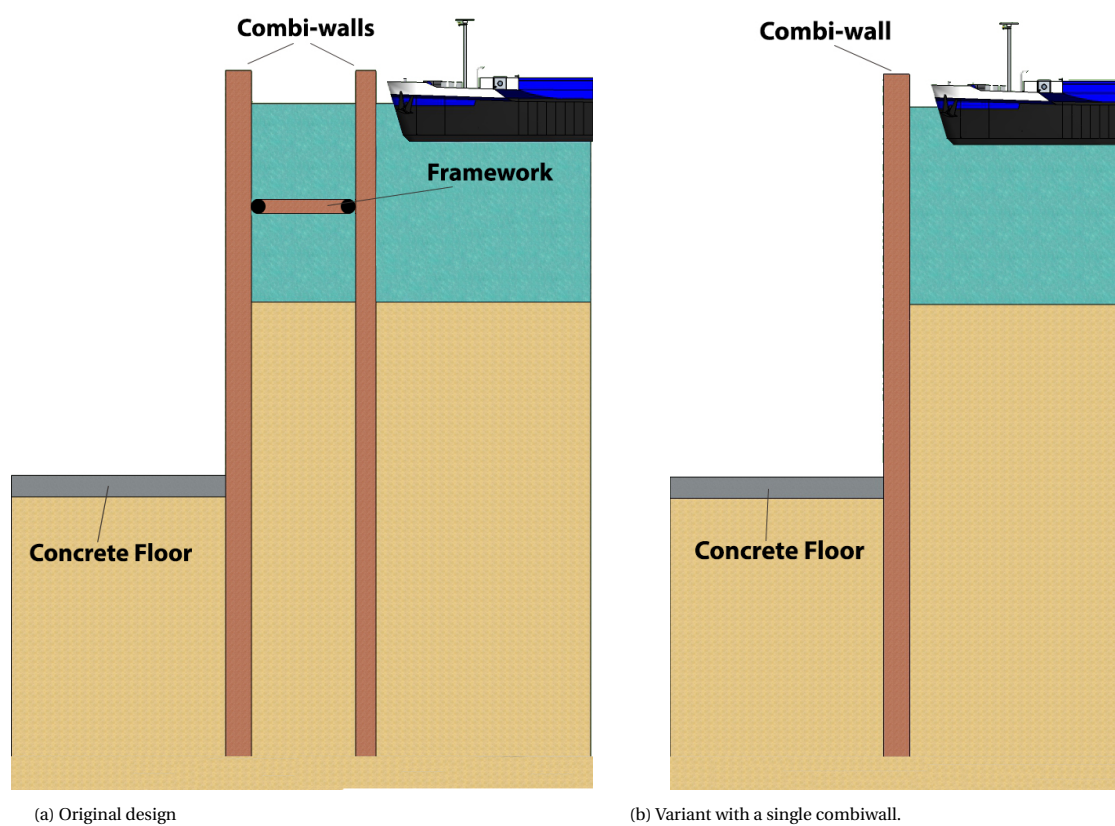
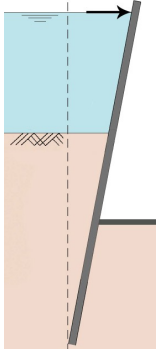
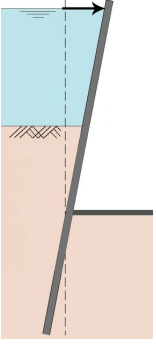
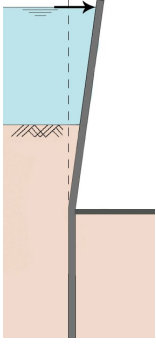
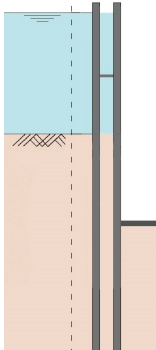
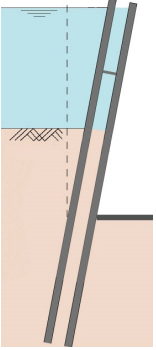
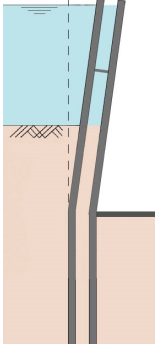


Figure 6.1: The two variants of the structure.

### 6.1.1. Failure mechanisms

The different failure mechanism which are important to check in case of a vessel collision are treated in Section 2.3.3. In Table 6.1 a short overview is given for the two variants.

Table 6.1: Different failure mechanisms for the two variants.

System	Failure mechanisms		
	Sliding along the base	Toppling of the wall	Structural failure
Single wall			
Double wall			

### 6.1.2. Assumptions

In order to perform the resistance calculations, some assumptions have been made which will be explained briefly.

#### Framework

In the original design by BAAK a framework is present, which introduces the forces due to the collision into the second combi-wall. It is assumed that this framework is infinitely rigid and is activating all piles in the structure. The framework is attached to the combi-walls with hinged connection.

#### Seagoing and inland going vessels

When a vessel collides with the structure, the point at which the vessel first touches the structure is called the point of impact. This point is of relevance for the resistance calculation of the structure, as a higher point of impact can result in significant additional bending moments. For seagoing vessels this point of impact is lower, due to the presence of a bulbous bow. However, based on the actual numbers and the analysis in Chapter 5, it can be assumed that inland going vessels will be governing. Therefore it is assumed that the point of impact will be located at water level at all times.

A second assumption is made in the application of the force. Due to deformations of the hull and the structure, the point of impact will increase over a small amount of time to an area of contact. When no redistributing measures are taken (such as a girder), this effect is not included in the calculations and the force will be taken as a point load.

## 6.2. Original design

The original design by BAAK consist of two combi-walls connected by a framework. This framework is assumed to be infinitely rigid and connects the primary wall with the inside secondary wall. The force introduced by the vessel will therefore be spread out over two instead of one wall, which increases the resistance of the structure. See Figure 6.2 for a more detailed overview of the situation.

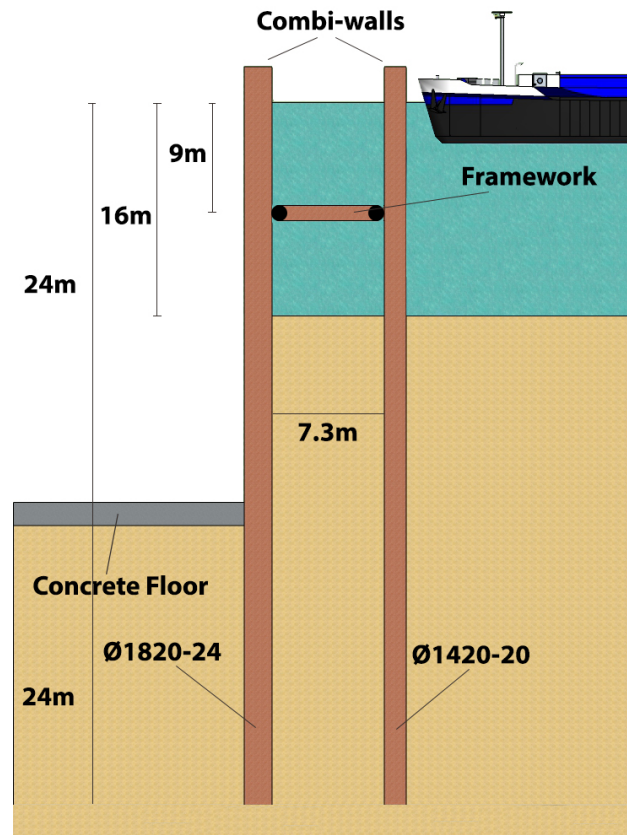


Figure 6.2: Details of the original design.

### 6.2.1. Characteristics of the combi-walls

From the figure it becomes clear that two types of combi-walls are used in the design. The primary retaining wall is the one bordering the channel and the secondary wall is placed in behind to protect the pit. In Table 6.2 the characteristics of both combi-walls are given.

Table 6.2: Characteristics of the elements for the original design.

Wall	Element	Steel	$E_s$ [N/mm <sup>2</sup> ]	$f_y$ [N/mm <sup>2</sup> ]	Diameter [mm]	Thickness [mm]	$D/te^2$ [-]	Length [m]
Primary	Tubular pile	X70	210,000	482	1820	24	125	48
	AZ Sheet piling	S355	210,000	355	-	12.2-13.0	-	48
Secondary	Tubular pile	X70	210,000	482	1420	20	125	48
	PU Sheet piling	S355	210,000	355	-	10.1-15.2	-	48

From the table it becomes clear that different types of sheet piling are being used in each wall. In the secondary wall a AZ-type of sheet piling is used, whereas in the primary wall a PU-type of sheet piling is used. The AZ-type sheet piling is mainly used because of its ability to allow some pile drift and horizontal displacements. The maximum allowed horizontal displacement without elastic or plastic deformation is 87 mm. Further rotation of the sheet piles will result in stresses in the interlocking of the sheet piles. See Figure 6.3 for a graphical display of the situation.

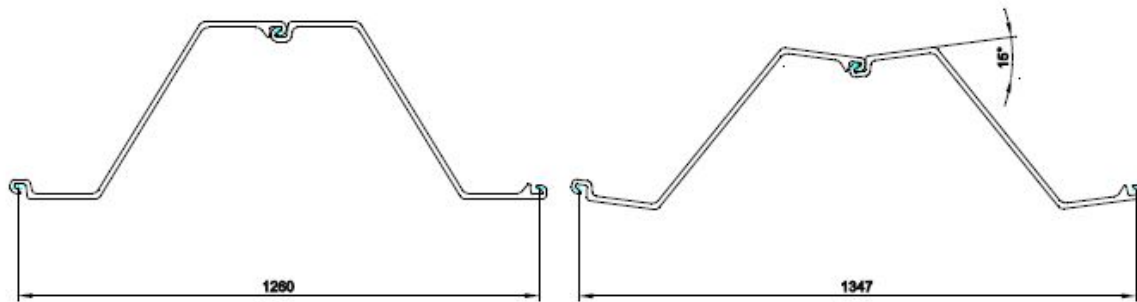


Figure 6.3: Tolerances in the AZ-sheet piling. Adapted from BAAK.

Sheet-piling of the PU-type does not allow for these deformations. All the interlocks (hinges) in the system are orientated at the same working line, which means that deformation directly leads to tension in the members. The two different types of combi-walls are presented in Figures 6.4 and 6.5.

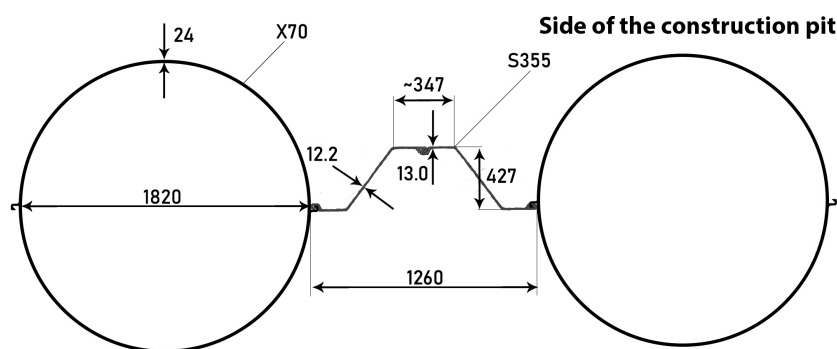


Figure 6.4: Characteristics of the primary combi-wall, distances in mm.

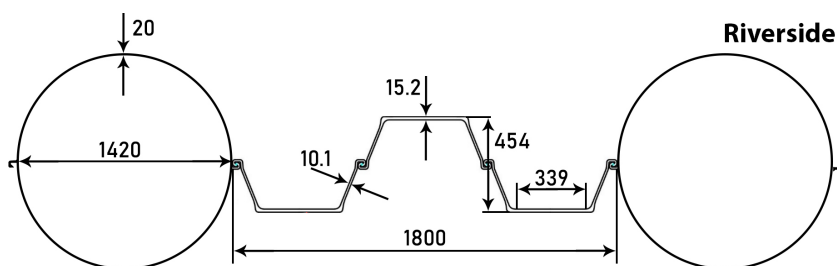


Figure 6.5: Characteristics of the secondary combi-wall, distances in mm.

### 6.2.2. Failure modes

In Chapter 2 the different failure modes for combi-walls under collision loading are given. In the case of a double combi-wall, the system is coupled and the failure modes will become a little bit different.

#### Horizontal stability

The first failure mechanism that needs to be checked is the horizontal capacity of the concrete floor. When assuming the structure to be completely rigid, the concrete floor should bear the horizontal load in order to prevent the walls from falling down.

Concrete strength	= 30 MPa
Thickness concrete layer	= 1.5 m
Total Resistance	= 30,000 kN/m

### Rotational stability

Another failure mode which can lead to severe consequences is when the piles are rotating around the concrete floor. In other words, if the pile is not driven far enough into the ground, this will lead to insufficient rotational resistance of the soil. The situation is illustrated in Figure 6.27. In this it is assumed that the two combi-walls act as one rigid structure with the turning point indicated in red.

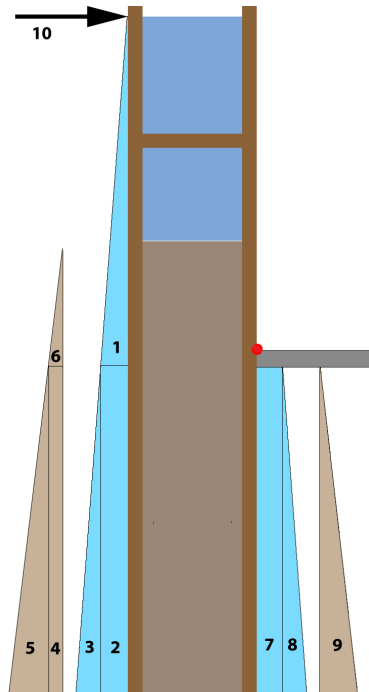


Figure 6.6: Schematization in order to assess the rotational stability of a tubular pile.

The maximum allowable force can be calculated by calculating the turning moment around the underwater concrete floor. For the soil pressures, the active and passive soil coefficients mentioned in Section 2.3.4 should be taken into account. In Table 6.10 the different parts are indicated and their contribution is calculated.

$$\overline{F_{Rotational}} = 6859 \text{ kN/m}$$

Table 6.3: Rotational stability of a tubular pile as part of a construction pit.

Section	Height [m]	Pressure Top [kN/m <sup>2</sup> ]	Pressure Bottom [kN/m <sup>2</sup> ]	Force [kN/m]	Arm [m]	Contribution [+/-]	Moment [kNm/m]
1 - Water	24	0	240	2880	8.00	+	23,040
2 - Water	24	240	240	5760	12	-	-69,120
3 - Water	24	240	480	2880	16	-	-46,080
4 - Passive Soil	24	72	72	5184	12	-	-62,208
5 - Passive Soil	24	72	288	7776	16	-	-124,416
6 - Active Soil	8	0	72	96	2.67	+	256
7 - Water	22.5	255	255	5737.5	11.25	+	64,547
8 - Water	22.5	255	480	2531.3	15	+	37,969
9 - Active Soil	22.5	0	202.5	759.4	15	+	11,390
<b>10 - Collision</b>	-	-	-	<b>6859</b>	24	+	164,622
Total	-	-	-	-	-	-	Σ0

### Local buckling

The local buckling mechanism should now be checked at two locations. When assuming that the connection with the framework is a clamped connection, the tubular pile of the primary wall should be checked just above the framework. The force on the secondary wall is introduced at a level of 9 meters below water surface and the wall should be checked for local buckling just above the concrete floor which is located 24 meters below water level (see Figure 6.7).

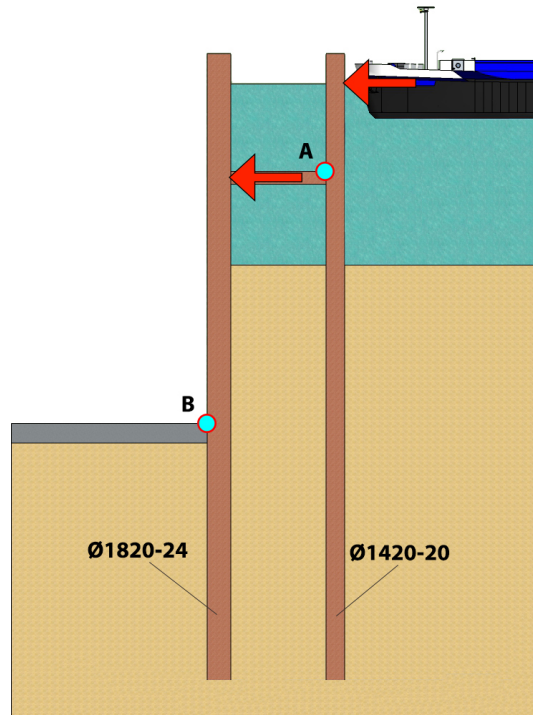


Figure 6.7: Point A and B should be checked for local buckling.

#### Location A

At location A the primary wall consists of a tubular pile connected to a framework. This connection is assumed to be a clamped connection. To determine the maximum allowable bending moment at location A, the different effects described in Chapter 2 should be taken into account. The calculated values can be found in Table 6.4 and a detailed calculation sheet can be found in Appendix H.

Table 6.4: Contribution of different factors on the total out-of-roundness at location A.

Cause	Ovalisation [mm]	Description
Production process	5.3	Normal class
Secondary members	0.0	Water pressures are balanced over the structure
Soil pressure	0.0	No soil pressures
Brazier effect	4.0	Effect of the bending moment
<b>Total</b>	<b>9.3</b>	

The maximum bending moment resistance and the buckling force for the primary wall will become as follows:

$M_{Rd}$	= 13,970 kNm
$F_{Buckle,pile}$	= 1552 kN
$F_{buckle}$	= 1093 kN/m



*Location B*

Local buckling can also occur at location B near the concrete floor of the construction pit. At this location the different effects causing ovalisation of the pile are higher due to the increased depth and different situation. See Table 6.5 for the details.

Table 6.5: Contribution of different factors on the total out-of-roundness at location B.

Cause	Ovalisation [mm]	Description
Production process	6.8	Normal class
Secondary members	14.7	24 meters of water
Soil pressure	9.0	8 meters of soil
Brazier effect	5.4	Effect of the bending moment
<b>Total</b>	<b>35.9</b>	

It is assumed that the piles and sheets are installed correctly and the forces from aberration of the sheet piles are neglected. At location B the pressure due to water and soil only exists on one side of the wall, resulting in a deformed sheet pile as can be seen in Figure 6.8. Beneath the underwater concrete floor, the pressures on both sides of the sheet piling are equal, and therefore cancel each other out.

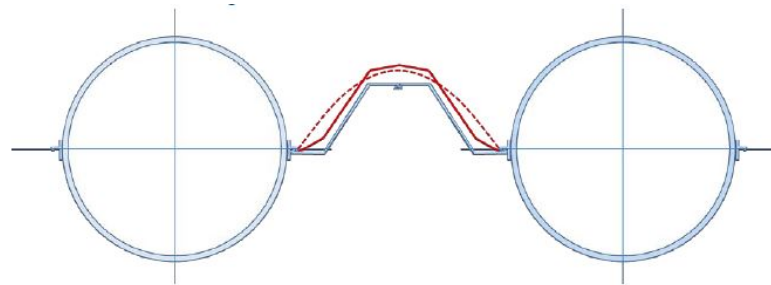


Figure 6.8: Water pressure deforming the secondary elements. Figure by BAAK.

$M_{Rd}$	= 25,414 kNm
$F_{Buckle,pile}$	= 2300 kN
$F_{buckle}$	= 1264 kN/m

### 6.2.3. Failure of the secondary members

Although failure of the interlocking is not likely to happen for the double wall variant, it should be reviewed. As the piles are coupled by the framework, the interlocking is not likely to fail. However, from the description of the case in Chapter 3 it becomes clear that failure of the interlocking could result in flooding of the construction pit, which is to be prevented.

Interlocking failure can occur in two ways. The first option is when a vessel collides with the structure and hits it exactly between two tubular piles. In this case the sheet piling is struck first, resulting in a heavy load on the locks. The second option is when after failure due to local buckling, the pile gives way. Tension will be generated in the interlocking due to the deformation of the pile, and the locks will fail. Failure after local buckling is treated in Section 6.2.4.

### Loading on the structure

In the case of interlocking failure, only the force of the colliding vessel is taken into account. As stated earlier it is assumed that the vessel will hit the structure at water level, which also means that there are no water pressures acting on the structure and pile drift will be minimal.

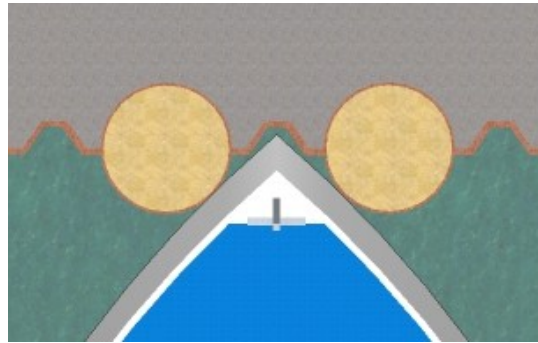


Figure 6.9: Vessel colliding precisely between two piles

It is assumed that the force of the colliding vessel can be distributed over the whole sheet pile as it will easily deform under the loading (see Figure 6.10). Further it is assumed that the tubular piles are not hit in this case and only the sheet pile is loaded.

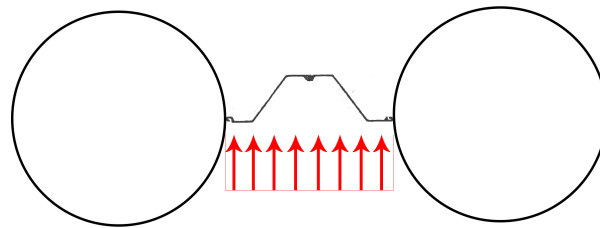


Figure 6.10: Distributed force on the secondary members.

### Interlocking type

There are multiple types of locking available. In this project two types of locking are used, the C6 lock and the C9 lock. The main difference in interlocking type is the way they are attached to the tubular pile. Both are welded to the tubular pile, although the size of locks are different (see Figures 6.11 & 6.12).

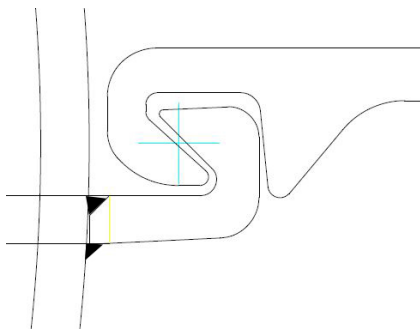


Figure 6.11: C6 Lock. Figure adapted from BAAK.

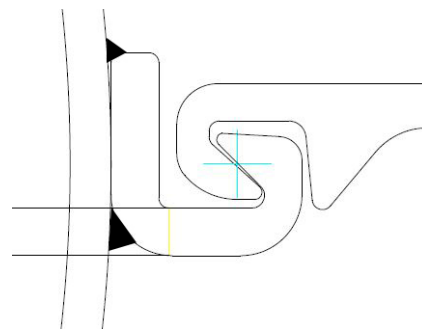


Figure 6.12: C9 Lock. Figure adapted from BAAK.

In general the C6 type of locking is used, but whenever the capacity is not sufficient (as can be the case for significant depth), C9 locking is used. When regarding interlocking failure at water level, only the C6 lock is relevant and evaluated.

Capacity of the locks

The bending moment at which yielding occurs in the outer fiber of a plate is  $M_{el} = f_y \cdot t^2/6$ . This bending moment may increase further in the areas with plastic deformation, reaching asymptotic  $M_{pl} = f_y \cdot t^2/4$  when the yield stress is reached throughout the whole cross-section. The neutral fiber forms the boundary between the zone in tension and the zone that is under pressure. The figures below show the principle in which it is clear that the cross-section will act as a hinge at bending moments that come close to  $M_{pl}$ .

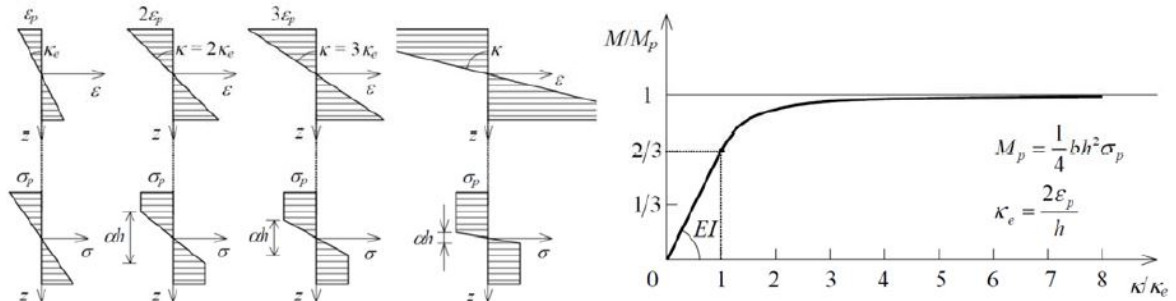


Figure 6.13: Stress/strain development with increasing bending moment (left) and bending moment/curvature (right)

The capacity of the locks is mainly determined by the properties of the material. The first thing that should be taken into account is the steel class, which is S355 for the secondary elements. Secondly, the thickness of the lock elements is of importance. With an increasing thickness a higher bending moment can be resisted.

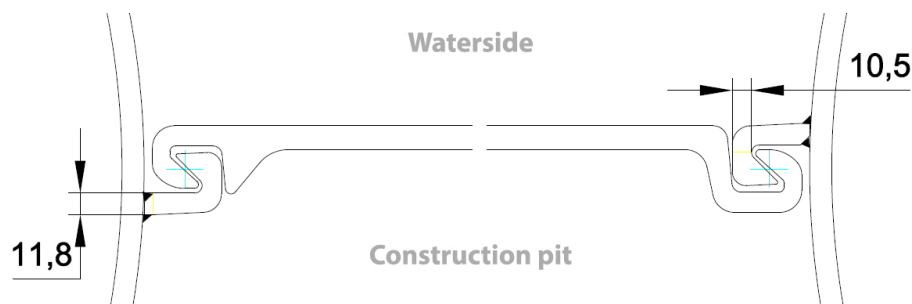


Figure 6.14: Overview of the interlocking: the locks have a different orientation. Figure adapted from BAAK.

Assuming that the sheet pile will deform and form an arch, the resultant force is acting under an angle of 40 to 60 degrees on the locks. The two locks of an AZ profile have a different orientation, which also means that the resistance of both locks is different. As can be seen in Figure 6.15, the resultant forces are assumed to be acting at the end of the secondary elements. From this figure it also becomes clear that the left lock is loaded more than the right lock, as the working line of the force on the right is almost passing through the attachment point of the lock. For the right lock, the governing part is not the attachment with the tubular pile, but the nod in the lock itself.

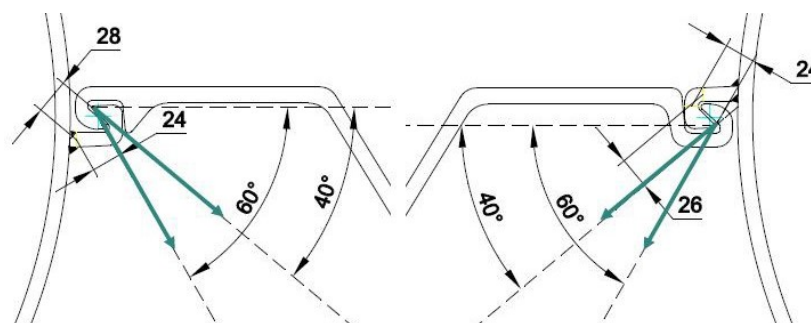


Figure 6.15: Assumed working lines of secondary element forcing. Figure adapted from BAAK.

Due to the forces on the sheet piles, the stresses in the locks will build up and the locks will be worked open as is illustrated in Figure 6.16. Due to this plastic behavior of the left lock, the arm of the force is increasing, reducing the bending moment capacity of the lock. On the right-hand side this is not the case, as after initial clamping the lock of the sheet pile is opening up.

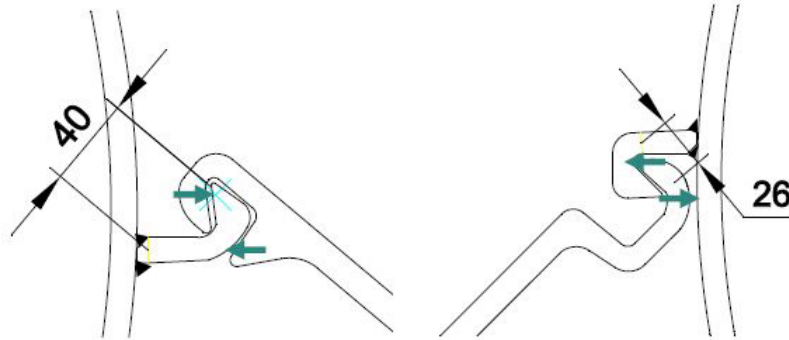


Figure 6.16: Forces acting on the locks after plastic deformation of the locks. Figure adapted from BAAK.

The maximum force on the locks can then be calculated using the bending moment capacity formulas and the arm given in Figure 6.16. The resulting maximum forces for the different states are given in Table 6.6. From this table it becomes clear that the left lock is the governing lock.

Table 6.6: Maximum force on the interlocking system.

Element	Thickness [mm]	State	Moment capacity [kNm/m]	Arm [mm]	Maximum Force [kN/m]
Lock left	11.8	Elastic	8.3	40	207
		Plastic	12.4	40	310
Lock right	10.5	Elastic	6.5	26	250
		Plastic	9.8	26	375

### Maximum force

The failure force for this failure mode can be found by dividing the total force by the length of the sheet piles between the tubular elements. The distance between the primary members is 1.26 meters.

$$\begin{aligned} F_{Interlocking,Elastic} &= 329 \text{ kN/m} \\ F_{Interlocking,Plastic} &= 492 \text{ kN/m} \end{aligned}$$

Failure of interlocking can only occur for vessels that are small enough to hit the secondary members without hitting the primary members (i.e. with the pointy bow of a tug boat or small fishing boat). After penetrating the secondary members, the primary retaining wall has failed. However, in the case with a double end-wall, the construction pit is still safe and as all vessels will have a width larger than 1.26 meters, the vessel will still collide with the tubular piles.

### 6.2.4. Influence of interlocking after local buckling

After local buckling of the tubular pile (assuming no force was acting directly on the secondary element) the interlocking could take up some additional forces. In this section this hypothesis is described in more detail.

#### Post-buckling behavior

After buckling the pile will deform largely and the bending moment capacity will be decreased to values of 40% to 60% of the original value (Van Es, 2016). The post-buckling bending moment capacity can be estimated using Formula 6.1.

$$M_{pb;d}(X_n) = \frac{M_{pb;m}(X_n)}{y_M^*} = \frac{(A \cdot \frac{D_n}{t_n \cdot e_n^2} + B) \cdot (D_n - t_n)^2 \cdot t_n \cdot \sigma_{y;n}}{y_M^*} \quad (6.1)$$

In which:

$\epsilon$	= Cross-sectional slenderness	$\rightarrow \epsilon^2 = 235/\sigma_y$
A	= Dimensionless coefficient	$\rightarrow A = -2.65 \cdot 10^{-3}$
B	= Dimensionless coefficient	$\rightarrow B = 1.04 \cdot 10^0$
$y_M^*$	= Model factor	$\rightarrow y_M^* = 1.28$
$X_N$	= Nominal value of a input parameter	

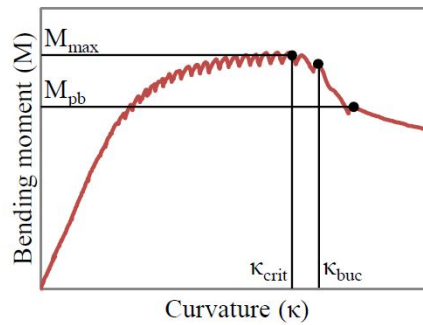


Figure 6.17: Moment-curvature diagram with post-buckling (Van Es, 2016).

As more research into the post-buckling behavior of tubular piles is lacking, the values found by Van Es are a preliminary estimation. Looking at Figure 6.18 a value of 40% seems reasonable but conservative, as this value is lower than what would be expected for a tube with a cross-sectional slenderness of 125.

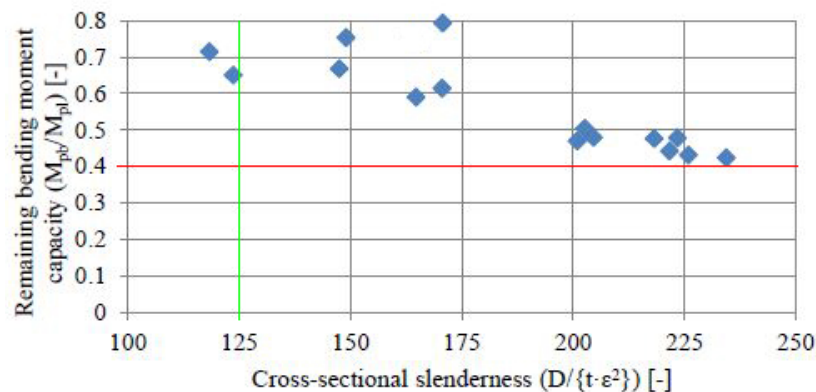


Figure 6.18: Overview of the remaining post-buckling bending moment capacity of the tested specimens (Van Es, 2016).

### Deformation after buckling

After buckling, the tubular pile will start to deform into the pit and the maximum displacement of the pile will be at the top of the pile. After some initial deformation (see Figure 6.3), the interlocking will begin to resist some forces. These forces can be regarded as positive and resisting. The collision force is acting at the height of the water level. It is assumed that only the top meter of the pile will reach the maximum allowable deviation of the pile. This will result in two extra resisting forces coming from the interlocking with the sheet piles.

### Angle of impact

Important for this situation is the angle of impact of the collision. Dependent on the collision angle, the pile can buckle away in multiple directions. Neglecting the ovalisation and its effect on the direction of buckling, it is assumed that the pile will buckle in the same direction as the forcing (see Figure 6.19). The two limit cases will be described as the 'head-on' collision and the 'brushing' collision of the structure.

#### *Head-on collision*

As can be seen from the figure, during the head-on collision, the two sheet piles connecting to the pile are being pulled under an angle. This angle, assuming a maximum lengthening of the sheet pile of 87 mm (see again Figure 6.3), is calculated to be 20.7 degrees. This value is less than half of the angle used in the previous section for calculating the limit values for the interlocking. The working line of the forces will therefore pass closer to the governing section in the interlocking, reducing the arm of the force and resulting in a higher bending moment capacity. In order to be conservative, still the limit values for an angle of 45 degrees are used. See Table 6.6 for the specific values.

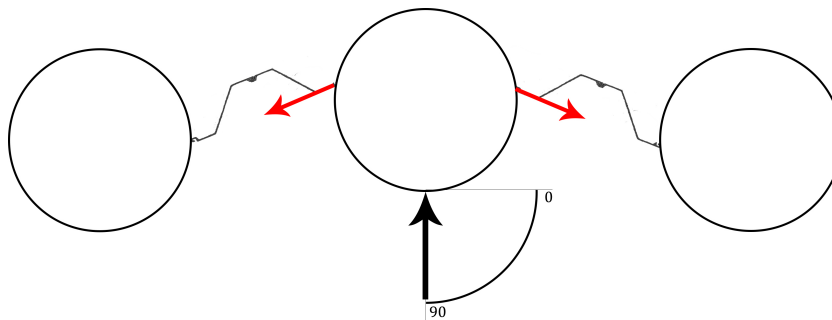


Figure 6.19: The head-on collision case, the angle of impact 90 degrees.

#### *Brushing collision*

The brushing case is a theoretical one, as a collision can never be completely parallel to the structure. However, this approach will give a limit value for the impact angle of 0 degrees, where-after the intermediate impact angles will be estimated. When colliding under an angle of 0 degrees, the sheet piles are loaded in the line of the structure. It is assumed that the compressive strength of the sheet pile is minimal and only tension forces can be resisted. In this manner only one sheet pile is activated when colliding under an angle. The only case when both sheet piles take up tension forces is during a head-on collision.

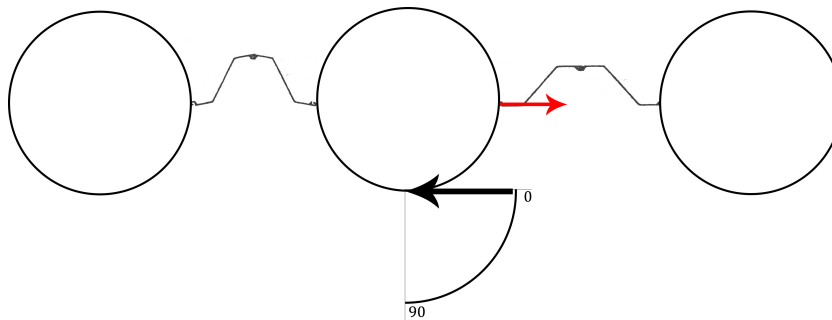


Figure 6.20: The 'brushing' collision case, angle of impact is zero degrees.

The force at the interlocking in the 'brushing' case is acting at a distance of approximately 16mm of the turning point, see Figure 6.21.

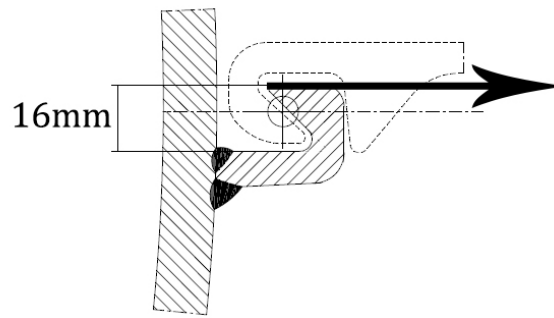


Figure 6.21: The 'brushing' collision case with a force and a arm of 16 mm. Figure adapted from BAAK.

#### Failure forces due to influence of the interlocking

Combining the post-buckling behavior and the capacity of the interlocking, one can set-up a relationship between the angle of impact and the failure force. When assuming a linear relation between angle of impact and the failure force, the graph in Figure 6.22 arises.

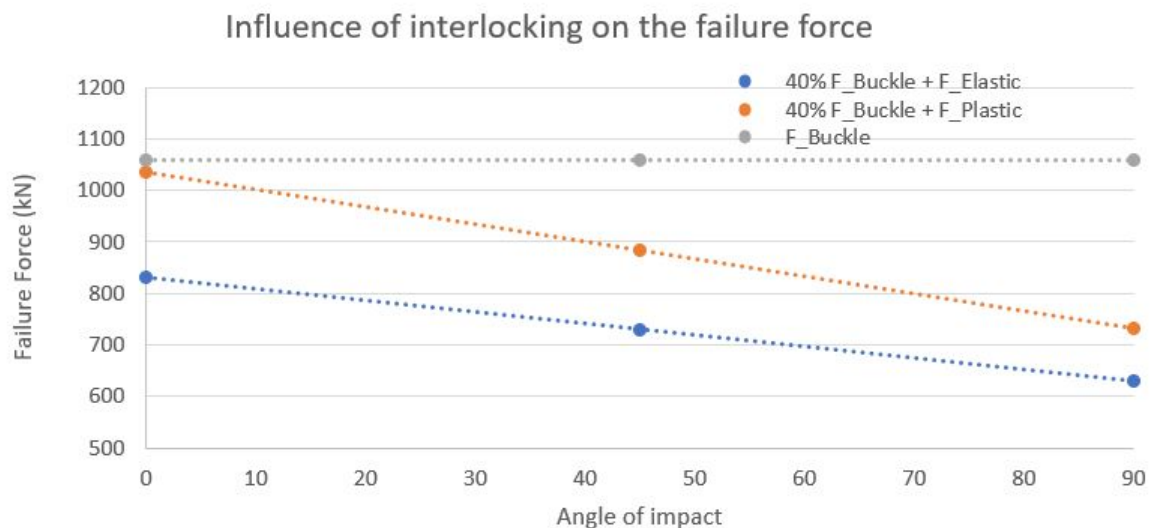


Figure 6.22: Influence of interlocking on the post-buckling behavior.

The failure force of this mode is dependent on the angle of impact  $\alpha$ . The maximum value is 1035 kN for a complete parallel collision and decreases with an increasing impact angle. It can be concluded that after buckling a significant residual resistance is present in the structure, however this resistance is lower than the original force on the structure after which buckling occurred.

#### 6.2.5. Failure of the welded joints

In the previous calculations plastic deformation is allowed in the interlocking system. This is only acceptable as long as the interlocking itself is welded properly to the pile. It is important to check this part of the interlocking, as high tension forces can occur.

Joints can be welded in several different ways as can be seen in Figure 6.23. The parameter that is important for the calculation of the strength of the welds, is the effective throat of the weld. From the figure it becomes clear that the effective thickness varies depending on the type of welding.

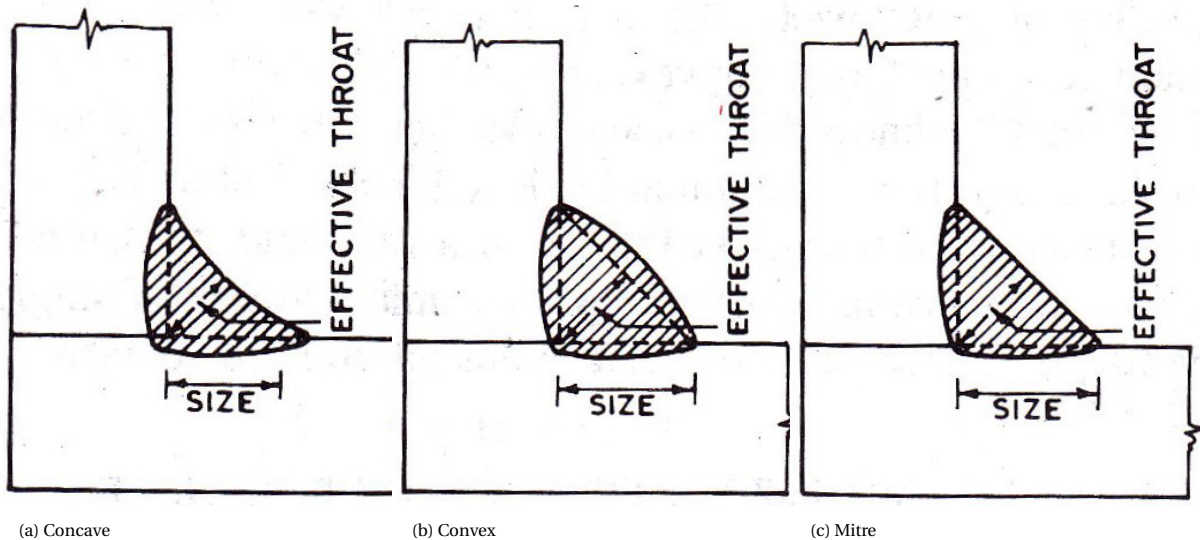


Figure 6.23: Three types of welded joints. Adapted from <http://ecoursesonline.iasri.res.in/>

According to the EN1993-1-8 (2005) the design weld resistance per unit length can be given as:

$$F_{w,Rd} = f_{vw,d} \cdot a \quad (6.2)$$

In which:

- $F_{w,Rd}$  = design weld resistance per unit length
- $f_{vw,d}$  = design shear strength of the weld
- $a$  = effective throat thickness

The design shear strength of the weld can be calculated using:

$$f_{vw,d} = \frac{f_u / \sqrt{3}}{\beta_w \cdot \gamma_{M2}} \quad (6.3)$$

In which:

- $f_u$  = nominal ultimate tensile strength of the weaker part joined
- $\beta_w$  = correlation factor, 0.9 for S355 steel.
- $\gamma_{M2}$  = model factor, 1.25 for yielding fail mechanism

In the design by BAAK a mitre filled weld (see Figure 6.23c) with a minimal throat thickness of 8 mm is used. For the welds in this design the weld resistance can be calculated and is found to be:

$$F_{w,Rd} = \frac{510 \text{ MPa}}{0.9 \cdot 1.25 \cdot \sqrt{3}} \cdot 8 = 2100 \text{ kN/m}$$

When comparing this value to the maximum force in the locks from Section 6.2.3, the failure of the welded joints can be considered non-governing.



### 6.2.6. Summary

In this section the strength of the double endwall is calculated. The failure forces can be summarized as follows:

Table 6.7: Failure forces for the different failure modes.

Failure Force		Magnitude	
$F_{Sliding}$	=	30,000	kN/m
$F_{Rotational}$	=	6,859	kN/m
$F_{Buckling,A}$	=	1,093	kN/m
$F_{Buckling,B}$	=	1,264	kN/m
$F_{Interlocking,Elastic}$	=	329	kN/m
$F_{Interlocking,Plastic}$	=	492	kN/m
$F_{Welding}$	=	1,667	kN/m

From this table it becomes clear that buckling of the tubular elements is the governing failure mechanism. Failure of the interlocking is disregarded, as a minor breach of the sheetpiles does not endanger the lives of the workers in the construction pit.

#### Influence of the framework

The now calculated failure forces are based on calculation per meter. However, due to the presence of the framework, the piles in the wall are coupled and the strength of the structure is increased. The end-wall in the case of the Maasdelatunnel is made out of a maximum of 12 piles. When assuming that the coupling between framework and piles is excellent, the resistance is increased with a factor of 12.

### 6.3. Single combi-wall

Instead of a double combi-wall, a new variant is proposed consisting of a single combi-wall. It should be checked which amount of forcing this structure can withstand. In Figure 6.24 the detailed overview of the variant is given. The depth of the construction pit is the same as for the original design and for the size of the tubular elements the larger one of the two, used in the double wall, is chosen.

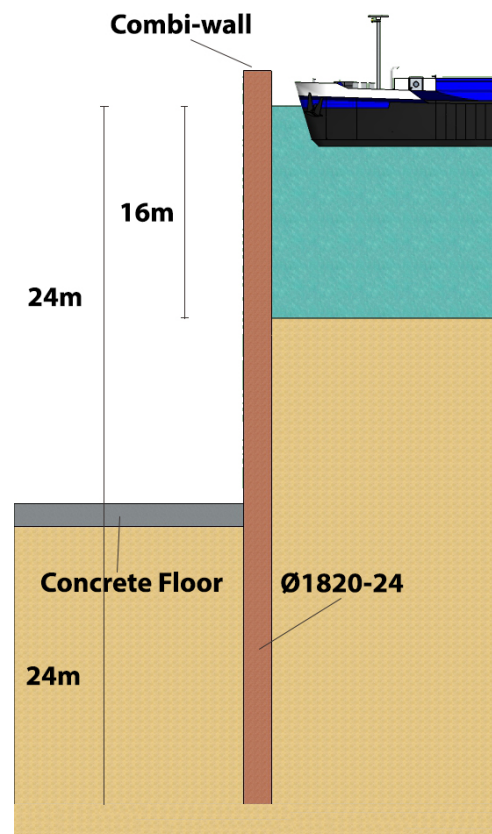


Figure 6.24: Details of the single combi-wall variant.

The characteristics for this variant are given in Table 6.8.

Table 6.8: Characteristics of the elements for the single combi-wall.

Wall	Element	Steel	$E_s$ [N/mm <sup>2</sup> ]	$f_y$ [N/mm <sup>2</sup> ]	Diameter [mm]	Thickness [mm]	$D/t\epsilon^2$ [-]	Length [m]
Primary	Tubular pile	X70	210,000	482	1820	24	125	48
	AZ Sheet piling	S355	210,000	355	-	12.2-13.0	-	48

#### Soil resistance

To determine the pile deformation, the stiffness of the soil should be known. Out of the data obtained from BAAK the soil properties for the case of the Blankenburg are known (see Appendix A). To ease up the calculation, it is assumed that the soil only consist of sand. The p-y curves (mentioned in section 2.3.4) of Reese et al. (1974) are used for sandy soils. Here only the results of the calculation are shown. The complete calculation method can be found in Appendix F.

#### 6.3.1. Local buckling

The governing section for failure due to local buckling can be found at the place where the biggest bending moments occur. In the model this place is located at the underwater concrete layer level (see also Figure 6.25), located at a depth of approximately 24 meters.

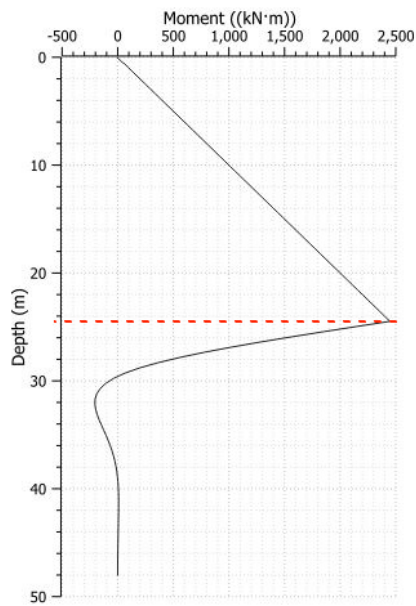


Figure 6.25: Governing cross-section regarding local buckle

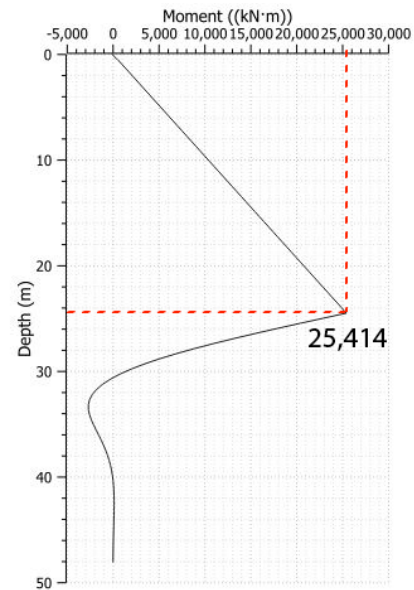


Figure 6.26: Bending moment for a total force on the pile of 1058.9 kN.

### Combining the ovalisations

The values of  $a$  caused by the different ovalizing effects shall be combined in order to calculate the critical strain and the bending moment resistance of the tube. In Table 6.9 the total ovalisation is given for the tubular pile of which the characteristics are given in Table 6.2.

Table 6.9: Contribution of different factors on the total out-of-roundness for a single combi-wall.

Cause	Ovalisation [mm]	Explanation
Production process	6.8	Normal class
Secondary members	14.7	24 meters of water
Soil pressure	9.0	8 meters of soil
Brazier effect	5.4	Effect of the bending moment
<b>Total</b>	<b>35.9</b>	

### Iteration process

The bending moment resistance of the pile is in a small amount dependent on the acting bending moment, as the Brazier effect is a second order effect. A bigger bending moment will result in more ovalisation which reduces the bending moment resistance. After some iterations a value of 26,489 kNm is found.

$$\overline{M_{Rd}} = 25,414 \text{ kNm}$$

This resistance value can then be translated into a force on top of the pile. Assuming that the pile is clamped at the underwater concrete floor, the calculation becomes rather simple. One should note that assuming a clamped connection is conservative, as small rotations may occur lowering the actual bending moment in the pile. As the soil is calculated to be quite stiff at a depth of 24 meters (see Appendix F), this reduction is neglected and a value for  $F_{buckle}$  is found.

$$\overline{F_{Buckle,Pile}} = 1058.9 \text{ kN}$$

$$\overline{F_{Buckle}} = 582 \text{ kN/m}$$

### 6.3.2. Rotational stability

Another failure mode which can lead to severe consequences is when the piles are rotating around the concrete floor. The situation is illustrated in Figure 6.27. In this it is assumed that the two combi-walls act as one rigid structure with the turning point indicated in red.

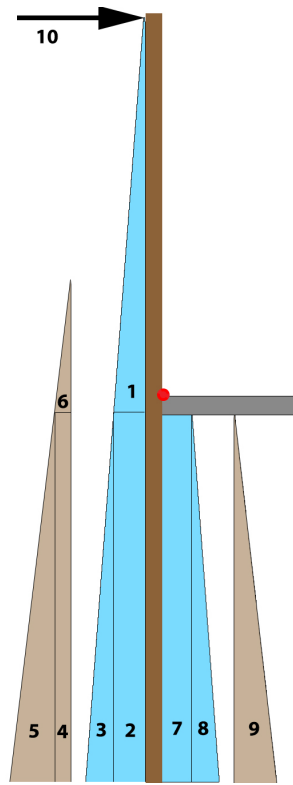


Figure 6.27: Schematization in order to assess the rotational stability of a single tubular pile.

The maximum allowable force can be calculated by calculating the turning moment around the underwater concrete floor. For the soil pressures the active and passive soil coefficients, mentioned in Section 2.3.4, should be taken into account. In Table 6.10 the different parts are indicated and their contribution is calculated.

$$\underline{F_{Rotational} = 6859 \text{ kN/m}}$$

Table 6.10: Rotational stability of a tubular pile as part of a construction pit.

Section	Height [m]	Pressure Top [kN/m <sup>2</sup> ]	Pressure Bottom [kN/m <sup>2</sup> ]	Force [kN/m]	Arm [m]	Contribution [+/-]	Moment [kNm/m]
1 - Water	24	0	240	2880	8.00	+	23040
2 - Water	24	240	240	5760	12	-	-69120
3 - Water	24	240	480	2880	16	-	-46080
4 - Passive Soil	24	72	72	5184	12	-	-62208
5 - Passive Soil	24	72	288	7776	16	-	-124416
6 - Active Soil	8	0	72	96	2.67	+	256
7 - Water	22.5	255	255	5737.5	11.25	+	64547
8 - Water	22.5	255	480	2531.3	15	+	37969
9 - Active Soil	22.5	0	202.5	759.4	15	+	11390
<b>10 - Collision</b>	-	-	-	<b>6859</b>	24	+	164622
Total	-	-	-	-	-	-	$\Sigma 0$

### 6.3.3. Summary

In this section the strength of the single end-wall is calculated. The failure forces can be summarized as follows:

Table 6.11: Failure forces for the different failure modes.

<b>Failure Force</b>	<b>Magnitude</b>	
$F_{Sliding}$	= 45,000	kN/m
$F_{Rotational}$	= 6,859	kN/m
$F_{Buckling}$	= 582	kN/m
$F_{Interlocking,Elastic}$	= 292.7	kN/m
$F_{Interlocking,Plastic}$	= 438.4	kN/m
$F_{Welding}$	= 2100	kN/m

From this table it becomes clear that buckling is the governing failure mechanism. Failure of the interlocking is disregarded as all vessels will eventually hit the primary elements of the end-wall and a minor breach due to interlocking failure does not endanger the lives of the workers.

## 6.4. Conclusion

The resistance of the structure largely determines the safety of the pit. The design with double end-wall has higher resistance due to the decreased arm of the impact force with respect to the turning point. Furthermore, the effects of the framework can not be neglected. The framework couples all the piles in the wall and also couples the primary wall with the secondary wall, making it a more robust system.

In the case of a single end-wall, the governing failure mechanism is the buckling of the primary elements. As no framework is present in this design, the piles should be considered separately. After local buckling of a pile, the bending moment resistance is reduced. Due to the lack of research in the residual strength of tubular piles, a conservative value of 40% is taken. Combining this residual strength with the tension capacity of the secondary members, some additional strength can be found. However, this value will be lower than the failure load for local buckling of the pile.

An overview of the failure forces for the two variant is given in Table 6.12.

Table 6.12: Failure forces for different failure mechanisms

System	Failure mechanisms		
	Sliding along the base	Toppling of the wall	Structural failure
<b>Double end-wall</b>	45,000 kN/m	6,859 kN/m	1,093 kN/m
<b>Single end-wall</b>	45,000 kN/m	6,859 kN/m	582 kN/m

## Sensitivity analysis for the end-wall

*In this chapter the previous chapters (the probability of a collision, the magnitude of the force and the resistance of the structure) are combined to give an estimate of the probability of failure and to estimate the safety of the construction pit. In Section 7.1 the safety of the construction pit is treated. Section 7.2 treats the different parameters which can be adapted and their influence on the safety of the construction pit. The conclusions based on this chapter are given in Section 7.3.*

### 7.1. Safety of the construction pit

As stated already in Chapter 2, the safety of the pit is determined by the individual risk criteria. In this section the required safety level is determined.

#### 7.1.1. Individual risk

From statistical data it can be concluded that the extent to which participation in an activity is voluntary strongly influences the level of risk that is accepted (Jonkman et al., 2017). Higher levels of risk are accepted for activities that are voluntary and have a (personal) benefit. Much smaller risks are accepted for activities that are involuntary, without benefit and imposed by others. A policy factor ( $\beta$ ) is introduced to account for the amount of voluntariness of an activity. The baseline is defined as the individual risk for young men who are at risk from driving in traffic, for this value ( $10^{-4}$ ) a  $\beta$  values of 1 is used see Table 7.1.

Table 7.1: Accident statistics and proposed policy factor and characteristics of the activity (Jonkman et al., 2017)

Prob. of Death (per year)	Example / Application	$\beta$	Voluntariness	Benefit
$10^{-2}$	Mountain climbing	100	Voluntary	Direct benefit
$10^{-3}$	Driving a motor cycle	10	Voluntary	Direct benefit
$10^{-4}$	Driving a car	1	Neutral	Direct benefit
$10^{-5}$	Flooding	0.1	involuntary	Some benefit
$10^{-6}$	Factory / LPG Station	0.01	Involuntary	No benefit

People working in a construction pit tend to do this involuntarily, but have some benefit from it in form of salary, therefore a  $\beta$  value of 0.1 is proposed as a limit value. The individual risk limit can then be calculated using Equation 7.1.

$$IR < \beta \cdot 10^{-4} \quad (7.1)$$

If the conditional probability of death due to an accident  $P(d|f)$  is known, the accepted probability of failure can be calculated using Equation 7.2.

$$P_f \leq \beta \cdot 10^{-4} / P_{d|f} \quad (7.2)$$

In case of complete flooding of the pit, the conditional probability of death is set to 1 and the resulting limit value for the construction pit becomes:

$$P_f \leq 10^{-5}$$

### 7.1.2. Probability of failure of the end-wall

In Chapter 4 the probability of a collisions is estimated, after which in Chapter 5 the relative frequency of the magnitude of the collision forces is given based on the actual data of the Scheur. In Chapter 6 the failure forces for the end-wall are determined.

Now the different sections can be put together, to estimate the probability of failure of the end-wall. In Table 7.2 the calculated failure probability for 1 tubular pile is given. This is the basic situation from which other parameters are being varied to look at their influence on the probability of failure.

Table 7.2: Failure probability of the single end-wall, 1 activated tubular pile.

Single end-wall - 1 Tubular pile			
Load		Resistance	Safety
P(Collision)	$P(F > F_{failure})$	$F_{failure}$	P(Failure end-wall)
2.730 E-06	0.986	1.058 MN	2.692 E-06

Table 7.3: Failure probability of the double end-wall, 12 activated tubular piles.

Double end-wall - 12 Tubular piles			
Load		Resistance	Safety
P(Collision)	$P(F > F_{failure})$	$F_{failure}$	P(Failure end-wall)
2.730 E-06	0.386	13.116 MN	1.054 E-06

A graphical representation of the resistance of the structure and the corresponding failure probability is given in Figure 7.1. The added area on the left of the presented lines is the probability that a collision can be resisted.

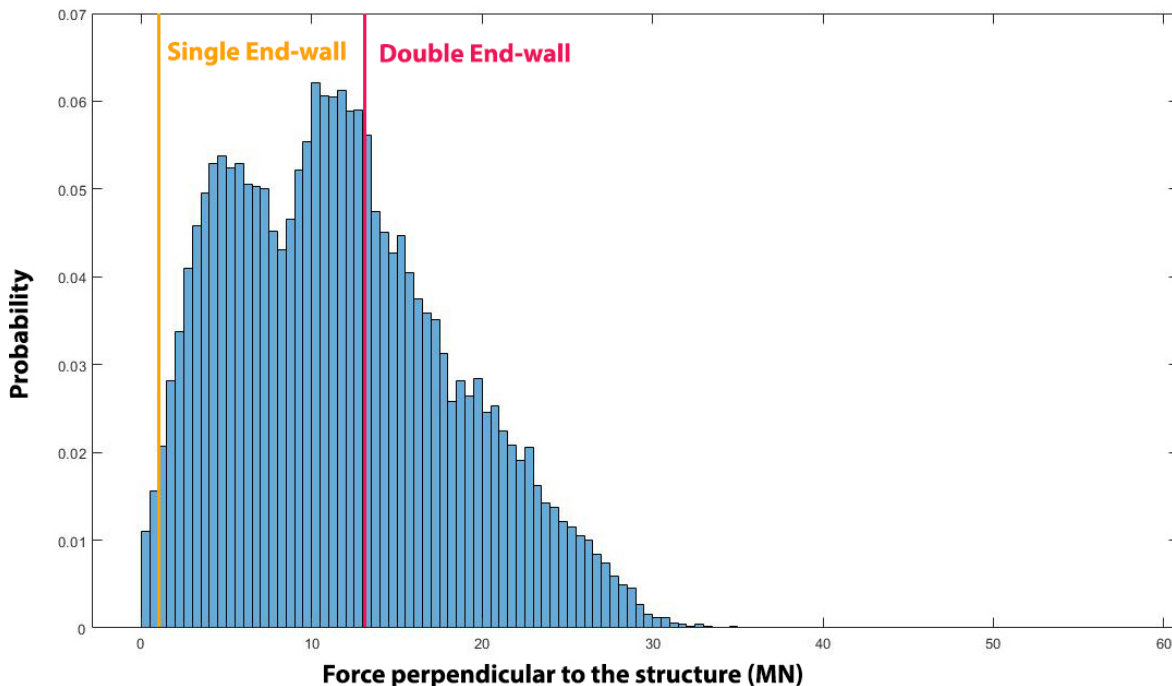


Figure 7.1: Resistance of the structure. Single end-wall (Orange) and double end-wall (Pink).



## 7.2. Parameters to study

In the previous chapters three different aspects of a ship collision in the Scheur are treated, namely the probability of collision, the magnitude of the forcing and the resistance of the structure. To give more insight on which measures are feasible to improve the safety of the pit, a sensitivity analysis is done. For each of the three aspects two cases are selected based on their importance or ease of adaptability.

#	Aspect	#	Parameter	Description
A	- Probability of a collision	1	- Type of vessel	At the Scheur the fleet consists of seagoing and inland going vessels. In order to take measures to prevent failure of the pit, it is interesting to know which vessel type is the governing one and what the failure probabilities are, related to this type.
		2	- Traffic distribution	From Chapter 4 it can be concluded that the most influential parameter which can easily be adapted, is the traffic distribution. By implementing regulations, the project owner can ensure that vessels do not encounter each other in the channel.
B	- Magnitude of the force	1	- Angle of the pit	The construction pit at the North side of the Scheur is constructed under an angle of 30 degrees with the waterway. In Chapter 5 it was argued that the angle of the pit could influence the magnitude of the force. It is interesting to see what the influence of the angle is and if this is beneficial for the design or not.
		2	- Friction coefficient	The reduction factor ( $\delta$ ), which is used for calculation of the impact force for vessels colliding under an angle, is based on the friction between vessel and structure. When changing the material of the structure, the friction coefficient can be lowered which influences the magnitude of the impact force.
C	- Resistance of the structure	1	- Number of activated piles	A single pile will lead to failure in 98.6% of the cases (see Section 7.1.2). When a rigid structure is formed, more piles can be activated, increasing the resistance of the structure.
		2	- Filled piles	Failure of the tubular piles is directly coupled to the buckling resistance of the pile. When filling the piles with sand or concrete, the amount of ovalisation of the pile is reduced, leading to a higher resistance of the structure.

## A1 - Type of vessel

At the project location the fleet exists of inland and seagoing vessels. As seagoing vessels are bigger and have a larger DWT, the general sense is that these vessels will be the governing ones. However, due to their low relative frequency in the fleet, this might not be true. In order to see their separate contribution to the probability of failure, the different type of vessels are split and examined.

In Table 7.4 the difference between the two types of vessels becomes clear. The probability of failure of the end-wall is about 11% higher for inland going vessels. This is mainly due to the fact that the probability of a collision is higher. The probability that the force will exceed the failure force is in the same order of magnitude.

Table 7.4: Comparison between seagoing and inland going vessels.

	<b>P(Collision)</b>	<b>Case</b>	<b>P(F &gt; F<sub>failure</sub>)</b>	<b>P(Failure end-wall)</b>
<b>Seagoing</b>	2.518 E-06	1 Pile	0.979	2.465 E-06
<b>Inland going</b>	2.760 E-06	1 Pile	0.987	2.724 E-06

When considering that seagoing vessels make up only 12.4% of the fleet, the probability that a collision of a seagoing vessel will result in failure, will decrease even more. This is also visualized in Figure 7.2. In this figure the area of both graphs combined has a total area of 1. The area in the right figure, the seagoing vessels, is significantly smaller meaning a lower probability.

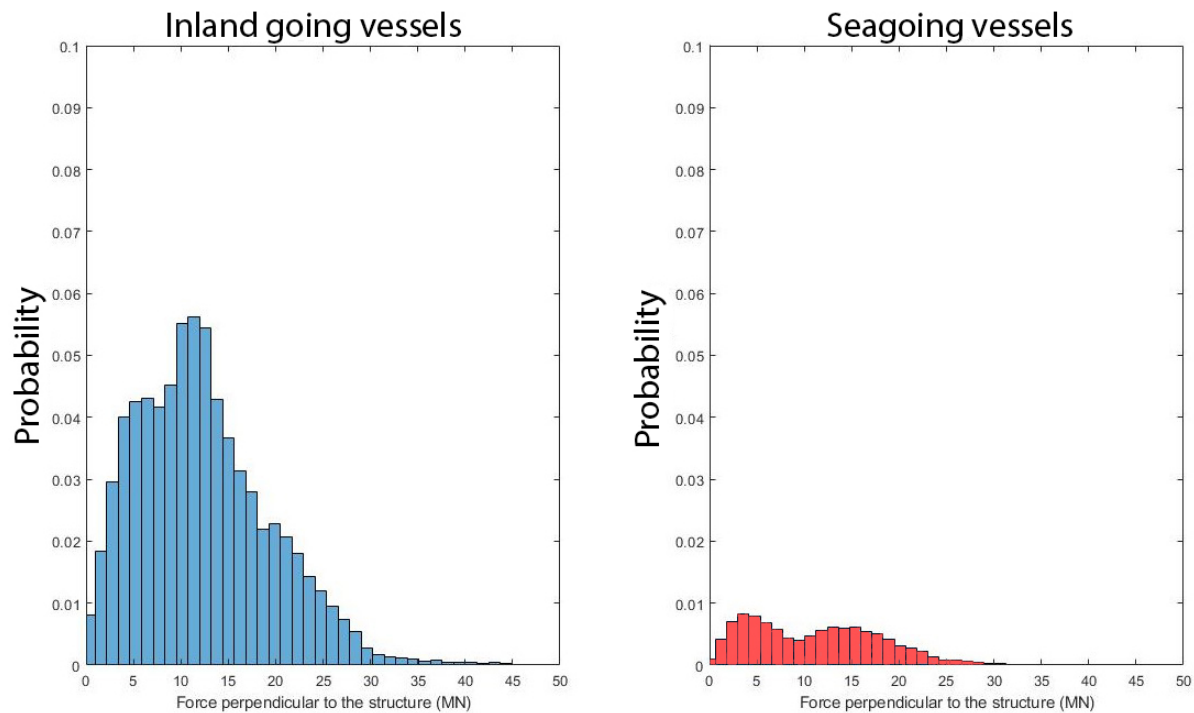


Figure 7.2: The relative frequency of collision force for inland going (left) and seagoing (right).

## A2 - Traffic distribution

In Chapter 4 different measures are proposed in order to reduce the probability of a collision. One of the most influential nodes is the traffic distribution. This describes the probability of a vessel encountering another vessel in the waterway. The proposed solution is to impose regulations, regulating shipping in the channel in such a way that blocks of incoming and outgoing vessels are created. This concept is also known from aviation, although there it is implemented to maximize capacity of the airport.

By implementing these regulations, vessels are prohibited to sail in two directions in the channel. Every thirty minutes the sailing direction changes, ensuring enough window for all vessels to sail towards or from the harbor. The positive effect of this measure is given in Table 7.5.

Table 7.5: Influence of the different states of two nodes on the probability of a collision.

Node	Positive difference
Traffic distribution	3.80 E-07

1 Tubular Pile - $P_f$
2.692 E-06

The total failure probability of the end-wall can now be calculated and is given in Table 7.6.

Table 7.6: Failure probability with imposed .

Pilot presence on all vessels			
Load		Resistance	Safety
P(Collision)	$P(F > F_{failure})$	$F_{failure}$	P(Failure end-wall)
2.350 E-06	0.986	1.058 MN	2.317 E-06

Implementing these regulations certainly results in longer waiting times for vessels, which consequently also has economic consequences. Another side effect which could occur after implementing these regulations, is that the amount of overtaking vessels will increase. Due to the waiting time, the vessels will be more concentrated together possibly resulting in an increase of overtaking. The additional risks connected to this are unknown and are not part of this research. The optimization of these regulations and how they should be implemented is out of the scope of this research, but further research is recommended to give insight in all consequences and side effects.

### B1 - Angle of the pit

In the case of the Blankenburg connection one of the construction pits is built under an angle. To determine the influence of this design choice, the construction site on the south side of the Scheur is placed under different angles (see Figure 7.3). This method is changing the probability of occurrence of forces on the structure and will therefore influence the failure of the end-wall.

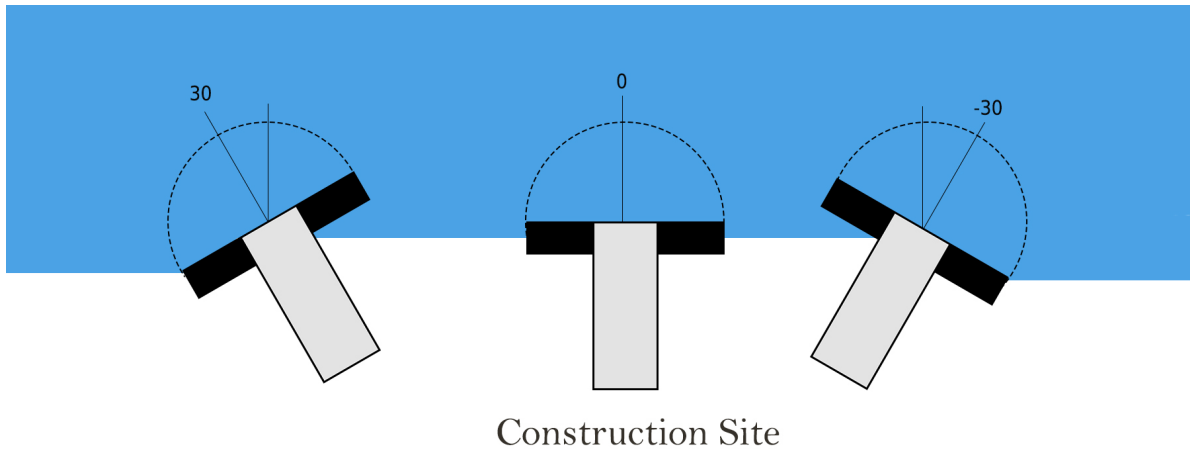


Figure 7.3: Definition of the angles of the construction pit.

In Table 7.7 the probability of failure of the end-wall is given for the different angles. In this case it is assumed that 10 piles are activated and the effect of the angle is based on that situation. As can be seen in the table, for small positive angles (see Figure 7.3 for the positive/negative definition) a small reduction of the probability is observed.

Table 7.7: Failure probability of the end-wall for different angles.

Angle	1 Tubular pile under an angle			10 Tubular piles under an angle		
	$P(F > F_{failure})$	$P(\text{Failure end-wall})$	Change %	$P(F > F_{failure})$	$P(\text{Failure end-wall})$	Change %
30	0.635	1.734 E-06	-35.6	0.473	1.291 E-06	-14.6
20	0.714	1.949 E-06	-27.6	0.480	1.310 E-06	-13.4
10	0.853	2.329 E-06	-13.5	0.500	1.365 E-06	-9.7
0	0.986	2.692 E-06	0	0.554	1.512 E-06	0
-10	0.999	2.727 E-06	+1.3	0.668	1.824 E-06	+20.6
-20	0.996	2.719 E-06	+1.0	0.714	1.949 E-06	+28.9
-30	0.932	2.544 E-06	-5.5	0.719	1.963 E-06	+29.8

When placing the construction site under a negative angle, the probability of failure increases, but is steady for all negative angles. This is not what was to be expected and can be explained by the fact that impact angles greater than 90 degrees, are assumed to be perpendicular to the structure.

## B2 - Friction coefficient

For the calculations in the single pile model, it is assumed that both the structure and the hull of the colliding vessel are made of steel. This is an important fact, as the friction between the two surfaces causes a ship to 'stick' or to 'slide'. In the calculations with both surfaces made of steel, a friction coefficient of  $\mu=0.5$  is used which was proposed by the ROK. Zhang and Pedersen (1999) did some research into the influence of the friction coefficient in the case of ship collisions. In Figure 7.4 their graphs are compared with the energy reduction graph based on the values of the ROK.

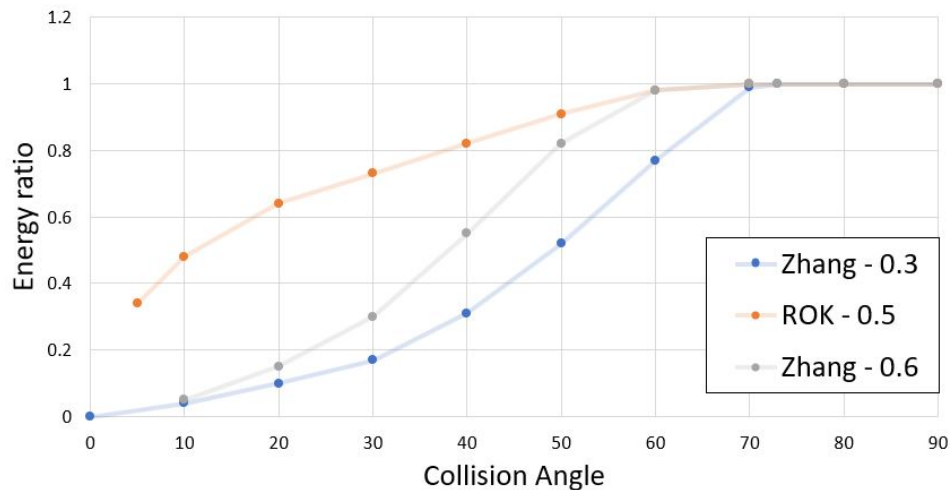


Figure 7.4: Energy reduction for different friction coefficients and impact angles.

In Appendix E a more detailed explanation of friction is given. In case of a collision on a construction pit, five different ways are distinguished to reduce the friction between the vessel and the construction:

1. Make the surface smoother
2. Make use of lubrication
3. Reduce forces acting on the surface
4. Reduce the friction surface
5. Replace sliding elements with rolling elements

Considering the single combi-wall variant and the above stated options, one can say that the outside of the combi-wall should be smooth (1). This can be achieved by placing a girder in front of the combi-wall, preventing the vessel to get stuck in the space between two piles. Additionally, the surface of the girder should be lubricated or equipped with material with a lower friction coefficient (2). As only the resistance part can be changed, option (3) is not a viable solution for this case. The last two options are difficult to achieve, as the collision force should be resisted. Reducing the height of the girder in order to minimize the surface area(4), would result in less spreading of the force and higher chances of penetrating the hull of the ship. The same holds for rolling fenders(5); when crushed during collision they will loose their friction reduction effectiveness.

In the situation that will be calculated, it is assumed that one pile is equipped with carbon, resulting in a friction coefficient of 0.14. As no graph and values are available for  $\mu=0.14$ , a safe value of 0.3 is chosen and Figure 7.4 is used to determine the energy reduction.

Table 7.8: Failure probability of the end-wall for reduced friction coefficient.

I Tubular pile and reduced friction			
Load		Resistance	Safety
P(Collision)	$P(F > F_{failure})$	$F_{failure}$	P(Failure end-wall)
2.730 E-06	0.721	1.058 MN	1.968 E-06

### C1 - Amount of activated piles

In order to strengthen the structure, an infinite rigid beam can be placed in front of the structure, activating multiple piles in order to resist the collision load. For this calculation the amount of activated piles will be increased to an amount of 10, see Figure 7.5.

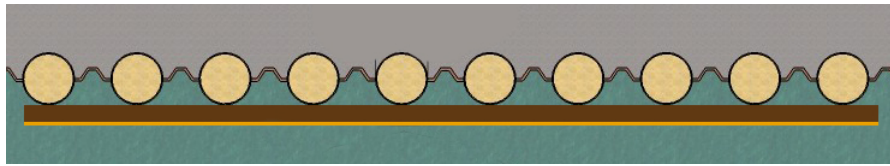


Figure 7.5: Activating multiple piles by using a girder.

Due to the increased number of activated piles, the failure probability of the end-wall will change and the value is given in Table 7.9.

Table 7.9: Failure probability of the end-wall for 10 tubular piles.

10 Tubular piles			
Load		Resistance	Safety
P(Collision)	$P(F > F_{failure})$	$F_{failure}$	P(Failure end-wall)
2.730 E-06	0.554	10.58 MN	1.512 E-06

Table 7.10: Failure probability of the end-wall for 20 tubular piles.

20 Tubular piles			
Load		Resistance	Safety
P(Collision)	$P(F > F_{failure})$	$F_{failure}$	P(Failure end-wall)
2.730 E-06	0.119	21.16 MN	3.249 E-07

The change in failure probability can also be illustrated using Figure 7.6. In this figure the blue area represents the amount of collisions which can be resisted by a single tubular pile. The white area are the additional collisions which can be resisted when activating 10 piles instead of one, and the same holds for the green area and 20 activated piles. The red bar charts are the collisions which still result in failure. As can be seen from the figure, increasing the number piles is beneficial till an amount of approximately 28 piles (resistance of 30MN).

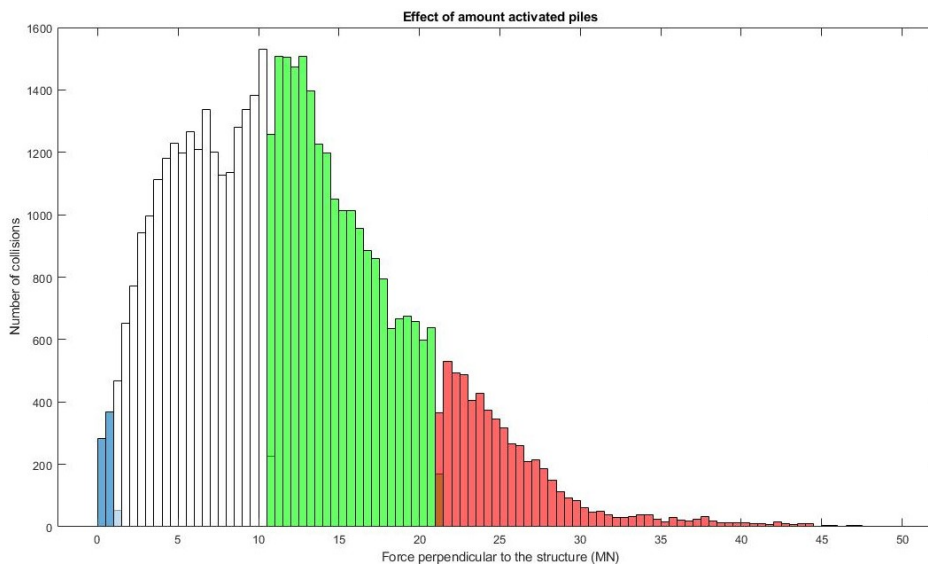


Figure 7.6: Distribution of collision forces for n=50,000 and the resistance for 1 (blue), 10 (white) and 20 (green) activated tubular piles.

## C2 - Filled tubular piles

An other option in making the combi-wall more resistant is filling the piles with sand or concrete. In this way the ovalisation of the pile is hindered, increasing the local buckling limit. For the sand filled tubes the used approach is that the sand fill's resistance against compression provides extra spring stiffness  $k = q / a$  to the steel ring, see Figure 7.7. The action of the sand matrix in preventing ovalization is primarily elastic and occurs at low strains. Although the failure mechanism of the sand fill and the behavior of the sand-fill when subjected to large deformations and small volume decrease may be rather complex, for the elastic compression of sand a simple 1D elastic model suffices (HASKONINGDHV, 2018).

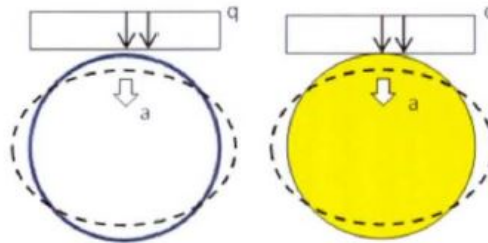


Figure 7.7: Stiffness of the steel tube and of the sand volume (CUR211, 2014).

The out-of-roundness for the sand-filled pile can be calculated as follows:

$$a_{sand-filled} = a_{empty} \cdot \frac{k_{steel}}{k_{steel} + k_{sand}} \quad (7.3)$$

In which:

$$k_{steel} = \frac{12EI}{r^4}$$

$$EI = \frac{1}{12} \cdot E_{steel} \cdot t^3$$

$$k_{sand} = \frac{E_{sand}}{r}$$

A safe value for  $E_{sand}$  of 10MPa is recommended by HASKONINGDHV (2018). The reduction factor for the out-of-roundness due to tensile forces, soil pressure and overall curvature is determined to be 0.29. The failure force for the single combi-wall is now increased to a value of 1292 kN.

Table 7.11: Failure probability of the end-wall for 1 sand-filled tubular pile.

<b>1 Tubular pile sand-filled</b>			
Load		Resistance	Safety
P(Collision)	P(F>F <sub>failure</sub> )	F <sub>failure</sub>	P(Failure end-wall)
2.730 E-06	0.981	1.292 MN	2.678 E-06

When replacing the sand with concrete, a higher compressive strength is achieved, which would lead to a higher buckling resistance. However, when computing the resistance it is found that the increase in buckling load is minimal (see Table 7.12).

Table 7.12: Failure probability of the end-wall for 1 concrete-filled tubular pile.

<b>1 Tubular pile concrete-filled</b>			
Load		Resistance	Safety
P(Collision)	P(F>F <sub>failure</sub> )	F <sub>failure</sub>	P(Failure end-wall)
2.730 E-06	0.979	1.375 MN	2.672 E-06

### 7.3. Conclusion

Several different methods are described in this chapter in order to decrease the probability of failure of the single end-wall. In Table 7.13 the different measures are listed and the failure probability is given. A factor is given which indicates how many times safer the construction would be when applying the method listed.

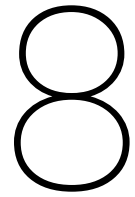
Table 7.13: Summary of the different measures

<b>Summary</b>		
Adaptation	P(Failure end-wall)	Factor
Single pile	2.692 E-06	1.00
Traffic Distribution	2.317 E-06	1.16
Angle of 10 degrees	2.329 E-06	1.16
Friction Coefficient	1.968 E-06	1.37
10 Piles	1.512 E-06	1.78
20 Piles	3.249 E-07	8.29
Sand-filled piles	2.678 E-06	1.01

From this table it can be concluded that coupling of the piles is the most beneficial method in increasing the safety of the pit. A combination of some of these measures can lead to an even higher safety level.

Although filling the piles with sand or concrete, leads to higher resistance, the increase in safety is minimal and this method is considered not beneficial for the Blankenburg case.





## Conclusions and recommendations

*This chapter closes off the research with the conclusions based on the findings. In Section 8.1 the conclusions are drawn, after which in Section 8.2 the recommendation for further research are given.*

### 8.1. Conclusions

The goal of this study was to explore the option of replacing the double end-wall in the design by BAAK with single end-wall. To this end, the probability and magnitude of the load were calculated first.

From different studies, it was concluded that a collision event is often caused by human failure. In order to capture decision-making and communication on board a vessel, a Bayesian Network was constructed to estimate the probability of a collision. The Bayesian Network used in this thesis was taken from existing models used for the Finnish Gulf and adapted to local conditions on several nodes. The outcome of the model was validated using historical data and a difference of 10% was found (2.730 E-06 collisions/year/km in Bayesian network vs. 2.529 E-06 collisions/year/km using historical data). The model over-predicts the actual accidents, or the historical data does not contain all accidents, which is a known phenomenon in the navigation industry. Hence, keeping in mind that the difference between historic and model collisions was 10% at most, but probably less, and given the difference in reliability between historic and model outputs, the output of the model was assumed to be an adequate estimation of the collision probability for this thesis. The main influential parameters in the Bayesian network were selected for BAAK, and measures to reduce the probability of collision were proposed, such as imposing a in- and outgoing window and additional training of pilots.

In addition to the probability of collision, the magnitude of the force (and the location of impact) is also an important factor in determining the load on the structure. . As a mixed fleet is present at the Scheur and a lot of different parameters could have influence on the magnitude of the force, a Monte Carlo simulation was used. The model provided more detailed information about the loading on the structure and the governing types of vessels. It was concluded that there is a small difference in loading between the North and the South side of the river. This is due to the effect of the tidal stream on the velocity of the vessel.

In order to accurately compare the double to the single end-wall, the resistance of both variants to a potential load was calculated. In the calculation of the double end-wall the framework had an important role in the distribution of the forces along the structure. It could be concluded that the double end-wall could resist a 2x times higher load than the single end-wall. The single end-wall was more vulnerable, due to the additional loading by water and soil pressures. In both cases local buckling was the governing failure mechanism.

The required safety limit for the entire construction pit was found after assessing the risk at an individual level. Combining the loads and resistance to calculate the failure probability of a single pile, resulted in a safe value for a single pile ( $2.692 \cdot 10^{-6} < 10^{-5}$ ). More importantly however, the probability of a collision is already low enough to provide safety for the construction pit, making the failure probability of a single pile less critical. The variant with a single end-wall will therefore be sufficient when regarding ship collisions. However, the single pile will fail during 98.6% of the collisions, which can be considered as undesirable because if a

collision occurs it is almost certain that the construction will fail.

In order to increase the level of safety regarding ship collisions even more, several options are discussed. In each of the three main areas of this thesis, two measures are proposed to reduce the probability of failure. From the analysis it was concluded that measures influencing the magnitude of the force or the resistance of the structure are most beneficial in reducing the probability of failure. The probability of a collision, which is calculated using the Bayesian Network, is already low making measures in this area less beneficial. It is also concluded that the most beneficial method of increasing the safety, is increasing the number of activated piles. The safety can be increased with a factor of 8.3, when activating 20 instead of 1 pile.

Finally, from the sensitivity analysis it was also concluded that turning the pit in its orientation with the shipping lane, has a significant influence on safety of the construction pit. This can either be positive or negative, within a range of -15% to +30% for 10 activated piles. As the pit on the North side of the Scheur is built under a negative angle of 30 degrees, one can conclude that turning of the pit by BAAK has a negative influence and the probability of failure is increased with 30% in comparison with constructing it perpendicular to the waterway.

## 8.2. Recommendations

Following from the results and models used in this research, a number of recommendations are made for further research.

### Detailed study into Bayesian Network

In the adaptation of the model of the Finnish Gulf some assumptions and crude estimates are made, which increase the uncertainty in the model. For a more reliable model, parameters for this location and its conditions should be examined carefully first.

Moreover, not all values for the conditional probability for the (original) model of the Finnish Gulf were known or could be retrieved. Based on literature and engineering judgment these values were estimated, however, more research is needed to better understand the model and determine which parameters are influenced by local conditions.

In the current network the presence of the construction pit does not lead to a higher probability of collision, as there is no evidence or data to support this claim. However, one could argue that this could influence the probability of a collision and therefore it is recommended to do further research to support this claim.

### Studying the effects of imposing regulations

In Chapter 4 it was proposed to impose regulations on ship traffic to establish an in and out going window. These regulations should be further worked out in order to give a better insight in the effectiveness of this measure. Besides that, the side effects of this measure should be mapped out and reviewed.

### Improving the probabilistic model

The probabilistic model constructed in Chapter 5 is an estimation of the collision process at the Scheur. In the model the different parameters are estimated based on data, research or engineering judgment and this leaves space for improvement.

In the current model all vessels will turn with their minimum turning radius. However, vessels can also collide with the structure when they are sailing on the wrong course for a longer period of time. This is not included in the model, as it was assumed that all vessels will turn in the vicinity of the construction pit. This assumption most likely leads to higher impact loads on the structure, as the angle of impact will be higher. However, this leaves space for further research and optimization of the model.

In the current model vessels are assumed to be fully loaded and uniformly distributed within their DWT class. Further research is required to confirm these assumptions or to come up with a better estimation.

### Residual strength of combi-walls

In this thesis it was assumed (based on [Van Es \(2016\)](#)) that a tubular pile has a residual capacity of 40% of the original bending moment capacity after local buckling. As the existing codes and guidelines do not consider residual capacity and only one study could be found in this area of interest, further research is recommended in this area.

### Friction coefficient

In the calculation of the magnitude of the force, the friction coefficient plays an important role. When comparing the reduction values of the [ROK \(2017\)](#) and the values suggested by [Zhang and Pedersen \(1999\)](#), a significant difference is noticed. Additional research is needed to better establish the influence of friction and how to determine the reduction.

### Vessel aspects

In the calculations performed in this thesis most aspect concerning the vessel are neglected. The focus was on the collision forces and the resistance of the structure. However, the deformability of the colliding vessel, the shape of the bow and the dynamic behavior of the vessel could be of influence on the collision process. Further research is recommended to implement these factors into the calculations.



# Bibliography

- Agency, European Maritime Safety (2015). Risk acceptance criteria and risk based damage stability. final report, part 1: Risk acceptance criteria. Technical report.
- Akchurin, A., Bosman, R., Lugt, P., and van Drogen, M. (2015). On a model for the prediction of the friction coefficient in mixed lubrication based on a load-sharing concept with measured surface roughness. *Tribology letters*, 59(1):19.
- Ancel, E., Shih, A., Jones, S., Reveley, M., Luxhøj, J., and Evans, J. (2015). Predictive safety analytics: inferring aviation accident shaping factors and causation. *Journal of Risk Research*, 18(4):428–451.
- BAAK (2019). Data and findings by baak. Technical report.
- Brown, D.A.; Turner, J.P.; Castelli, R.J.; (2010). Drilled shafts manual. Technical report, FHWA.
- Consultants, The Øresund Link (1994). Ship collision frequencies - tunnel, island and peninsula. Technical report, Øresundkonsortiet.
- CUR166 (2012). Infra, damwandconstructies. Technical report.
- CUR211 (2014). *CUR211E Kademuren/Quay walls*, volume 2 of *The Netherlands*.
- de Oña, J., Mujalli, R. O., and Calvo, F. J. (2011). Analysis of traffic accident injury severity on spanish rural highways using bayesian networks. *Accident Analysis and Prevention*, 43(1):402–411.
- DNV (2005). Formal safety assessment of electronic chart display and information system. Technical report.
- EAU (2015). *Recommendations of the committee for waterfront structures harbours and waterways EAU 2012*. John Wiley and Sons.
- EN1991-1-1 (2005). Eurocode 1 - actions on structures part 1-6: General actions actions during execution. Technical report, CEN.
- EN1991-1-7 (2006). Eurocode 1 - actions on structures - part 1-7: General actions - accidental actions. Technical report, CEN.
- EN1993-1-6 (2005). Eurocode 3: Design of steel structures - part 1-6: Strength and stability of shell structures. Technical report, CEN.
- EN1993-1-8 (2005). Eurocode 3: Design of steel structures - part 1-8: Design of joints. Technical report, CEN.
- EN1993-4-3 (2009). Eurocode 3: Design of steel structures - part 4-3: Pipelines. Technical report, CEN.
- European Maritime Safety Agency (2017). Overview of marine casualties and incidents. Technical report, European Maritime Safety Agency.
- Gresnigt, A. (1987). Plastic design of buried steel pipelines in settlement areas.
- HASKONINGDHV (2018). Recommendations design method combined walls preliminary design blankenburg tunnel. Technical report, HASKONINGDHV NEDERLAND B.V.
- Havenbedrijf Rotterdam (2015). Mer verdieping nieuwe waterweg, botlek en 2e petroleumhaven. Technical report.
- Hänninen, M. and Kujala, P. (2012). Influences of variables on ship collision probability in a bayesian belief network model. *Reliability Engineering and System Safety*, 102:27–40.

- Johnson, K., Greenwood, J., and Poon, S. (1972). A simple theory of asperity contact in elasto-hydro-dynamic lubrication. *Wear*, 19(1):91–108.
- Jonkman, S., Steenbergen, R., Morales-Nápoles, O., Vrouwenvelder, A., and Vrijling, J. (2017). *Probabilistic Design: Risk and Reliability Analysis in Civil Engineering*. Technische Universiteit Delft.
- Joustra, N. and Pater, R. (1993). Aanvaarbeasting door schepen op starre constructies. Master's thesis, Delft University of Technology.
- Koller, D. and Friedman, N. (2009). *Probabilistic graphical models: principles and techniques*. MIT press.
- Kostis, N. (2016). Local buckling of sand-filled steel tubes for combined walls.
- Loodswezen (2018). Jaarverslag 2018. Technical report.
- Lutzen, M. (2001). *Ship collision damage*. Phd, Technical University of Denmark.
- MARIN (2017). Sea shipping emissions 2015: Netherlands continental shelf, 12-mile zone and port areas. Technical report, MARIN.
- Martins, M. R. and Maturana, M. (2013). Application of bayesian belief networks to the human reliability analysis of an oil tanker operation focusing on collision accidents. *Reliability Engineering and System Safety*, 110:89–109.
- Mazaheri, A., Montewka, J., Kotilainen, P., Sormunen, O., and Kujala, P. (2015). Assessing grounding frequency using ship traffic and waterway complexity. *The Journal of Navigation*, 68(1):89–106.
- Mazaheri, A., Montewka, J., and Kujala, P. (2016). Towards an evidence-based probabilistic risk model for ship-grounding accidents. *Safety science*, 86:195–210.
- Minorksy, V. (1959). An analysis of ship collisions with reference to protection of nuclear powered plants. *Journal of Ship Research*, 1-4.
- Motora, S., Fujino, M., Sugiura, M., and Sugita, M. (1971). Equivalent added mass of ships in collisions. *Selected Papers, J of Soc of Naval Arch of Japan*, 7.
- Neapolitan, R. (2004). *Learning bayesian networks*, volume 38. Pearson Prentice Hall Upper Saddle River, NJ.
- NV, Havenbedrijf Rotterdam (2019). Operationeel stromingsmodel rotterdam. Technical report.
- Onderzoeksraad voor de veiligheid (2018). Bouwen aan constructieve veiligheid. Technical report, Onderzoeksraad voor de veiligheid.
- Perera, W. (2018). Development of a post-tensioned masonry retaining wall system. In *International Conference on Sustainable Built Environment*, pages 394–410. Springer.
- Port of Rotterdam (2012). Hydrometeobundel nr. 4. Technical report.
- Rankine, W. (1856). On the stability of loose earth. *Proceedings of the Royal Society of London*, pages 185–187.
- Reese, L., Cox, W., and Koop, F. (1974). Analysis of laterally loaded piles in sand. *Offshore Technology in Civil Engineering Hall of Fame Papers from the Early Years*, pages 95–105.
- Reynolds, J. (1976). Ship-turning characteristics in different water depths. *Safety at Sea International*, (90).
- Rijkswaterstaat (2015). Tracébesluit / mer blankenburgverbinding. Technical report.
- ROK (2017). Richtlijn ontwerp kunstwerken. Technical report, Rijkswaterstaat.
- Rotterdam Port Authority (2018). Port information guide. Technical report, International Harbour Masters Association.
- Roubos, A., Groenewegen, L., and Peters, D. (2017). Berthing velocity of large seagoing vessels in the port of rotterdam. *Marine Structures*, 51:202–219.

- Tunnel, D.-W. (2018). Retrieved from <https://www.dwtunnel.com/history/>, 2019(7-10-19).
- Van Es, S. (2016). *Inelastic local buckling of tubes for combined walls and pipelines*. PhD thesis.
- Verheij, H.J.;Stolker, C.;Groenveld, R. (2008). *Inland waterways*. Technical report, TU Delft.
- Verruijt, A. and Van Baars, S. (2007). *Soil mechanics*. VSSD Delft, the Netherlands.
- Wang, Y., Xie, M., Chin, K., and Fu, X. (2013). Accident analysis model based on bayesian network and evidential reasoning approach. *Journal of Loss Prevention in the Process Industries*, 26(1):10–21.
- Winkel, J., Kostis, N., Peters, D. J., and van Es, S. (2017). Experiments and fem-simulations of local buckling of sand-filled tubular piles. *ce/papers*, 1(2-3):1305–1314.
- Zhang, S. and Pedersen, P. T. (1999). *The mechanics of ship collisions*. PhD thesis, Technical University of Denmark.
- Zhang, S., Pedersen, P. T., and Ocakli, H. (2014). Collision analysis of ships and jack-up rigs. In *Proceedings of the 7th International Conference on Thin-Walled Structures (ICTWS)*.





# List of Figures

1.1	Three recent examples of temporary construction pits vulnerable to ship collisions. . . . .	1
1.2	The different steps in this thesis visualized in a diagram. . . . .	3
1.3	The different steps and the corresponding chapters in this thesis. . . . .	4
2.1	The safety principle . . . . .	5
2.2	Distribution of $Z = R-S$ and the reliability index . . . . .	6
2.3	Relationship between acceptable risk and failure probability of a system . . . . .	8
2.4	Total amount of marine accidents per year . . . . .	9
2.5	Distribution of casualty events with a ship . . . . .	9
2.6	Relationship between accidental events and the main contributing factors . . . . .	10
2.7	Influence of waterway systems on the probability . . . . .	11
2.8	Wind wall near Rozenburg . . . . .	11
2.9	Influence of vessel characteristics on the probability . . . . .	12
2.10	Influence of human factors on the probability . . . . .	12
2.11	Different type of ship motions . . . . .	13
2.12	Ship impact under an angle . . . . .	15
2.13	Coefficient of eccentricity . . . . .	16
2.14	Example of sheet piling . . . . .	18
2.15	Example of a combi wall in water . . . . .	18
2.16	Concrete pile wall with heavy top load . . . . .	19
2.17	Crane excavating a trench during construction of a diaphragm wall . . . . .	19
2.18	A simple L-shaped retaining wall . . . . .	20
2.19	A cofferdam with a concrete slab on top . . . . .	20
2.20	Cellular cofferdam . . . . .	21
2.21	The application of a 'terre armee' method . . . . .	21
2.22	Different failure mechanisms of a retaining wall . . . . .	21
2.23	Failure modes for a combi-wall . . . . .	22
2.24	Single pile model . . . . .	23
2.25	Soil failure modes . . . . .	24
2.26	Different cross-section classes. . . . .	25
2.27	Cross-section classes and analysis methods . . . . .	26
2.28	Radius $r'$ in an ovalised cross-section. . . . .	27
2.29	Measurement of diameters for assessment of out-of-roundness . . . . .	28
2.30	Ovalisation due to initial out-of-roundness. . . . .	29
2.31	Possibilities of a aberration in the piles. . . . .	29
2.32	Case with tensile forces from secondary members . . . . .	30
2.33	Case with soil pressure on one side . . . . .	30
3.1	Location of the Blankenburg connection near Rotterdam . . . . .	33
3.2	Blankenburg connection . . . . .	34
3.3	The construction process of an immersed tunnel . . . . .	34
3.4	Different tunnel element sizing . . . . .	35
3.5	Placement of the tunnel element in the pit . . . . .	35
3.6	Location of the construction sites in the Scheur . . . . .	39
3.7	Construction principle . . . . .	39
3.8	Plan view of the construction site at the south bank. . . . .	40
3.9	Construction of the end wall including framework . . . . .	41
3.10	Dimensions of the end wall . . . . .	41
3.11	Combi wall of tubular piles with AZ26 sheet piling. . . . .	42

3.12	Combi wall of tubular piles with PU28 sheet piling . . . . .	42
3.13	Scenario 1 - Evasive maneuver . . . . .	43
3.14	Scenario 2 - Traffic intensity . . . . .	43
3.15	Scenario 3 - Tug assistance . . . . .	43
3.16	Scenario 4 - Human failure . . . . .	44
3.17	Scenario 5 - Local bathymetry and conditions . . . . .	44
3.18	Scenario 6 - Technical problem or error . . . . .	44
3.19	Governing construction phases. . . . .	46
3.20	Design by BAAK of the construction pit at the South bank. . . . .	46
4.1	Bayesian belief network for ship grounding in the Finnish Gulf . . . . .	49
4.2	Grounding accidents happening in the Gulf of Finland (1989–2010) . . . . .	50
4.3	'Type of ship' node in the model. . . . .	53
4.4	The distribution of wind near Rozenburg . . . . .	53
4.5	Amount of hours with limited sight at the waters around the Port of Rotterdam. . . . .	54
4.6	The 'Meteorological conditions' node in the model. . . . .	54
4.7	'Pilot presence' node connected with the 'Type of ship' in the model. . . . .	54
4.8	Bayesian belief network for ship collision at the Scheur . . . . .	55
4.9	Setting the evidence of the model . . . . .	56
4.10	Number of accidents per kilometer . . . . .	56
5.1	Sketch of the basic situation. . . . .	61
5.2	Vessel colliding with structure . . . . .	62
5.3	Input parameters . . . . .	63
5.4	Relative frequency of vessel class . . . . .	64
5.5	Distribution of dead weight within a vessel class. . . . .	65
5.6	Correlation between DWT and vessel length . . . . .	65
5.7	Correlation between DWT and vessel draught . . . . .	65
5.8	Correlation between DWT and vessel beam width . . . . .	66
5.9	Area of application . . . . .	66
5.10	Estimated velocity of sea-going vessels . . . . .	66
5.11	Tidal fluctuations at the project location . . . . .	67
5.12	Model approximation of the tide at the project location. . . . .	67
5.13	Tidal stream fluctuations at the project location . . . . .	68
5.14	Model approximation of the tidal stream at the project location. . . . .	68
5.15	Squat effect on vessels in shallow waters. . . . .	69
5.16	The location of the vessel is assumed to be Gaussian distributed. . . . .	70
5.17	Flow chart of the calculation process . . . . .	74
5.18	Calculation example of the collision model. . . . .	75
5.19	Forces on the structure on the North side of the Scheur . . . . .	76
5.20	Forces on the structure on the South side of the Scheur . . . . .	76
5.21	Correlation between $F_{dx}$ and $F_{dy}$ for the South side. . . . .	77
6.1	The two variants of the structure. . . . .	79
6.2	Details of the original design. . . . .	81
6.3	Tolerances in the AZ-sheet piling. . . . .	82
6.4	Characteristics of the primary combi-wall, distances in mm. . . . .	82
6.5	Characteristics of the secondary combi-wall, distances in mm. . . . .	82
6.6	Schematization in order to assess the rotational stability of a tubular pile. . . . .	83
6.7	Point A and B should be checked for local buckling. . . . .	84
6.8	Water pressure deforming the secondary elements . . . . .	85
6.9	Vessel colliding precisely between two piles . . . . .	86
6.10	Distributed force on the secondary members. . . . .	86
6.11	C6 Lock . . . . .	86
6.12	C9 Lock . . . . .	86
6.13	Stress/strain development and bending moment . . . . .	87
6.14	Overview of the interlocking . . . . .	87

6.15 Assumed working lines of secondary element forcing . . . . .	87
6.16 Forces acting on the locks after plastic deformation of the locks . . . . .	88
6.17 Moment-curvature diagram with post-buckling . . . . .	89
6.18 Overview of the remaining post-buckling bending moment capacity . . . . .	89
6.19 The head-on collision case, the angle of impact 90 degrees. . . . .	90
6.20 The 'brushing' collision case, angle of impact is zero degrees. . . . .	90
6.21 The 'brushing' collision case with a force and a arm of 16 mm. . . . .	91
6.22 Influence of interlocking on the post-buckling behavior. . . . .	91
6.23 Three types of welded joints . . . . .	92
6.24 Details of the single combi-wall variant. . . . .	94
6.25 Governing cross-section regarding local buckle . . . . .	95
6.26 Bending moment for a total force on the pile of 1058.9 kN. . . . .	95
6.27 Schematization in order to assess the rotational stability of a single tubular pile. . . . .	96
7.1 Resistance of the structure . . . . .	100
7.2 The relative frequency of collision force for inland going (left) and seagoing (right). . . . .	102
7.3 Definition of the angles of the construction pit. . . . .	104
7.4 Energy reduction for different friction coefficients and impact angles. . . . .	105
7.5 Activating multiple piles by using a girder. . . . .	106
7.6 Distribution of collision forces . . . . .	106
7.7 Stiffness of the steel tube and of the sand volume . . . . .	107
A.1 Soil classification . . . . .	124
A.2 Probing with local friction measurement(1). . . . .	125
A.3 Probing with local friction measurement(2). . . . .	126
B.1 Sample Bayesian Network . . . . .	130
E.1 Lubricated friction . . . . .	146
E.2 Influence of the friction coefficient . . . . .	147
F.1 Soil failure modes . . . . .	149
F.2 Typical PY-Curve. . . . .	150
F.3 Correction factors. . . . .	151
F.4 PY-curve for z = 10m. . . . .	152
F.5 Stiffness of the soil with curve fitting. . . . .	152

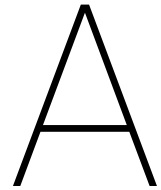


# List of Tables

2.1	Target values for $\beta$ in Ultimate Limit State	7
2.2	Indicative values for dynamic collision force of seagoing vessels	14
2.3	Reduction factors as function of the impact angle	15
2.4	Characteristics of a New-Panamax container vessel	17
2.5	Comparison of the different methods	17
2.6	Classification of cross-sections	25
2.7	Recommended values for $U_r$	28
3.1	The different phases of the project	36
3.2	Consequences of failure of a ship collision.	45
4.1	Existing BBN models for ship-grounding accidents	48
4.2	Grounding frequency of the studied waterways	52
4.3	Influence of the different states of nodes on the probability of a collision	57
4.4	Maximum effect when changing a node for the better.	58
4.5	Proposed measures for nodes which can be adapted by the project owner.	59
4.6	Proposed measures for nodes which can be adapted by the project owner.	60
5.1	Amount of seagoing vessels per DWT class per year	63
5.2	Dead Weight Tonnage per DWT-Class	63
5.3	Amount of inland going vessels per DWT class per year	64
5.4	Total amount of vessels per DWT class per year	64
5.5	Influence of the depth on the turning radius	69
5.6	Dependence of the width of the shipping lane on the draught of the vessel.	70
5.7	Overview of the input parameters for the probabilistic model.	71
5.8	Vessel classes and the 95% characteristic impact force.	77
6.1	Different failure mechanisms for the two variants.	80
6.2	Characteristics of the elements for the original design.	81
6.3	Rotational stability of a tubular pile as part of a construction pit.	83
6.4	Total out-of-roundness for location A	84
6.5	Total out-of-roundness for location B	85
6.6	Maximum force on the interlocking system.	88
6.7	Failure forces for the different failure modes.	93
6.8	Characteristics of the elements for the single combi-wall.	94
6.9	Total out-of-roundness for a single combi-wall	95
6.10	Rotational stability of a tubular pile as part of a construction pit.	96
6.11	Failure forces for the different failure modes.	97
6.12	Failure forces for different failure mechanisms	98
7.1	Accident statistics and proposed policy factor and characteristics of the activity	99
7.2	Failure probability of the single end-wall	100
7.3	Failure probability of the double end-wall	100
7.4	Comparison between seagoing and inland going vessels.	102
7.5	Influence of the different states of two nodes on the probability of a collision.	103
7.6	Failure probability with imposed.	103
7.7	Failure probability of the end-wall for different angles.	104
7.8	Failure probability of the end-wall for reduced friction coefficient.	105
7.9	Failure probability of the end-wall for 10 tubular piles.	106

---

7.10	Failure probability of the end-wall for 20 tubular piles. . . . .	106
7.11	Failure probability of the end-wall for 1 sand-filled tubular pile. . . . .	107
7.12	Failure probability of the end-wall for 1 concrete-filled tubular pile. . . . .	107
7.13	Summary of the different measures . . . . .	108
A.1	Width and depth restrictions for the channel. . . . .	123
A.2	Characteristic subsoil values . . . . .	124
A.3	Classification of soil. . . . .	124
A.4	Navigational conditions at the Scheur . . . . .	127
E.1	Friction coefficient with steel . . . . .	146
E1	Assumed soil properties and pile diameter. . . . .	150
E2	Basic $k$ value . . . . .	151



# General requirements and boundary conditions

*For the project some general requirements and boundary conditions are applicable, which are described in this appendix.*

## **A.1. Design lifetime of the structure**

A key technical aspect of the structure is the lifetime. A common design lifetime for civil engineering projects is 50 years. The Blankenburg connection is a project that will be executed over the period 2018-2024. The tunnel itself has to be made with a larger design lifetime, however, the temporary construction site will be removed after finishing the project. The construction treated in this thesis will therefore be considered as a temporary construction: the lifetime of the structure will be close to the project duration (6 years). As some delay should be accounted for, a design lifetime of 10 years is required.

## **A.2. Shipping lane**

The construction pit is partly located in the Scheur, which is a busy shipping route and blockage of this route can cause, amongst others, huge financial consequences. The port of Rotterdam allows blockage of the shipping lane only for shorter periods of time, meant for placing the tunnel elements. However, protective measures should be located outside of the shipping lane.

The dimensions of this shipping lane are given in Table A.1. This is the minimal width that should be kept at all times (except for the time when placing the elements), and also a minimal depth is required by the port authorities.

Table A.1: Width and depth restrictions for the channel.

Channel	Width	Depth
Dredged channel	230 m	16.2 m
Complete channel	370 m	10.0 m

### A.3. Geotechnical conditions

The soil conditions at the project location can be determined using the data from CPT soundings done by Fugro in preparation of the Blankenburg project.

For the calculations the Dutch standard will be used (NEN 9997-1). The characteristic values for different soil types are given in table A.2.

Table A.2: Characteristic subsoil values according to NEN 9997

Primary material	Admixture	Consistency	$\gamma_{dry}$ [kN/m <sup>3</sup> ]	$\gamma_{sat}$ [kN/m <sup>3</sup> ]	$\varphi$ [°]	$c$ [kPa]
Gravel	Slightly silty	Loose	17	19	32.5	0
		Medium	18	20	35.0	0
		Dense	19-20	21-22	37.50-40.0	0
Sand	Clean	Loose	17	19	30.0	0
		Medium	18	20	32.5	0
		Tight	19-20	21-22	35.0-40.0	0
Sand	Gravel	Medium/Tight	19	21	35.0	0

#### A.3.1. Classification of soil

Before the CPT are shown, the classification according to Robertson is given as this is used to determine the soil properties.

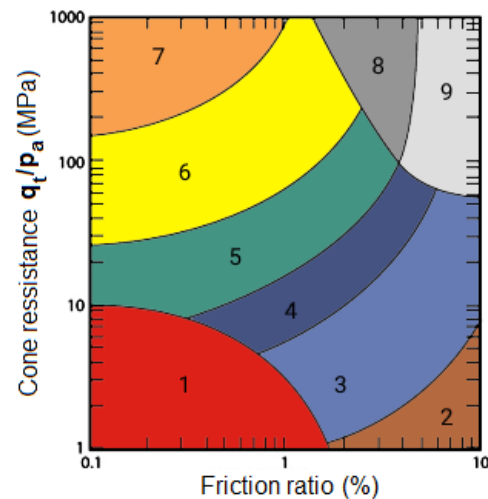


Figure A.1: Soil classification by Robertson (1990)

Table A.3: Classification of soil.

Zone	Soil Behavior Type (SBT)
1	Sensitive, fine grained
2	Organic soils - clay
3	Clay - silty clay to clay
4	Silt mixtures - clayey silt to silty clay
5	Sand mixtures - silty sand to sandy silt
6	Sands - clean sand to silty sand
7	Gravelly sand to dense sand
8	Very stiff sand to clayey sand*
9	Very stiff fine grained*

\* Heavily overconsolidated or cemented



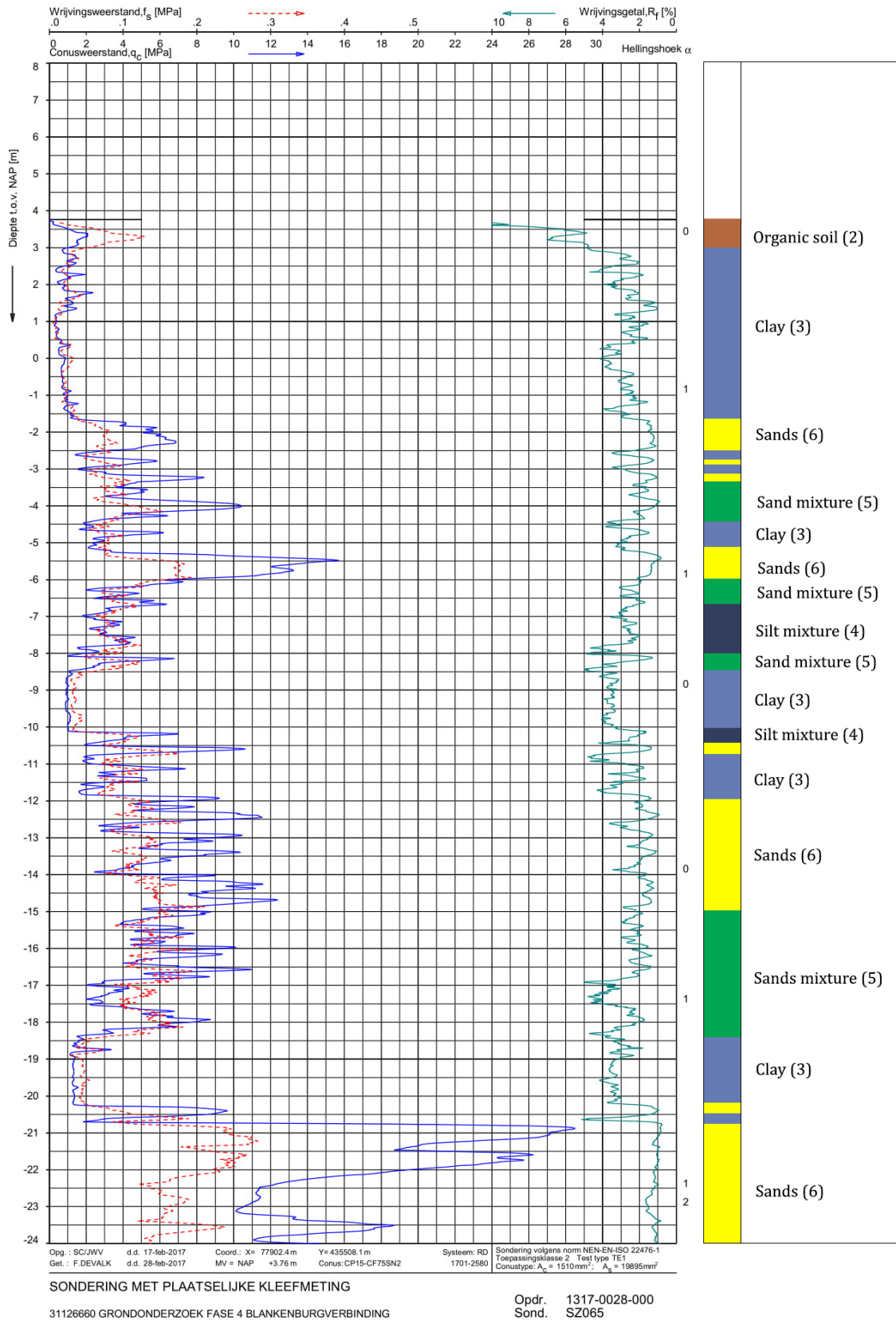


Figure A.2: Probing with local friction measurement(1).

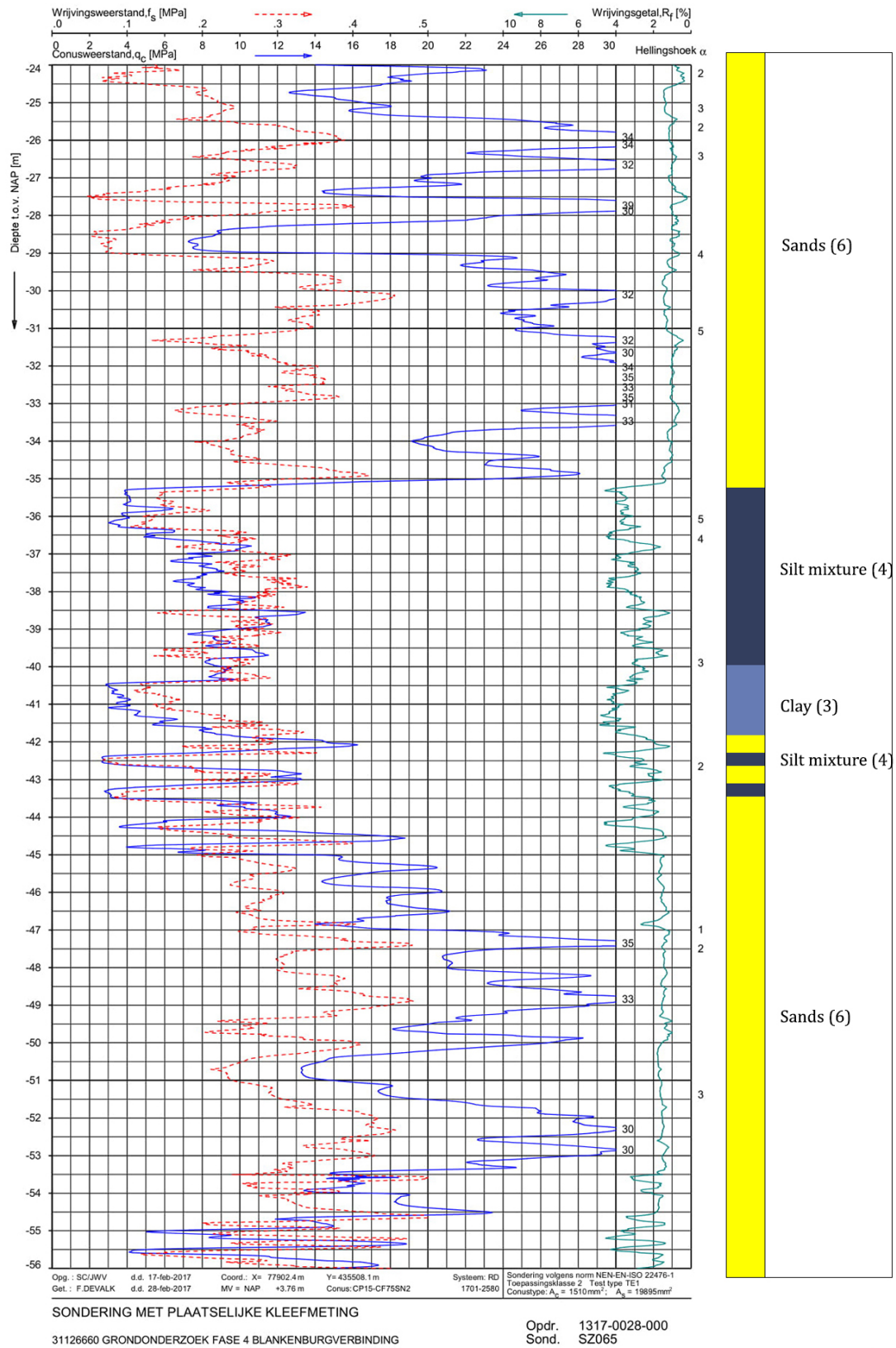


Figure A.3: Probing with local friction measurement(2).

## A.4. Navigational conditions

Navigation in the channel can also be influenced by external conditions; these conditions are discussed briefly in table A.4.

Table A.4: Navigational conditions at the Scheur (Rotterdam Port Authority, 2018)

Condition	Description
Buoys	In the waterway buoys are present to highlight the shipping lane. During construction additional buoys will be placed in order to highlight the presence of the temporary works. By night, flashing lights on top of the buoys will alert captains to the new situation.
Nautical paper charts	Paper charts of the channel are available, but the charts are not likely to be updated often enough to include temporary works.
Nautical electronic charts	As electronic charts can be updated more regularly, temporary works will have the possibility to be implemented and shown on the charts.
Officer on duty	An officer from the Harbour Control Center will be available 24 hours a day, to provide information about the shipping lanes and maneuverability.
Wind	The prevailing winds are coming from the south west to south, force 2 or 3 Beaufort. The relative frequency of wind forces greater than force 5 Beaufort is 2%. (see Appendix G)
Tide	In a period of 24 hours there are 2 high waters and 2 low waters, with different amplitudes. The tide amplitude ranges from -0.40 till 1.45 meter (see Appendix G). A special phenomenon manifests itself at Hoek van Holland, which has a double low tide with the second low water lower than the first. Strong and sustained winds from the north west raise water levels along the Dutch coast. Strong and sustained winds from the south-east have the opposite effect.
Fog	The frequency of visibility less than 1500 meters is 1,4%. The frequency of visibility less than 500 meters is 0,6%.
Ice	The waterway is open at all times, there is no forming of ice.
Water Density	The density of the water ranges from $1020 \text{ kg/m}^3$ at high water to $1000 \text{ kg/m}^3$ at low water.



# B

## Bayesian Networks - Basics

In this appendix a short introduction is given about Bayesian Networks and how they work.

### B.1. Basic concepts in probability theory

Events are formally defined by assuming that there is a space of possible outcomes, which is denoted by  $\Omega$ . In addition, there is a set of measurable events  $S$  to which probabilities will be assigned, such that each event  $\alpha \in S$  is a subset of  $\Omega$ . The probability distribution  $P$  is then defined as follows:

**Definition 3.1** A probability distribution  $P$  over  $(\Omega, S)$  is a mapping from events in  $S$  to real values that satisfies the following conditions:

- $P(\alpha) \geq 0$  for all  $\alpha \in S$
- $P(\Omega) = 1$
- If  $\alpha, \beta \in S$  and  $\alpha \cap \beta = \emptyset$ , then  $P(\alpha \cup \beta) = P(\alpha) + P(\beta)$

The first condition states that probabilities are not negative. The next statement states that the “trivial event”, which allows all possible outcomes, has the maximal possible probability of 1. The final condition states that the probability that one of two mutually disjoint events will occur is the sum of the probabilities of each event.

In case of a Bayesian Network, events are dependent on each other, which is also called conditional probability. The probability of event  $\beta$  given  $\alpha$  is defined as:

$$P(\beta|\alpha) = \frac{P(\alpha \cap \beta)}{P(\alpha)}$$

Other important definitions are the definitions of Independence and Conditional Independence. Independence refers to a random variable that is unaffected by all other variables. A dependent variable is a random variable whose probability is conditional on one or more other random variables.

**Definition 3.2** Two events  $A$  and  $B$  are **independent** if one of the following holds:

1.  $P(A|B) = P(A)$  and  $P(A) \neq 0, P(B) \neq 0$
2.  $P(A \cap B) = P(A) \cdot P(B)$

Conditional independence describes the relationship among multiple random variables, where a given variable may be conditionally independent of one or more other random variables. This does not mean that the variable is independent per se; instead, it is a clear definition that the variable is independent of specific other known random variables.

**Definition 3.3** Two events  $A$  and  $B$  are **conditionally independent** given  $C$ , denoted by  $I(A, B|C)$ , if  $P(C) \neq 0$  and one of the following holds:

1.  $P(A|B \cap C) = P(A|C)$  and  $P(A|C) \neq 0, P(B|C) \neq 0$

$$2. P(A, B|C) = P(A|C) \cdot P(B|C)$$

A probabilistic graphical model, such as a Bayesian Network, provides a way of defining a probabilistic model for a complex problem by stating all of the conditional independence assumptions for the known variables, whilst allowing the presence of unknown (latent) variables.

As such, both the presence and the absence of edges (connection between nodes, i.e. see Figure B.1) in the graphical model are important in the interpretation of the model.

Next one of the most important theorems for conditional probabilities is needed, namely Bayes' Theorem:

**Bayes' Theorem** Given two events  $\alpha$  and  $\beta$  such that  $P(\alpha) \neq 0$  and  $P(\beta) \neq 0$ , the following holds:

$$P(\alpha|\beta) = \frac{P(\beta|\alpha) \cdot P(\alpha)}{P(\beta)}$$

### B.1.1. Graph theory

Probabilistic graphical models are defined by a graph  $G=(V,E)$ , where  $V$  is the set of nodes and  $E$  the set of edges of the graph. There are two types of graphical models using two different types of edges, namely directed and undirected. When edges are undirected, it is possible to start in one node and by following the edges end up in the same node again. In this case one speaks of a Markov network. In a directed graph this is not possible and a directed acyclic graph is created, also called a Bayesian Network (Koller and Friedman, 2009).

In the case of human failure influencing ship collision, all edges are assumed to be directed, so a Bayesian Network is used. This means that the graph has to be a directed acyclic graph (DAG). An important definition concerning directed acyclic graphs comes from Neapolitan (2004):

**Definition 3.3** Given a DAG  $G = (V,E)$  and nodes  $X, Y$  in  $V$ :

- $Y$  is called **parent** of  $X$  if there is an edge from  $Y$  to  $X$ .
- $Y$  is called a **descendent** of  $X$  and  $X$  is called an **ancestor** of  $Y$  if there is a path from  $X$  to  $Y$
- $Y$  is called a **non-descendent** of  $X$  if  $Y$  is not a descendent of  $X$

An example of a simple Bayesian Network can be found in literature (Koller and Friedman, 2009). A patient can have two diseases, Flu or Hay fever, which both have one plausible common cause: the season of the year. Both disease have a common effect; the congestion of the nostrils and it is assumed that Flu also causes Muscle-Pain. This network is graphical represented in Figure B.1.

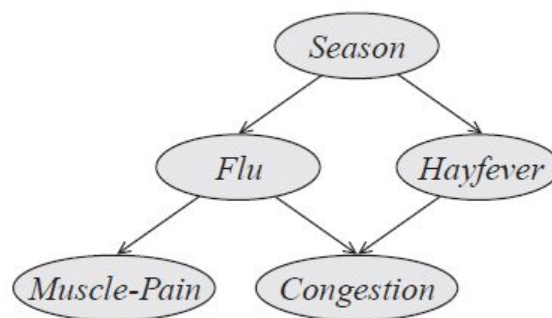


Figure B.1: Sample Bayesian Network (Koller and Friedman, 2009).

### B.1.2. Setting up a Bayesian Network

The construction of a Bayesian network is the process of going from a given event to a Bayesian network. In reality this is not as simple as it sounds, and constructing a model can be quite challenging since a real life event in all its complexity now has to be put into a network structure and parameters. This task breaks

down into several components, each of which can be quite subtle. Unfortunately, modeling mistakes can have significant consequences for the quality of the answers obtained from the network, and may go at the cost of using the network in practice. Three different aspects of setting the model up will be briefly reviewed (Koller and Friedman, 2009):

#### Picking variables

When one wants to model a domain, there are many possible ways to describe the relevant entities and their attributes. Choosing which random variables to use in the model is often one of the most difficult tasks, and this decision has implications throughout the model. A common problem when choosing variables is using ill-defined variables. These are variables which can not be clearly answered by a measurable parameter, or just raise more questions than they answer.

#### Picking structure

When all variables are determined, different structures can be made that are consistent with the same set of in-dependencies. One successful approach is to choose a structure that reflects the causal order and dependencies, so that causes are parents of the event. Such structures tend to work well. In general, there are many weak influences that can be modeled, but then the network can become very complex.

#### Picking probabilities

Another challenging task in constructing a network manually is obtaining *probabilities from people*. This task is somewhat easier in the context of causal models, since the parameters tend to be natural and more interpretable. Nevertheless, people generally dislike committing to an exact estimate of probability.

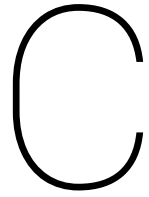
*Zero probabilities:* a common mistake is to assign a probability of zero to an event that is extremely unlikely, but not impossible. The problem is that one can never condition away a zero probability, no matter how much evidence there is. When an event is unlikely but not impossible, giving it probability zero is guaranteed to lead to irrecoverable errors. As a general rule, very few things (except definitions) have probability zero, and one must be careful in assigning zeros.

*Orders of magnitude:* Small differences in very low probability events can make a large difference to the network conclusions. Thus, a (conditional) probability of  $10^{-4}$  is very different from  $10^{-5}$ .

*Relative values:* The qualitative behavior of the conclusions reached by the network — the value that has the highest probability — is fairly sensitive to the relative sizes of  $P(x|y)$  for different values  $y$  of  $PaX$ . For example, it is important that the network encode correctly that the probability of having a high fever is greater when the patient has pneumonia than when he has the flu.







## Bayesian Network - Description of nodes

In this appendix the nodes used in the Bayesian belief network are described and the (conditional) probabilities are given. The nodes are ordered alphabetically.

### Adequate alarm

The node describes the usage of a grounding alarm to warn the crew on the bridge. Based on the amount of training, the alarm is used or not.

Lack of training	Yes	No
In_use	0.8	0.95
Not_in_use	0.2	0.05

The conditional probability in this node is based on [Mazaheri et al. \(2016\)](#) and [DNV \(2005\)](#).

### Authority gradient

The node describes the authority gradient at the ship. The gradient between the officer on deck and the rest of the crew influences the decision making. Three different categories are distinguished; steep, optimal and negative. Steep means that the officers makes all the decisions and does not take in feedback. In optimal conditions, the officer and crew work together and there is room for suggestions. In a negative environment, the officer is not able to make good decisions as the crew is too important in the process.

Steep	0.35
Optimal	0.6
Negative	0.05

The conditional probability in this node is based on [DNV \(2005\)](#).

### Being off course

The node describes if the vessel is off course. This node is mainly influenced by its parental nodes, which are 'Navigational Error', 'Loss of control' and 'Traffic Distribution'.

Navigational Error	Yes					
	No		Partial		Total	
Traffic distribution	Encounter	Free	Encounter	Free	Encounter	Free
Yes	0.85	0.75	0.95	0.85	0.9999	0.9999
No	0.15	0.25	0.05	0.15	0.0001	0.0001

		No					
		No		Partial		Total	
Encounter	Free	Encounter	Free	Encounter	Free	Encounter	Free
0.051	0.001	0.15	0.05	0.3	0.3		
0.949	0.999	0.85	0.95	0.7	0.7		
0	0	0	0	0	0		

The conditional probability in this node is partly based on Mazaheri et al. (2016) and engineering judgment.

Bridge design

The node describes the design of the bridge. The states defined for this node are the following:

Inadequate	0.1
Conventional	0.8
Solo	0.1

The probability in this node is based on DNV (2005).

BRM

The node describes the existence of a Bridge Resource Management (BRM) system. The BRM node covers optimisation of human resources on the bridge given the technical system and bridge design. An optimisation of the human resources is strongly related to communication and task responsibilities. The existence of a BRM system means that the system is developed and implemented, as well as maintained according to the intensions.

Safety culture	Excellent	Standard	Poor
Exist	0.5	0.2	0.1
Non	0.5	0.8	0.9

The probability in this node is based on Hänninen and Kujala (2012).

Collision

The node states the probability for a collision, which is has conditioned probability depending on the 'Being off course' and 'Waterway complexity'.

Being of course	Yes			No		
Waterway com...	Difficult	Managable	Easy	Difficult	Managable	Easy
Yes	0.000624	0.000524	0.000444	6.24e-05	4.44e-05	2.92e-05
No	0.999376	0.999476	0.999556	0.9999376	0.9999556	0.9999708

The conditional probability in this node is partly based on DNV (2005) and Mazaheri et al. (2015).

Communication, cooperation, monitoring

Depending on the existence of a Bridge Resource Management system, the node describes the level and the quality of the communication between the bridge personnel.

BRM	Exist											
Competence	High						Low					
Authorthy Grad...	Steep		Optimal		Negative		Steep		Optimal		Negative	
Visibility	Good	Poor	Good	Poor	Good	Poor	Good	Poor	Good	Poor	Good	Poor
Adequate	0.9	0.8	0.95	0.85	0.85	0.75	0.85	0.75	0.9	0.8	0.8	0.7
Inadequate	0.1	0.2	0.05	0.15	0.15	0.25	0.15	0.25	0.1	0.2	0.2	0.3

Non													
High							Low						
Steep		Optimal			Negative		Steep		Optimal			Negative	
Good	Poor	Good	Poor	Good	Poor	Good	Poor	Good	Poor	Good	Poor	Good	Poor
0.75	0.65	0.8	0.7	0.7	0.6	0.7	0.6	0.75	0.65	0.65	0.55	0.25	0.35
0.25	0.35	0.2	0.3	0.3	0.4	0.3	0.4	0.25	0.35	0.35	0.45		

The conditional probability in this node is based on [Hänninen and Kujala \(2012\)](#).

### Competence

Competence is a combination of knowledge, skills and attitude. The node reflects the Officer on watch's (OOW) knowledge, the level of training, the way he uses his knowledge and the attitude he has towards the tasks he is set to perform, e.g. to follow procedures and work instructions. This also reflects the technical competence on use of equipment.

Lack of training	Yes	No
High	0.5	0.9
Low	0.5	0.1

The conditional probability in this node is based on [DNV \(2005\)](#).

### Cumulated tasks

The node described the amount of cumulated tasks at the bridge of the ship. More tasks can result in having not a good overview of the situation.

Manning	Adequate					
Sudden Situati...	Yes			No		
Bridge Design	Inadequate	Conventional	Solo	Inadequate	Conventional	Solo
Yes	0.15	0.01	0.1	0.1	0.0001	0.05
No	0.85	0.99	0.9	0.9	0.9999	0.95

Inadequate					
Yes			No		
Inadequate	Conventional	Solo	Inadequate	Conventional	Solo
0.9	0.7	0.8	0.8	0.4	0.7
0.1	0.3	0.2	0.2	0.6	0.3

The conditional probability in this node is based on [Mazaheri et al. \(2016\)](#).

### Detection

The node joins the nodes 'Visual detection' and other input, and describes whether the OOW has detected the danger, either with visual means or navigational equipment.

Signal quality	Good						Poor					
Visibility	Good			Poor			Good			Poor		
Technical failure	Yes	No	Yes	No	Yes	No	Yes	No	Yes	No	Yes	No
► Yes	0.6	0.9	0.5	0.85	0.6	0.7	0.2	0.4	0.6	0.7	0.2	0.4
No	0.4	0.1	0.5	0.15	0.4	0.3	0.8	0.6	0.4	0.3	0.8	0.6

The conditional probability in this node is based on [DNV \(2005\)](#).

### Incapacitated

The node describes the OOW's physical capability. The capability is assessed to be reduced if the OOW is e.g. intoxicated or affected by an illness, and incapable if the OOW is asleep, not present, dead, etc.

► Capable	0.99996
Reduced	1e-05
Incapable	3e-05

The conditional probability in this node is based on [DNV \(2005\)](#) and [Hänninen and Kujala \(2012\)](#).

### Lack of training

The node describes the lack of training among the crew. The level of training can influence their competence to handle the ship. The training itself is influenced by the safety culture which is present on the ship.

Safety culture	Excellent	Standard	Poor
Yes	0.07	0.1	0.2
No	0.93	0.9	0.8

The conditional probability in this node is based on [Hänninen and Kujala \(2012\)](#).

### Loss of control

The node describes the probability for loss of control of the ship due to technical failures. If the control is lost, nothing can prevent it from continuing towards the danger, i.e. towards the structure.

Technical failure	Yes		No	
Lack of training	Yes	No	Yes	No
► No	0.7	0.8	0.9	0.999
Partial	0.25	0.15	0.09	0.0009
Total	0.05	0.05	0.01	0.0001

The conditional probability in this node is based on engineering judgment.

### Maintenance routine

The node described the probability that the maintenance routine is followed on the ship. This is dependent on the safety culture present on the ship.

Safety culture	Excellent	Standard	Poor
Followed	0.95	0.8	0.6
Not_Followed	0.05	0.2	0.4

The conditional probability in this node is based on [DNV \(2005\)](#).

### Manning

The node described the probability of adequate manning of the bridge. This is dependent on the safety culture present on the ship.

Safety culture	Excellent	Standard	Poor
Adequate	0.99	0.9	0.8
Inadequate	0.01	0.1	0.2

The conditional probability in this node is based on [DNV \(2005\)](#).

### Meteorological conditions

The node describes the most important weather conditions relevant for the operation. The states defined for this node are influenced by the seasons and are the following:

Season	Winter	Summer	Spring	Autumn
Good	0.5	0.8	0.6	0.6
Storm_Rain	0.1973	0.1381	0.2886	0.1993
Windy	0.2	0.05	0.1	0.15
Fog_misty	0.1027	0.0119	0.0114	0.0507

The conditional probability in this node is based on [Port of Rotterdam \(2012\)](#).

### Navigation method

The node describes the method used to navigate the channel and it is influenced by the 'Voyage preparation'.

Voyage prepar...	Properly	Poor
Traditional	0.19	0.4
Advanced	0.81	0.6

The conditional probability in this node is based on [Hänninen and Kujala \(2012\)](#).

### Navigational error

The node describes the probability of a navigational error based on the input coming from the 'Incapacitated' and 'Situational Awareness' node.

Incapacitated	Capable			Reduced			Incapable		
Situational awa...	Fully	Partial	No	Fully	Partial	No	Fully	Partial	No
► Yes	0.05	0.2	0.3	0.1	0.15	0.5	0.4	0.6	0.8
No	0.95	0.8	0.7	0.9	0.85	0.5	0.6	0.4	0.2

The conditional probability in this node is based on engineering judgment.

### Pilot presence

The node describes the presence of a pilot. In this model it is assumed that 98% of the seagoing vessels will have a pilot and that a pilot will be absent at inland going vessels.

Type of ship	Seagoing	Inland
Present	0.98	0
Absent	0.02	1

The conditional probability in this node is based on [Loodswezen \(2018\)](#).

### Pilot vigilance

Influenced by the task responsibilities and the communication level between the bridge personnel and the pilot, this node shows the effect of having a pilot present to correct a critical course.

Pilot presence	Present	Absent
Able_To_Correct	0.9	0
Not_Able	0.1	1

The conditional probability in this node is based on [DNV \(2005\)](#).

**Safety culture**

The node describes how well the vessel operator deals with safety issues and how well the operator promotes a good safety mindset among its employees. By safety issues it is meant both technical safety onboard the vessel (e.g. standard of life saving equipment) and vessel design, in addition to work procedures/instructions, working conditions, training, drills, attitude, etc.

Excellent		0.1
Standard		0.5
Poor		0.4

The conditional probability in this node is based on [DNV \(2005\)](#) and [Hänninen and Kujala \(2012\)](#).

**Season**

The node describes the four different seasons, each having a probability of 0.25 per definition.

Winter		0.25
Summer		0.25
Spring		0.25
Autumn		0.25

**Signal quality**

The signal quality on the radar display is influenced by the weather conditions and the tuning of the radar system. It is assessed that 1 of 1,000 times the radar is displaying poor signal quality in good weather and with the radar tuned to the conditions. Poor signal quality means that it may not be possible to detect the danger on the radar. The other probabilities in the node's CPT are an adjustment of this figure based on engineering judgment.

Meteorological ...	Good	Storm_Rain	Windy	Fog_misty
▶ Good	0.999	0.8	0.999	0.999
Poor	0.001	0.2	0.001	0.001

The conditional probability in this node is based on [DNV \(2005\)](#) and engineering judgment.

**Situational awareness**

The node described the situational awareness of the crew on the bridge. This node is influenced by several other nodes, resulting in a effect on the 'Navigational error' node.

Navigation met.	Traditional								Advanced							
	High				Low				High				Low			
Compliance	Able_To_Correct		Not_Able		Able_To_Correct		Not_Able		Able_To_Correct		Not_Able		Able_To_Correct		Not_Able	
Pilot vigilance	Yes	No	Yes	No	Yes	No	Yes	No	Yes	No	Yes	No	Yes	No	Yes	No
Detection	0.99	0	0.95	0	0.9	0	0.75	0	0.88	0	0.83	0	0.75	0	0.7	0
Partial	0.01	0.8	0.05	0.7	0.09	0.7	0.18	0.5	0.05	0.8	0.1	0.5	0.15	0.5	0.2	0.3
No	0	0.2	0	0.3	0.01	0.3	0.07	0.5	0.07	0.2	0.07	0.5	0.1	0.5	0.1	0.7

The conditional probability in this node is based on engineering judgment.

**Sudden situational change**

The node describes the probability that a situation is changed abruptly, requiring intervention of the crew.

Yes		0.23
No		0.77

The conditional probability in this node is based on [DNV \(2005\)](#) and [Mazaheri et al. \(2016\)](#).

### Technical failure

The node described the probability of technical failure. This node is dependent on the maintenance routine and the redundancy of the equipment.

Technical Red...	Redundant		Scarce	
	Followed	Not_Followed	Followed	Not_Followed
Yes	9e-07	1.5e-06	9e-06	1.5e-05
No	0.9999991	0.9999985	0.999991	0.999985

The conditional probability in this node is based on [DNV \(2005\)](#).

### Technical redundancy

The node described the overall redundancy of equipment on-board the ship.

Safety culture	Excellent	Standard	Poor
Redundant	0.999	0.9	0.7
Scarce	0.001	0.1	0.3

The conditional probability in this node is based on [DNV \(2005\)](#).

### Traffic distribution

The node described the probability of encountering traffic which could lead to 'Loss of control'.

Encounter	0.4
Free	0.6

The probability in this node is based on data provided by the Port of Rotterdam and a calculation of the amount of meeting points.

### Type of ship

The node described the probability of a vessel being a seagoing vessel or an inland going vessel.

Seagoing	0.124
Inland	0.876

The conditional probability in this node is based on statistical data available for the mixed fleet in the Scheur.

### Visibility

The node defines the probability distribution for the visibility, conditional on the weather. The states defined for this node are the following:

Metreological c...	Good	Stom_Rain	Windy	Fog_misty
Good	1	0.75	1	0
Poor	0	0.25	0	1

The conditional probability in this node is based on [DNV \(2005\)](#).

### Voyage preparation

This node describes the quality of the passage planning. 'Poor' means that the trade is not sufficiently planned or that the planned route exposes the vessel to a higher risk than necessary. The node also reflects the ability to detect unknown hazards in the route.

Safety culture	Excellent		Standard		Poor	
	Present	Absent	Present	Absent	Present	Absent
Properly	0.99	0.9	0.85	0.6	0.75	0.4
Poor	0.01	0.1	0.15	0.4	0.25	0.6

The conditional probability in this node is based on [DNV \(2005\)](#) and [Hänninen and Kujala \(2012\)](#).

### VTS

The node shows the probability of that a Vessel Traffic Service (VTS) is monitoring the ship traffic in the area.

Yes	0.75
No	0.25

The conditional probability in this node is based on [Hänninen and Kujala \(2012\)](#).

### Waterway complexity

The node described the complexity of the waterway experienced on the bridge. It is dependent on the visibility and the location of the vessel.

Visibility	Good	Poor
Difficult	0	0.02
Managable	0	0.27
Easy	1	0.71

The conditional probability in this node is based on engineering judgment and [Chapter 4](#).



D

Inland vessels

## Types of vessels

## Bureau Voorlichting Binnenvaart

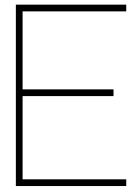
Class		
I	 <b>Spits</b> Length 38,5 meters - width 5,05 meters - draught 2,20 meters - cargo capacity 350 tonnes	 14 x
II	 <b>Campine vessel</b> Length 55 meters - width 6,60 meters - draught 2,59 meters - cargo capacity 655 tonnes	 22 x
III	 <b>Dortmund-Ems canal vessel</b> Length 67 meters - width 8,20 meters - draught 2,50 meters - cargo capacity 1.000 tonnes	 40 x
IV	 <b>Rhine-Herne canal vessel</b> Length 85 meters - width 9,50 meters - draught 2,50 meters - cargo capacity 1.350 tonnes	 54 x
Va	 <b>Large Rhine vessel</b> Length 110 meters - width 11,40 meters - draught 3,00 meters - cargo capacity 2.750 tonnes	 120 x
Vb	 <b>Large Rhine vessel</b> Length 135 meters - width 11,40 meters - draught 3,5 meters - cargo capacity 4.000 tonnes	 160 x
Vla	 <b>Two lighter pushing unit</b> Length 172 meters - width 11,40 meters - draught 4 meters - cargo capacity 5.500 tonnes	 220 x
Vlb Vlc	 <b>Four or six lighter pushing unit</b> Length 193 meters - width 22,80 / 34,20 meters - diepgang 4 meters - laadvermogen 11.000 / 16.500 tonnes	 440 / 660 x
Va	 <b>Standard tank vessel</b> Length 110 meters - width 11,40 meters - diepgang 3,50 meters - cargo capacity 3.000 tonnes	 120 x

## Types of vessels

## Bureau Voorlichting Binnenvaart

Class		 380 x
Vb	<p><b>Large tank vessel</b>            Length 135 meters - width 21,80 meters -            draught 4,40 meters - cargo capacity 9.500 tonnes</p>	
Va		 60 x
Va	<p><b>Car vessel</b>            Length 110 meters - width 11,40 meters -            draught 2,00 meters - cargo capacity 530 cars</p>	
III		 16 x
III	<p><b>Container vessel (Campine class)</b>            Length 63 meters - width 7 meters -            draught 2,50 meters - cargo capacity 32 TEU</p>	
Va		 100 x
Va	<p><b>Standard container vessel</b>            Length 110 meters - width 11,40 meters -            draught 3,00 meter - cargo capacity 200 TEU</p>	
Vb		 250 x
Vb	<p><b>Large container vessel</b>            Length 135 meters - width 17 meters -            draught 3,50 meters - cargo capacity 500 TEU</p>	
Va		 72 x
Va	<p><b>Ro-ro vessel</b>            Length 110 meters - width 11,40 meters -            draught 2,50 meters</p>	
Vlb		 240 x
Vlb	<p><b>Coupled formation (vessel with pushed lighter)</b>            Average length 185 meters - width 11,40 meters -            draught 3,50 meters - cargo capacity 6.000 tonnes</p>	
Vlb		 240 x
Vlb	<p><b>Coupled formation (vessel with pushed vessel)</b>            Average length 185 meters - width 11,40 meters -            draught 3,50 meters - cargo capacity 6.000 tonnes</p>	





# Friction

*In this appendix the phenomena of friction will be examined in detail, as friction plays an important role in defining the amount of reduction that can be applied on the angled impact force.*

## E.1. Definition

Friction is a force resisting relative motion and may occur at the interface between two objects and prevent them from sliding freely against each other. The coefficient of friction ( $\mu$ ) is a number that is the ratio of the resisting force of friction divided by the normal or perpendicular force pushing the object together (Equation E.1).

$$\mu = \frac{F_f}{F_n} \quad (\text{E.1})$$

where  $F_f$  is the friction force and  $F_n$  is the applied normal force. The friction coefficient is influenced by the properties of the surfaces, surroundings, surface features, presence of lubricant and other factors.

Mainly three types of friction can be distinguished, namely dry or lubricated friction, rolling friction and fluid friction. Dry friction occurs when two surfaces slides against each other, rolling friction or rolling resistance can be found when a train moves over the rails and fluid friction occurs when objects move through a fluid or gas.

When look at dry friction, two types of friction are distinguished: static and dynamic friction. The static friction is defined as the ratio of the maximum friction force prior to relative motion to the normal force. The dynamic or kinetic friction is defined as the ratio of the friction force during sliding to the applied normal force. Generally, the static friction is larger than the dynamic one.

Another aspect or distinction that can be made is between dry or lubricated friction. Since for regular engineering materials dry friction is significantly higher than the friction of lubricant layers, the friction could be decreased by introducing a lubricant film or layer and introducing lubricated friction.

## E.2. Dry Friction

There are three laws of dry friction formulated 200 years ago, which are the basic beginning points of every dry friction related calculation.

1. Friction force is proportional to the normal load (first Amonton's law)
2. Friction force is independent of the apparent contact area (second Amaonton's law)
3. Kinetic friction is independent of sliding speed (Coulomb's law)

### E.3. Lubricated friction

Lubricated friction can be divided into three regimes: Boundary (BL), Mixed (ML) and Elastohydrodynamic (EHL). The lubricated friction depends on the operations conditions such as sliding speed, lubricant viscosity, temperature and some other factors. The friction coefficient as function of the lubricating conditions is showed in Figure E.1.

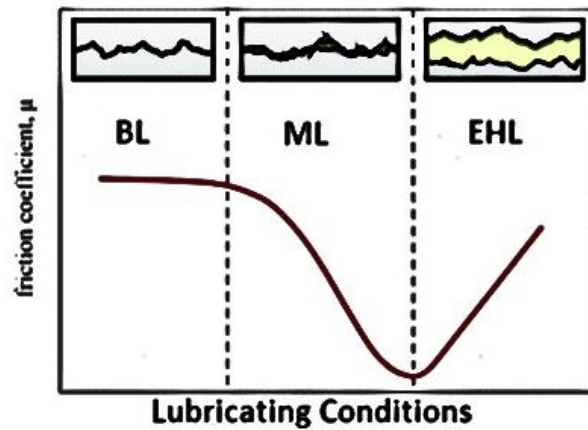


Figure E.1: Three regimes of lubricated friction

A simple theory (load sharing concept) to calculate coefficient of friction in lubricated contacts was proposed by Johnson et al. (1972). This theory considers the total friction coefficient as a sum of two components, dry and lubricant friction weighted by the corresponding areas. The theory was shown to match experimental data quite well in some cases (Akchurin et al., 2015).

### E.4. Friction at the interface of ship-structure

The most used material in building ships nowadays, is steel. The friction coefficient for steel interacting with different materials and in different states is given in Table E.1. From this table it can be seen that there is a significant difference between a static and dynamic state, but even more between a dry and a lubricated state.

Table E.1: Friction coefficient for steel interacting with different materials

Material combinations		Clean and dry surfaces		Lubricated and greasy surfaces	
		Static	Dynamic	Static	Dynamic
Steel	Cast Iron	0.4		0.21	
Steel	Carbon	0.14		0.12 - 0.14	
Steel	Plexiglas	0.4 - 0.5		0.4 - 0.5	
Steel	Steel	0.5 - 0.8		0.16	
Steel (Mild)	Aluminum	0.61	0.47		
Steel (Mild)	Cast Iron		0.23	0.183	0.133
Steel (Mild)	Lead	0.95	0.95	0.5	0.3
Steel (Mild)	Steel (Mild)	0.74	0.57		0.09 - 0.19
Steel (Hard)	Steel (Hard)	0.78	0.42	0.05 - 0.11	0.029 - 0.12

### E.5. Influence of the friction coefficient

Zhang and Pedersen (1999) developed a analytic approach to ship collisions, covering ship-ship collision, ship-rigid walls and ship impact with flexible offshore platforms. He also studied the impact force for two different values of the friction coefficient, namely  $\mu=0.3$  and  $\mu=0.6$ . In Figure E.2 the energy ratio is plotted against the angle of impact for the two different values of the friction coefficient.

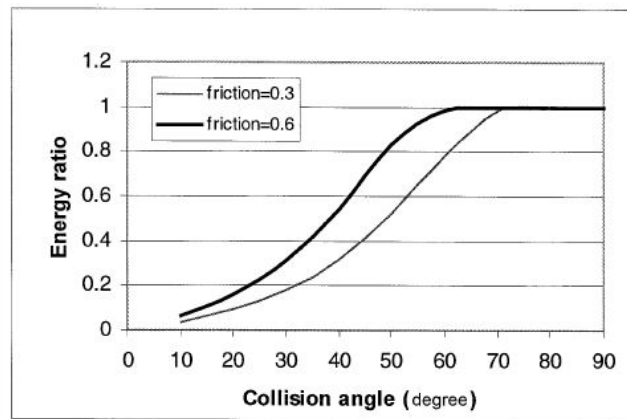


Figure E.2: Influence of the friction coefficient on the energy ratio (Zhang and Pedersen, 1999)

From the study and the figure it becomes clear that a lower friction coefficient is desirable, as even for bigger impact angles a reduction in the impact force can be assumed.

## E.6. Reducing the friction coefficient

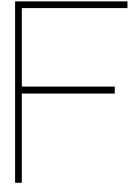
When looking at the friction coefficient, it can be concluded that a lower value is favorable, as the probability of sliding will increase and a lower value for the impact force perpendicular to the structure should be taken into account.

In the case of designing for ship impact, it is possible to look for mitigation measures that can lower the friction coefficient between the ship's hull and the protective structure. There are several ways of reducing the friction, some of them listed below:

1. Make the surface smoother
2. Make use of lubrication
3. Reduce forces acting on the surface
4. Reduce the friction surface
5. Replace sliding elements with rolling elements





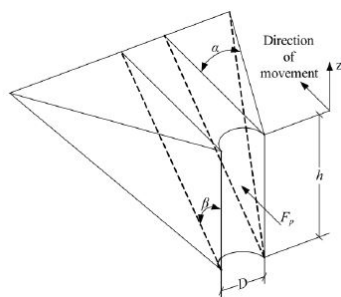


## Soil stiffness

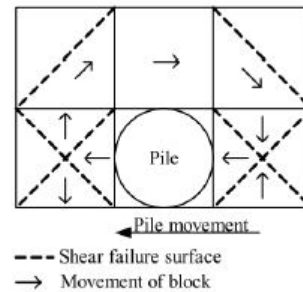
The soil stiffness around the piles can be determined using the  $p$ - $y$  curves (mentioned in section 2.3.4) of Reese et al. (1974). In this appendix the calculation method is explained.

### F.1. Calculation procedure

For the ultimate soil resistance of sand the following expressions based on the different failure mechanisms are given:



(a) Wedge failure for small depths.



(b) Block failure for high depths.

Figure F.1: Soil failure modes according to Reese et al. (1974).

The ultimate soil resistance at smaller depths can be described using the following formula:

$$p_{st} = \gamma' z \left[ \frac{K_0 \tan(\phi) \sin(\beta)}{\tan(\beta - \phi) \cos(\alpha)} + \frac{\tan(\beta)}{\tan(\beta - \phi)} (b + z \tan(\beta) \tan(\alpha)) + K_0 z \tan(\beta) (\tan(\phi) \sin(\beta) - \tan(\alpha)) - K_a b \right] \quad (E.1)$$

The formula related to the block failure at higher depths is this:

$$p_{st} = K_a b \gamma z \tan^8(\beta - 1) + K_0 b \gamma z \tan(\phi) \tan^4(\beta) \quad (E.2)$$

In Figure E2 a typical  $p_y$ -curve is showed with the key points displayed. In 8 steps this curve can be generated, which then describes the behavior of the soil at a certain depth.

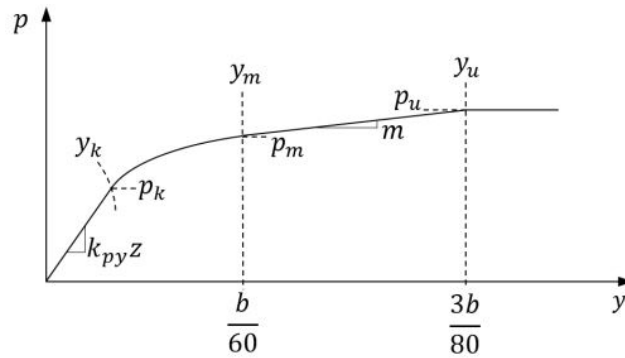


Figure E2: Typical PY-Curve.

### Step 1

Obtain soil internal the friction angle, the effective unit weight and pile diameter  $d$ .

Layer m NAP	Soil Type	Packing	Effective unit weight $\gamma' \text{ kN/m}^3$	Internal Friction Angle $\phi$	Diameter mm
0    -45	Sand	Medium	9	30	1820

Table E1: Assumed soil properties and pile diameter.

### Step 2

Compute the following parameters:

$$\alpha = \frac{\phi}{2} \quad \beta = 45 + \frac{\phi}{2} \quad K_0 = 0.4 \quad K_a = \tan^2(45 - \frac{\phi}{2}) \quad (\text{E3})$$

### Step 3

Compute ultimate soil resistance  $p_s$  per unit length of pile, at depth  $z$  of which is of interest, by taking the smaller of the values given by the following the equations E1 and E2.

### Step 4

Determine the point  $u$  and point  $m$

$$y_u = 3d/80, \quad p_u = A \cdot p_s \quad y_m = d/60, \quad p_m = B \cdot p_u$$

where  $d$  is pile diameter in any length unit,  $A$  is a correction factor from empiricism that can be found from empirical curves in Figure E3,  $B$  is another empirical factor that can be obtained from Figure E3. Note that for static case, use  $A_s$  and  $B_s$ , for cyclic case, use  $A_c$  and  $B_c$ .

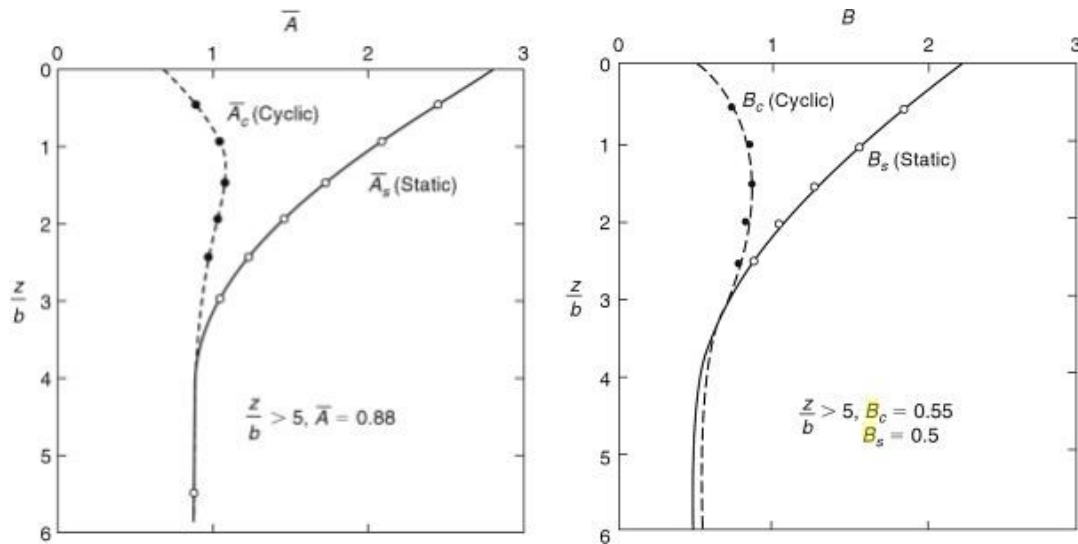


Figure E3: Correction factors.

**Step 5**

Find the initial slope of the p-y curve:

$$k_0 = k \cdot z \tag{E4}$$

where  $z$  is depth and  $k$  is sub-grade modulus for sand. A rough value of  $k$  can be found from Table E2.

Table E2: Basic  $k$  value according to Reese et al. (1974).

Relative Density	Loose	Medium	Dense
	MN/m <sup>3</sup>	MN/m <sup>3</sup>	MN/m <sup>3</sup>
Dry sand	6.8	24.4	61.0
Submerged sand	5.4	16.3	34.0

**Step 6**

Establish the parabolic section of the p-y curve in the form:

$$p = C \cdot y^{1/n} \tag{E5}$$

with:

$$n = \frac{p_m}{k_{mu} \cdot y_m}$$

$$C = \frac{p_m}{y_m^{1/n}}$$

$k_{mu}$  = slope between the point  $u$  and  $m$

**Step 7**

Determine the point  $k$ :

$$y_k = \left(\frac{C}{kz}\right)^{\frac{n}{n-1}}, \quad p_k = k \cdot z \cdot y_k \tag{E6}$$

**Step 8**

Plot the p-y-curve for the depth  $z$ .

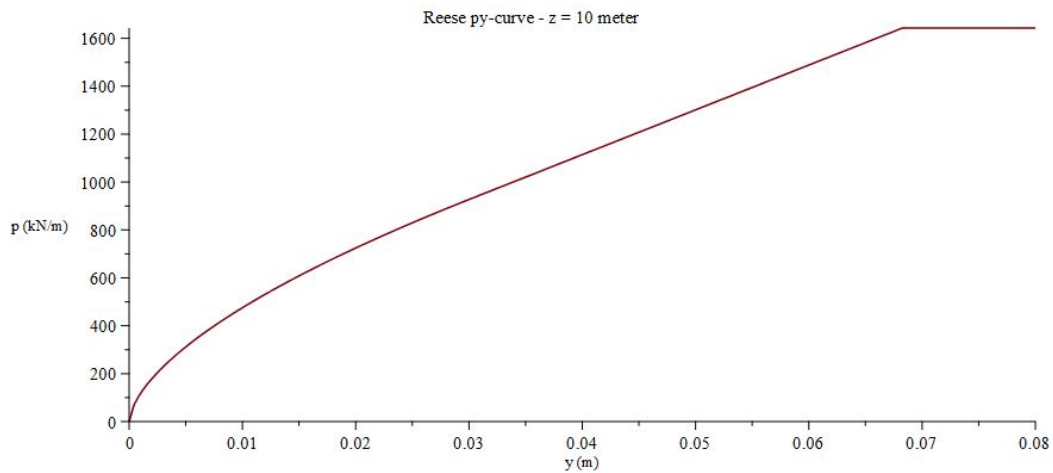


Figure E4: PY-curve for z = 10m.

### F.2. Results

For the calculation of the soil stiffness, the soil is divided in layers of 2 meters thickness. For each a layer a soil stiffness is calculated and a fit is made through these data points. The soil stiffness can then be made dependent on the depth  $z$  and put into the differential equation. The fit can be described by Equation E7 and the 6 constants.

$$k_{soil}(z) := p_1 \cdot z^5 + p_2 \cdot z^4 + p_3 \cdot z^3 + p_4 \cdot z^2 + p_5 \cdot z + p_6 \tag{E.7}$$

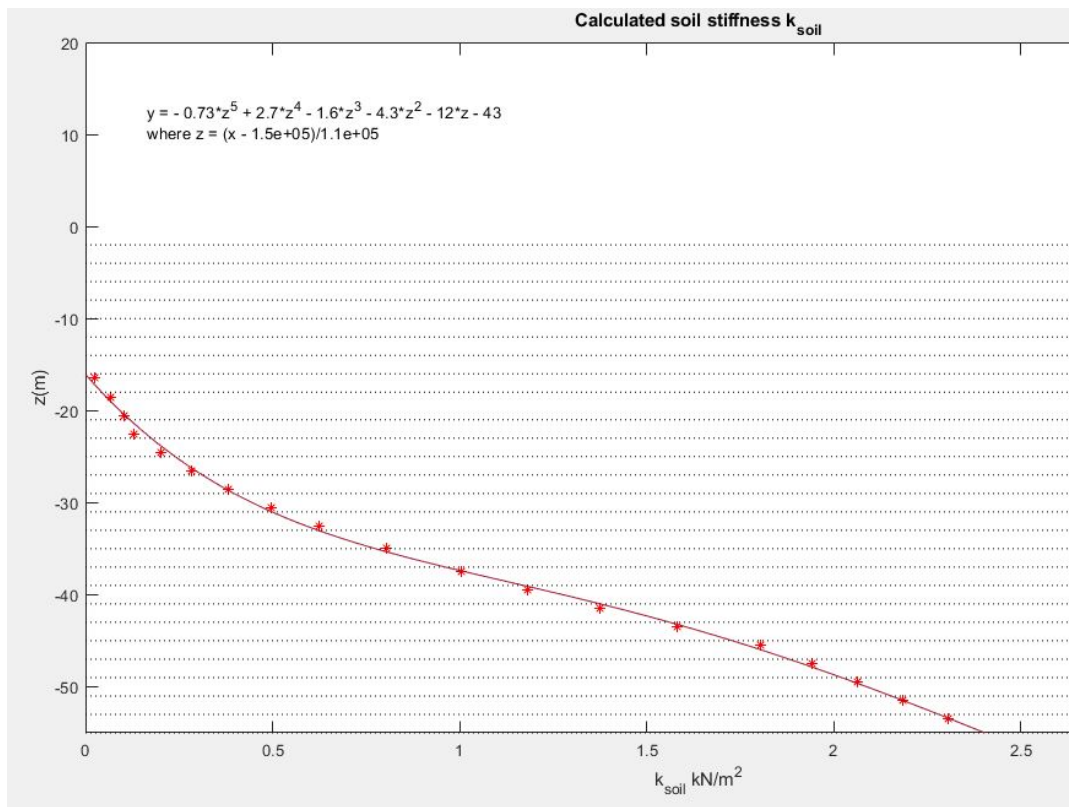


Figure E5: Stiffness of the soil with curve fitting.

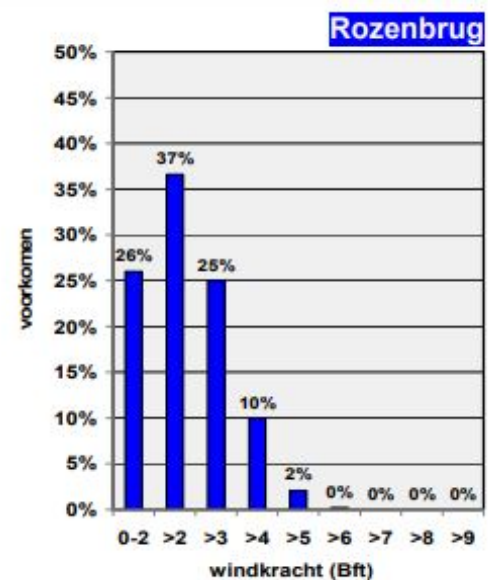
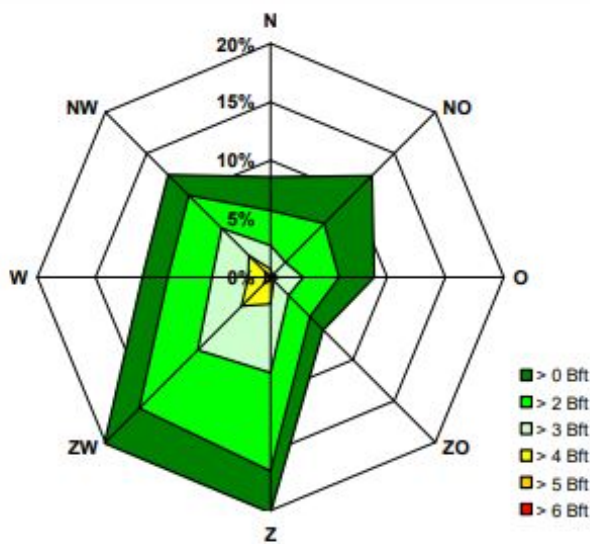
# G

## Navigational properties

*In this appendix figures are given related to the navigational properties in the Scheur.*

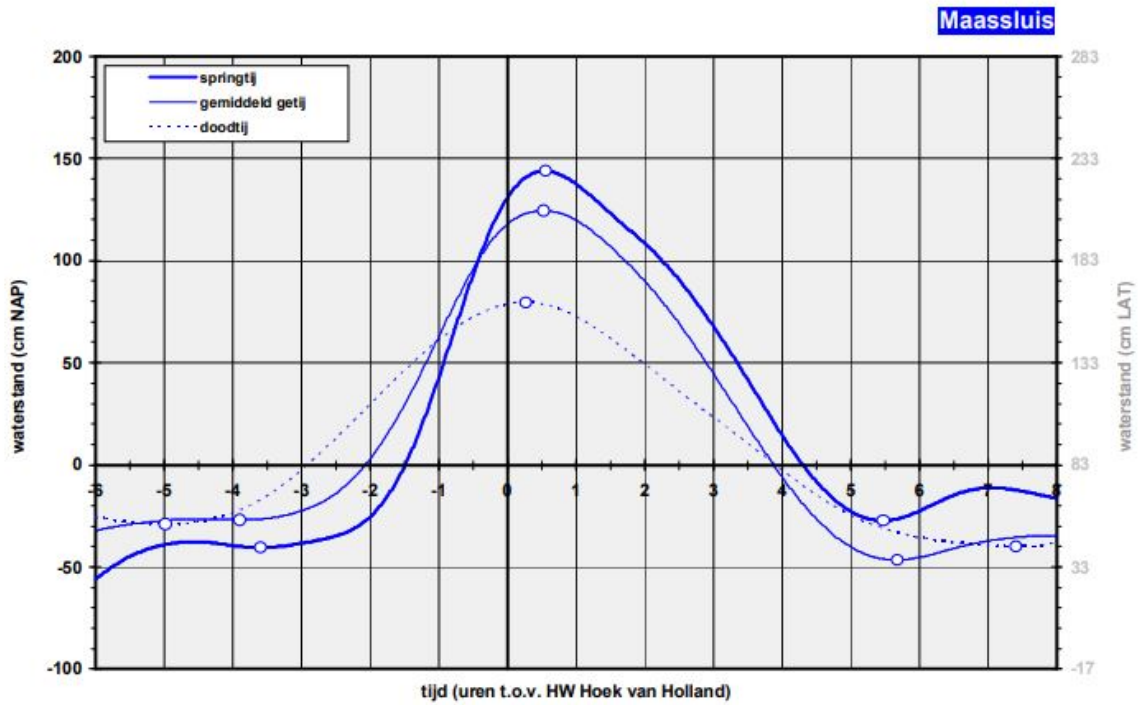
### G.1. Distribution of wind

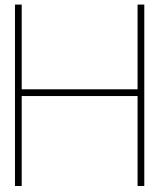
The wind is of importance for the navigability of the Scheur. This information is used in the Bayesian Belief Network in Chapter 4.



## G.2. Tide variation

At the project location, tide variations are present and should be described. As there is no data available of the exact location of the project, the data from Maassluis is taken as this is close by.





# Buckling calculation sheet

The local buckling resistance of the tubular elements is calculated using a Microsoft Excel calculation sheet.

## Parameters Steel Tube

### Material:

Steel grade		=	X70
Yield strength	$f_y$	=	482 N/mm <sup>2</sup>
Elasticity	$E_s$	=	210000 N/mm <sup>2</sup>
Material factor	$\beta_{MO}$	=	1.1

### Internal forces:

$M_{Ed}$	=	13970 kNm
$N_{Ed}$	=	0 kN
u.c.	=	1.00

### Dimensions:

Outer diameter of tube	$D_{out}$	=	1420 mm
Wall thickness of tube	$t$	=	20 mm
Radius of tube	$r = \frac{1}{2} \times (D_{out} - t)$	=	700.0 mm
Corrosion depth	c.d.	=	0 mm

### Structure characteristics:

Secondary members:	Yes
Soil pressures:	Yes
Sand Filled section:	No

### Design values:

Diameter of tube	$D_{des} = D_{out} - t - c.d.$	=	1400 mm
Wall thickness of tube	$t_{des} = t - c.d.$	=	20 mm
Radius of tube	$r_{des} = \frac{1}{2} \times D_{des}$	=	700.0 mm
Area	$A_{des} = \pi \times t_{des} \times D_{des}$	=	87965 mm <sup>2</sup>
Section modulus	$W_{des,pl} = \pi/4 \times t_{des} \times (D_{des})^2$	=	3.08E+07 mm <sup>3</sup>
	$W_{des,pl} = t_{des} \times (D_{des})^2$	=	3.92E+07 mm <sup>3</sup>
Moment of inertia	$I_{des} = \pi/8 \times t_{des} \times (D_{des})^3$	=	2.16E+10 mm <sup>4</sup>

### Initial out-of-roundness

Production class:		C	Normal
D	=	1420 mm	
Value for $U_r$	=	0.015	
Ovalization $a_{init}$	=	$1/4 \times U_r \times D$	
Ovalization $a_{init}$	=	5.3 mm	

Table for  $U_r$

Class	3			4		5	
	D < 0,50	0,50 < D < 1,25		D > 1,25			
A Excellent	0.014	0,007+0,0093(1,25-D)		0.007			
B High	0.020	0,010+0,0133(1,25-D)		0.010			
C Normal	0.030	0,015+0,0200(1,25-D)		0.015			

### Cross tensile forces from secondary members

Tensile Force  $F$  = maximal support reaction from secondary member;  $[0,5 \times f_{y,sp} \times t_{sp,min}^2 / (h_{pl,tot} - t_r)]$

### Parameters Secondary member

Steel grade		=	S355 -
Yield strength	$f_{y,sm}$	=	355 N/mm <sup>2</sup>
Elasticity	$E_s$	=	210000 N/mm <sup>2</sup>
Flange thickness	$t_{flange}$	=	13.0 mm
Web thickness	$t_{web}$	=	12.2 mm
Total height	$h_{sm,total}$	=	427 mm

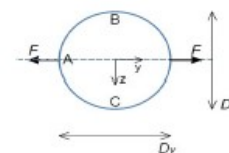
$$F = [0,5 \times f_{y,sm} \times t_{sm,min}^2 / (h_{sm,tot} - t_r)] = 0.0 \text{ kN/m}$$

$$DD_y = -(2/p - 1/2) F \times r_{des}^3 / EI = 0.00 \text{ mm}$$

$$B_{tensile \text{ force}} = 0.00 \text{ mm}$$

$$M_A = -1/p \times F \times r_{des} = 0.00 \text{ kNm}$$

$$M_B = (1/2 - 1/p) \times F \times r_{des} = 0.00 \text{ kNm}$$



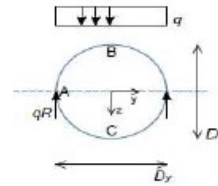
**Soil pressure**

Soil pressure acting at tube are:

	Side B	Side C	
$q_{eff}$	0	0	kN/m <sup>2</sup>

**One sided pressure**

$DD_s$	=	$-1/12 \times q \times r_{des}^4 / EI$	=	0.0 mm
$a_{soil\ press.}$	=	$abs[1/2 \times DD_s]$	=	0.0 mm
$M_A$	=	$-1/8 \times q \times r_{des}^2$	=	0.0 kNm
$M_B$	=	$(3/8 - 2/3p) \times q \times r_{des}^2$	=	0.0 kNm



**Overall curvature**

Internal forces:

$M_{Ed}$	=	13970 kNm
$N_{Ed}$	=	0 kN

Meridional stresses:

$s_{x,Ed,1}$	=	$M_{Ed} / W_{des}$	=	453.8 N/mm <sup>2</sup>
$s_{x,Ed,2}$	=	$N_{Ed} / A_{des}$	=	0.0 N/mm <sup>2</sup>
$s_{x,Ed}$	=	$s_{x,Ed,1} + s_{x,Ed,2}$	=	453.8 N/mm <sup>2</sup>

Yield limit  $f_y$  = 482 N/mm<sup>2</sup> >  $s_{x,Ed}$  p

$a_{curv.} = i_c^2 \times r_{des}^5 / t_{des}^2 = 4.0$  mm  
 $k = M_{Ed} / EI_{des} = 3.09E-06$  -

**Resulting ovalisation and circumferential moments for the empty tubes**

- Initial out-of-roundness	$a_{init.}$	=	5.3 mm
- Cross tensile forces	$a_{tensile\ force}$	=	0.0 mm
- Soil pressure	$a_{soil\ press.}$	=	0.0 mm
- Overall curvature	$a_{curv.}$	=	4.0 mm
<b>Resulting:</b>	$a_{empty}$	=	<b>9.3 mm</b>
- Resulting moment:	$M_A$	=	0.00 kNm
- Resulting moment:	$M_B$	=	0.00 kNm
- Moment capacity	$M_{p0,rd}$	=	$3/4 \times t_{des}^2 \times f_y \times g_{M0}^{-1} = 43.82$ kNm

**Bending moment evaluation for empty tubes**

As a result from the ovalisation, the radius of the top and bottom sides of the tube changes according:

$r' = r_{des} / (1 - 3 \times a_{empty} / r_{des}) = 729.2$  mm

This (larger) radius  $r'$  is input to the critical strain formula(s).

$D_{des} / t_{des} = 70 < 120$

Calculate critical strain  $e_{cr}$  according:

$\epsilon_{cr} = 0.25 \times t/r' - 0.0025 = 4.36E-03$  rad.  
 $e_y = f_{y,sp} / E = 2.30E-03$  kNm  
 kNm

$\mu = e_{cr} / e_y = 1.898 > 1,0$  p  
 $\theta = \sin^{-1}(1/\mu) = 0.555$   
 $M_{Ez} = 1/2 \times (\theta' \sin \theta + \cos \theta) \times M_{p1;d} = 16346$  kNm  
 $M_{p1;d} = D_{des}^2 \times t_{des} \times f_{y,sp} \times \gamma_{M0}^{-1} = 17177$  kNm

$M_{Ed}$	=	$g \times b_k \times b_s \times M_{Ez}$	=	13970 kNm
- $g$	=	$c_1/6 + 2/3$	=	1.00 kNm
- $c_1$	=	$[4 - 2 \times (3^{1/2} \times m_{eff,sd} / m_{pl,sd})]^{1/2}$	=	2.00 -
- $m_{eff,sd}$	=	$1/2 \times [M_A + M_B]$	=	0.00 -
- $m_{pl,rd}$	=	$3/4 \times t_{des}^2 \times f_y \times \gamma_{M0}^{-1}$	=	43.8 -
- $b_k$	=	$1 - 2a/3r$	=	0.991
- $b_s$	=	$0,625 + 0,125\mu$	=	0.862